Observatory science with eXTP

in 't Zand, J.J.M.; Maccarone, T.J.; Rowlinson, A.; Tauris, T.M.; Zhou, P.; Altamirano, D.; Bilous, A.; Casella, P.; Cavecchi, Y.; Chambers, F.; Costantini, E.; Degenaar, N.; Di Salvo, T.; Götz, D.; Homan, J.; Jonker, P.G.; Linares, M.; Stappers, B.W.; Vink, J.; Watts, A.L.; Wijnands, R.; eXTP Mission

DOI
10.1007/s11433-017-9186-1

Publication date
2019

Document Version
Author accepted manuscript

Published in
Science China: Physics, Mechanics and Astronomy

SCIENCE CHINA
Physics, Mechanics & Astronomy

• **Invited Review** •
The X-ray Timing and Polarimetry Frontier with eXTP

February 2019 Vol. 62 No. 2: 029506
doi: 10.1007/s11433-017-9186-1

Observatory science with *eXTP*

Jean J.M. in 't Zand[1], Enrico Bozzo[2], Jinlu Qu[3], Xiang-Dong Li[4], Lorenzo Amati[5], Yang Chen[4], Immacolata Donnarumma[6,7], Victor Doroshenko[8], Stephen A. Drake[9], Margarita Hernanz[10], Peter A. Jenke[11], Thomas J. Maccarone[12], Simin Mahmoodifar[9], Domitilla de Martino[13], Alessandra De Rosa[7], Elena M. Rossi[14], Antonia Rowlinson[15,16], Gloria Sala[17], Giulia Stratta[18], Thomas M. Tauris[19], Joern Wilms[20], Xuefeng Wu[21], Ping Zhou[15,4], Iván Agudo[22], Diego Altamirano[23], Jean-Luc Atteia[24], Nils A. Andersson[25], M. Cristina Baglio[26], David R. Ballantyne[27], Altan Baykal[28], Ehud Behar[29], Tomaso Belloni[30], Sudip Bhattacharyya[31], Stefano Bianchi[32], Anna Bilous[15], Pere Blay[33], João Braga[34], Søren Brandt[35], Edward F. Brown[36], Niccolò Bucciantini[37], Luciano Burderi[38], Edward M. Cackett[39], Riccardo Campana[5], Sergio Campana[30], Piergiorgio Casella[40], Yuri Cavecchi[41,25], Frank Chambers[15], Liang Chen[42], Yu-Peng Chen[3], Jérôme Chenevez[35], Maria Chernyakova[43], Jin Chichuan[44], Riccardo Ciolfi[45,46], Elisa Costantini[1,15], Andrew Cumming[47], Antonino D'Aì[48], Zi-Gao Dai[4], Filippo D'Ammando[49], Massimiliano De Pasquale[50], Nathalie Degenaar[15], Melania Del Santo[48], Valerio D'Elia[40], Tiziana Di Salvo[51], Gerry Doyle[52], Maurizio Falanga[53], Xilong Fan[54,55], Robert D. Ferdman[56], Marco Feroci[7], Federico Fraschetti[57], Duncan K. Galloway[58], Angelo F. Gambino[51], Poshak Gandhi[59], Mingyu Ge[3], Bruce Gendre[60], Ramandeep Gill[61], Diego Götz[62], Christian Gouiffès[62], Paola Grandi[5], Jonathan Granot[61], Manuel Güdel[63], Alexander Heger[58,64,121], Craig O. Heinke[65], Jeroen Homan[66,1], Rosario Iaria[51], Kazushi Iwasawa[67], Luca Izzo[68], Long Ji[8], Peter G. Jonker[1,69], Jordi José[17], Jelle S. Kaastra[1], Emrah Kalemci[70], Oleg Kargaltsev[71], Nobuyuki Kawai[72], Laurens Keek[73], Stefanie Komossa[19], Ingo Kreykenbohm[20], Lucien Kuiper[1], Devaky Kunneriath[74], Gang Li[3], En-Wei Liang[75], Manuel Linares[17], Francesco Longo[76], Fangjun Lu[3], Alexander A. Lutovinov[77], Denys Malyshev[8], Julien Malzac[78], Antonios Manousakis[79], Ian McHardy[59], Missagh Mehdipour[1], Yunpeng Men[80], Mariano Méndez[81], Roberto P. Mignani[82], Romana Mikusincova[83], M. Coleman Miller[84], Giovanni Miniutti[85], Christian Motch[86], Joonas Nättilä[87], Emanuele Nardini[88], Torsten Neubert[35], Paul T. O'Brien[89], Mauro Orlandini[5], Julian P. Osborne[89], Luigi Pacciani[7], Stéphane Paltani[2], Maurizio Paolillo[90], Iossif E. Papadakis[91], Biswajit Paul[92], Alberto Pellizzoni[93], Uria Peretz[29], Miguel A. Pérez Torres[94], Emanuele Perinati[8], Chanda Prescod-Weinstein[95], Pablo Reig[96], Alessandro Riggio[38], Jerome Rodriguez[62], Pablo Rodríguez-Gil[33,97], Patrizia Romano[30], Agata Różańska[98], Takanori Sakamoto[99], Tuomo Salmi[87], Ruben Salvaterra[82], Andrea Sanna[38], Andrea Santangelo[8], Tuomas Savolainen[100,101], Stéphane Schanne[62], Hendrik Schatz[102], Lijing Shao[19], Andy Shearer[103], Steven N. Shore[104,105], Ben W. Stappers[106], Tod E. Strohmayer[9], Valery F. Suleimanov[8], Jiří Svoboda[74], F.-K. Thielemann[107], Francesco Tombesi[9], Diego F. Torres[10], Eleonora Torresi[5], Sara Turriziani[108], Andrea Vacchi[109,110], Stefano Vercellone[30], Jacco Vink[15], Jian-Min Wang[3], Junfeng Wang[111], Anna L. Watts[15], Shanshan Weng[112], Nevin N. Weinberg[113], Peter J. Wheatley[114], Rudy Wijnands[15], Tyrone E. Woods[58], Stan E. Woosley[115], Shaolin Xiong[3], Yupeng Xu[3], Zhen Yan[42], George Younes[116], Wenfei Yu[42], Feng Yuan[42], Luca Zampieri[117], Silvia Zane[118], Andrzej A. Zdziarski[79], Shuang-Nan Zhang[3], Shu Zhang[3], Shuo Zhang[119], Xiao Zhang[4], Michael Zingale[120]

[1]*SRON Netherlands Institute for Space Research, Sorbonnelaan 2, 3584 CA Utrecht, The Netherlands,* [2]*Department of Astronomy, University of Geneva, 1290 Versoix, Switzerland,* [3]*Key Laboratory for Particle Astrophysics, CAS Institute of High Energy Physics, 19B Yuquan Road, Beijing 100049, China,* [4]*School of Astronomy and Space Science, Nanjing University, Nanjing 210023, China,* [5]*INAF-IASF Bologna, via P. Gobetti 101, 40129 Bologna, Italy,* [6]*ASI, Via del Politecnico snc, 00133 Roma, Italy,* [7]*INAF - Istituto di Astrofisica e Planetologie Spaziali. Via Fosso del Cavaliere 100, 00133 Roma, Italy,* [8]*Institut für Astronomie und Astrophysik Tübingen, Universität Tübingen, Sand 1, 72076 Tübingen, Germany,* [9]*NASA Goddard Space Flight Center, Code 662, Greenbelt, MD 20771, USA,* [10]*ICREA & Institute of Space Sciences (IEEC-CSIC), Campus UAB, Carrer de Can Magrans, s/n 08193 Barcelona, Spain,* [11]*CSPAR, SPA University of Alabama in Huntsville, Huntsville, AL 35805, USA,* [12]*Department of Physics, Texas Tech University, Lubbock, TX 79409, USA,* [13]*INAF Osservatorio Astronomico di Capodimonte, Salita Moiariello 16, 80131 Napoli, Italy,* [14]*Leiden Observatory, Leiden University, PO Box 9513, 2300 RA Leiden, the Netherlands,* [15]*Anton Pannekoek Institute, University of Amsterdam, Science Park 904, 1098 XH Amsterdam, The Netherlands,* [16]*ASTRON Netherlands Institute for Radio Astronomy, P.O. Box 2, 7990 AA Dwingeloo, the Netherlands,* [17]*Universitat Politecnica de Catalunya (UPC-IEEC), 08034 Barcelona, Spain,* [18]*Universitá degli Studi di Urbino 'Carlo Bo', 61029 Urbino, Italy,* [19]*Max-Planck-Institut für Radioastronomie, 53121 Bonn, Germany,* [20]*Dr. Karl-Remeis-Sternwarte and Erlangen Centre for Astroparticle Physics (ECAP), Friedrich Alexander Universität Erlangen-Nurnberg, Sternwartstr. 7, 96049 Bamberg, Germany,* [21]*Purple Mountain Observatory, Chinese Academy of Sciences, Nanjing 210008, China,* [22]*Instituto de Astrofysíca de Andalucia - CSIC, 18008 Granada, Spain,* [23]*Department of Physics and Astronomy, University of Southampton, Southampton, SO17 1BJ, UK,* [24]*IRAP, Université de Toulouse, CNRS, UPS, CNES, 31028 Toulouse, France,* [25]*Mathematical Sciences and STAG Research Centre, University of Southampton, Southampton, SO17 1BJ, UK,* [26]*New York University Abu Dhabi, PO Box 129188, Abu Dhabi, UAE,* [27]*Center for Relativistic Astrophysics, School of Physics, Georgia Institute of Technology, Atlanta, GA 30332, USA,* [28]*Physics Department, Middle East Technical University, 06531 Ankara, Turkey,* [29]*Department of Physics, Technion-Israel Institute of Technology, 32000 Haifa, Israel,* [30]*INAF Osservatorio Astronomico di Brera, via Bianchi 46, 23807 Merate (LC), Italy,* [31]*Tata Institute of Fundamental Research, Mumbai 400005, India,* [32]*Dipartimento di Matematica e Fisica, Università degli Studi Roma Tre, via della Vasca Navale 84, 00146 Roma, Italy,* [33]*Instituto de Astrofísica de Canarias, 38205 La Laguna, Tenerife, Spain,* [34]*Instituto Nacional de Pesquisas Espaciais - INPE, Av. dos Astronautas 1758, 12227-010, S.J. Campos-SP, Brazil,* [35]*National Space Institute, Technical University of Denmark (DTU Space), 2800 Kgs. Lyngby, Denmark,* [36]*Department of Physics and Astronomy, Michigan State University, East Lansing, MI 48824, USA,* [37]*INAF Osservatorio Astrofisico di Arcetri, Largo Enrico Fermi 5, 50125 Firenze, Italy,* [38]*Dipartimento di Fisica, Universitá degli Studi di Cagliari, SP Monserrato-Sestu km 0.7, 09042 Monserrato, Italy,* [39]*Department of Physics and Astronomy, Wayne State University, 666 W. Hancock St., Detroit, MI 48201, USA,* [40]*INAF Osservatorio Astronomico di Roma, Via Frascati 33, 00078 Monteporzio Catone, Roma, Italy,* [41]*Department of Astrophysical Sciences, Princeton University, Peyton Hall, Princeton, NJ 08544, USA,* [42]*Key Laboratory for Research in Galaxies and Cosmology, Shanghai Astronomical Observatory, Chinese Academy of Sciences, 80 Nandan Road, Shanghai 200030, China,* [43]*School of Physical Sciences, Dublin City University, Glasnevin, Dublin 9, Ireland,* [44]*Max-Planck-Institut für Extraterrestrische Physik, Giessenbachstrasse, 85748 Garching, Germany,* [45]*INAF, Osservatorio Astronomico di Padova, Vicolo dellOsservatorio 5, 35122 Padova, Italy,* [46]*INFN-TIFPA, Trento Institute for Fundamental Physics and Applications, Via Sommarive 14, 38123 Trento, Italy,* [47]*Department of Physics and McGill Space Institute, McGill University, 3600 rue University, Montreal, QC, H3A 2T8, Canada,* [48]*INAF/IASF Palermo, via Ugo La Malfa 153, 90146 Palermo, Italy,* [49]*INAF - Istituto di Radioastronomia, via Gobetti 101, 40129 Bologna, Italy,* [50]*Department of Astronomy and Space Sciences, Istanbul University, 34119, Beyazit, Turkey,* [51]*Universitá degli Studi di Palermo, Dipartimento di Fisica e Chimica, via Archira 36, 90123 Palermo, Italy,* [52]*Armagh Observatory, College Hill, Armagh, BT61 9DG, N. Ireland,* [53]*International Space Science Institute (ISSI), Hallerstrasse 6, 3012 Bern, Switzerland,* [54]*School of Physics and Electronics Information, Hubei University of Education, 430205 Wuhan, China,* [55]*SUPA, School of Physics and Astronomy, University of Glasgow, Glasgow G12 8QQ, UK,* [56]*Faculty of Science, University of East Anglia, Norwich Research Park, Norwich NR4 7TJ, UK,* [57]*Depts. of Planetary Sciences and Astronomy, University of Arizona, Tucson, AZ 85721, USA,* [58]*School of Physics and Astronomy, Monash University, Clayton VIC 3800, Australia,* [59]*Department of Physics and Astronomy, University of Southampton, Southampton SO17 1BJ, UK,* [60]*University of the Virgin Islands, John Brewers Bay, St Thomas, U.S. Virgin Islands 00802-9990, USA,* [61]*Department of Natural Sciences, The Open University of Israel, 1 University Road, PO Box 808, Raanana 4353701, Israel,* [62]*CEA Paris-Saclay, DRF/IRFU/Département d'Astrophysique, Laboratoire AIM (UMR 7158), 91191 Gif sur Yvette, France,* [63]*University of Vienna, Department of Astrophysics, Vienna, 1180, Austria,* [64]*University of Minnesota, School of Physics and Astronomy, Minneapolis, MN 55455, USA,* [65]*Department of Physics, University of Alberta, CCIS 4-181, Edmonton, AB T6G 2E1, Canada,* [66]*Eureka Scientific, Inc., 2452 Delmer Street, Oakland, CA 94602, USA,* [67]*ICREA & Institut de Ciéncies del Cosmos (ICCUB), Universitat de Barcelona (IEEC-UB), Martí i Franqués, 1, 08028 Barcelona, Spain,* [68]*Instituto de Astrofisica de Andalucia (IAA-CSIC), Glorieta de la Astronomia s/n, 18008 Granada, Spain,* [69]*Department of Astrophysics, IMAPP, Radboud University, 6500 GL Nijmegen, the Netherlands,* [70]*Faculty of Engineering and Natural Sciences, Sabanci University, Orhanli-Tuzla, 34956 Istanbul, Turkey,* [71]*Department of Physics, The George Washington University, 725 21st St. NW, Washington, DC 20052, USA,* [72]*Department of Physics, Tokyo Institute of Technology, Meguro, Tokyo 152-8551, Japan,* [73]*Department of Astronomy, University of Maryland, College Park, MD 20771, USA,* [74]*Astronomical Institute, Academy of Sciences, Bocni II 1401, 14131 Prague, Czech Republic,* [75]*GXU-NAOC Center for Astrophysics and Space Sciences, Department of Physics, Guangxi University, Nanning 530004, China,* [76]*Dip. di Fisica, Universitá di Trieste and INFN, Via Valerio 2, 34127 Trieste, Italy,* [77]*Space Research Institute of the Russian Academy of Sciences, Profsoyuznaya Str. 84/32, 117997 Moscow, Russia,* [78]*IRAP, Université de Toulouse, CNRS, UPS, CNES, 31028 Toulouse, France,* [79]*Nicolaus Copernicus Astronomical Center, Polish Academy of Sciences, Bartycka 18, 00-716 Warszawa, Poland,* [80]*Department of Astronomy, School of Physics, Peking University, Yi He Yuan Lu 5, Hai Dian District, Beijing 100871, China,* [81]*Kapteyn Astronomical Institute, University of Groningen, PO Box 800, 9700 AV Groningen, The Netherlands,* [82]*INAF Istituto di Astrofisica Spaziale e Fisica Cosmica, via E. Bassini 15, 20133 Milano, Italy,* [83]*Institute of Theoretical Physics, Faculty of Mathematics and Physics, Charles University, V. Holesovickach 2, 180 00 Praha 8, Czech Republic,* [84]*Department of Astronomy and Joint Space-Science Institute, University of Maryland, College Park, MD 20742-2421, USA,* [85]*Centro de Astrobiologia (CSIC-INTA), Dep. de Astrofsica, ESAC, PO Box 78, 28691 Villanueva de la Canada, Madrid, Spain,* [86]*Université de Strasbourg, CNRS, Observatoire Astronomique, UMR 7550, 67000, Strasbourg, France,* [87]*Tuorla Observatory, Department of Physics and Astronomy, University of Turku, Väisäläntie 20, 21500 Piikkiö, Finland,* [88]*INAF Osservatorio Astrofisico di Arcetri, Largo Enrico Fermi 5, 50125 Firenze, Italy,* [89]*Department of Physics and Astronomy, University of Leicester, University Road, Leicester LE1 7RH, UK,* [90]*Dipartimento di Fisica Ettore Pancini, Universitá di Napoli Federico II, via Cintia, 80126 Napoli, Italy,* [91]*Department of Physics and Institute of Theoretical and Computational Physics, University of Crete, 71003, Heraklion, Greece,* [92]*Raman Research Institute, Sadashivnagar, C. V. Raman Avenue, Bangalore 560080, India,* [93]*INAF, Osservatorio Astronomico di Cagliari, Via della Scienza 5, 09047 Selargius, Italy,* [94]*Instituto de Astrofísica de Andalucía - CSIC, 18008 Granada, Spain,* [95]*Department of Physics, University of Washington, Seattle, WA 98195-1560, USA,* [96]*IESL, Foundation for Research and Technology-Hellas, 71110, Heraklion, Greece,* [97]*Departamento de Astrofísica, Universidad de La Laguna, 38206 La Laguna, Tenerife, Spain,* [98]*N. Copernicus Astronomical Center, Bartycka 18, 00-716 Warsaw, Poland,* [99]*Department of Physics and Mathematics, Aoyama Gakuin University, Sagamihara, Kanagawa 252-5258, Japan,* [100]*Aalto University Metsahovi Radio Observatory, Metsahovintie 114, 02540 Kylmala, Finland,* [101]*Aalto University Department of Electronics and Nanoengineering, PL 15500, 00076 Aalto, Finland,* [102]*National Superconducting Cyclotron Laboratory, Michigan State University, East Lansing, MI 48824, USA,* [103]*Centre for Astronomy, National University of Ireland, Galway, H91 TK33, Ireland,* [104]*Dipartimento di Fisica 'Enrico Fermi', University of Pisa, 56127 Pisa, Italy,* [105]*INFN Sezione di Pisa, 56127 Pisa, Italy,* [106]*Jodrell Bank Centre for Astrophysics, School of Physics and Astronomy, The University of Manchester, Manchester M13 9PL, UK,* [107]*Department of Physics, University of Basel, Klingelbergstrabe 82, 4056 Basel, Switzerland,* [108]*Computational Astrophysics Laboratory - RIKEN, 2-1 Hirosawa, Wako, Saitama 351-0198, Japan,* [109]*Dep. of Mathematics, Computer science and Physics, University of Udine, Via delle Scienze 206, 33100 Udine, Italy,* [110]*INFN Italian National Institute for Nuclear Physics, c/o Area di Ricerca Padriciano 99, 34012 Trieste, Italy,* [111]*Department of Astronomy and Institute of Theoretical Physics and Astrophysics, Xiamen University, Xiamen, Fujian 361005, China,* [112]*Department of Physics and Institute of Theoretical Physics, Nanjing Normal University, Nanjing 210023, China,* [113]*Department of Physics, and Kavli Institute for Astrophysics and Space Research, Massachusetts Institute of Technology, Cambridge, MA 02139, USA,* [114]*Department of Physics, University of Warwick, Coventry CV4 7AL, UK,* [115]*Department of Astronomy and Astrophysics, University of California, Santa Cruz, CA 95064,USA,* [116]*Department of Physics, The George Washington University, Washington, DC 20052, USA,* [117]*INAF Astronomical observatory of Padova, 35122 Padova, Italy,* [118]*Mullard Space Science Laboratory, University College London, Holmbury St. Mary, Dorking, Surrey RH5 6NT, UK,* [119]*MIT Kavli Institute for Astrophysics and Space Research, Cambridge, MA 02139, USA,* [120]*Department of Physics and Astronomy, Stony Brook University, Stony Brook, NY 11794-3800, USA,* [121]*Astronomy Department, Shanghai Jiao Tong University, Shanghai 200240, China*

Received December 6, 2017; accepted February 9, 2018; published online August 30, 2018

In this White Paper we present the potential of the *enhanced X-ray Timing and Polarimetry* (eXTP) mission for studies related to *Observatory Science* targets. These include flaring stars, supernova remnants, accreting white dwarfs, low and high mass X-ray binaries, radio quiet and radio loud active galactic nuclei, tidal disruption events, and gamma-ray bursts. *eXTP* will be excellently suited to study one common aspect of these objects: their often transient nature. Developed by an international Consortium led by the Institute of High Energy Physics of the Chinese Academy of Science, the *eXTP* mission is expected to be launched in the mid 2020s.

Keywords: space research instruments, nuclear astrophysics, flare stars, accretion and accretion disks, mass loss and stellar winds, cataclysmic binaries, X-ray binaries, supernova remnants, active galactic nuclei, X-ray bursts, gamma-ray bursts, gravitational waves

PACS number(s): 07.87+v, 26.30.ca, 97.30.Nr, 97.10.Gz, 97.10.Me, 97.30.Qt, 97.80.Jp, 98.38.Mz, 98.54.Cm, 98.70.Qy, 98.70.rz, 04.30.Db

Citation: in 't Zand J.J.M., Bozzo E., Li X., Qu J., et al., Observatory science with *eXTP*, Sci. China-Phys. Mech. Astron. **62**, 029506 (2019), doi: 10.1007/s11433-017-9186-1

1 Introduction

The enhanced X-ray Timing and Polarimetry mission (eXTP) is a mission concept proposed by a consortium led by the Institute of High-Energy Physics of the Chinese Academy of Sciences and envisaged for a launch in the mid 2020s. It carries 4 instrument packages for the 0.5–30 keV bandpass, with the primary purpose to study conditions of extreme density, gravity and magnetism in and around compact objects in the universe. The mission concept provides for a low-Earth orbit with a low inclination ($< 15°$), incurring earth obscurations every one and a half hour for targets near the celestial equator such as the Galactic center region. The scientific payload of *eXTP* consists of: the Spectroscopic Focusing Array (SFA), the Polarimetry Focusing Array (PFA), the Large Area Detector (LAD) and the Wide Field Monitor (WFM).

The *eXTP* instrumentation is discussed in detail in Zhang et al. (2018), which includes a comparison with other instruments. We summarize as follows. The SFA is an array of nine identical X-ray telescopes covering the energy range 0.5–20 keV with a spectral resolution of better than 180 eV (full width at half maximum, FWHM) at 6 keV, and featuring a total effective area from $\sim$0.5 m^2 at 6 keV to $\sim$ 0.7 m^2 at 1 keV. The SFA angular resolution is required to be less than $\sim 1'$ (half-power diameter; HPD) and its sensitivity reaches 10^{-14} erg s^{-1} cm^{-2} (0.5–20 keV) for an exposure time of 10^4 ks. In the current baseline, the SFA focal plane detectors are silicon drift detectors that combine CCD-like spectral resolutions with very small dead times, and therefore are excellently suited for studies of the brightest cosmic X-ray sources at the smallest time scales.

The PFA consists of four identical X-ray telescopes that are sensitive between 2 and 8 keV, have an angular resolution better than 30″ (HPD) and a total effective area of $\sim$ 900 cm^2 at 2 keV (including the detector efficiency). The PFA features Gas Pixel Detectors (GPDs) to allow polarization measurements in the X-rays. It reaches a minimum detectable polarization (MDP) of 5% in 100 ks for a source with a Crab-like spectrum of flux 3×10^{-11} erg s^{-1} cm^{-2}. The spectral resolution is 1.1 keV at 6 keV (FWHM).

The LAD has a very large effective area of $\sim$ 3.4 m^2 at 8 keV, obtained with non-imaging silicon drift detectors, active between 2 and 30 keV with a spectral resolution of about 260 eV and collimated to a field of view of 1 degree (FWHM). The LAD and the SFA together reach an unprecedented total effective area of more than 4 m^2, compared to 0.7 m^2 for the largest flown instrument (Proportional Counter Array on the Rossi X-ray Timing Explorer; Jahoda et al., 2006).

The science payload is completed by the WFM, consisting of 6 coded-mask cameras covering 4 sr of the sky at a sensitivity of 4 mCrab for an exposure time of 1 d in the 2 to 50 keV energy range, and for a typical sensitivity of 0.2 mCrab combining 1 yr of observations outside the Galactic plane. The instrument will feature an angular resolution of a few arcminutes and will be endowed with an energy resolution of about 300 eV (FWHM). The WFM pairs the largest duty cycle of 30% for an imaging monitoring 2-30 keV device (e.g., compared to 8% for BeppoSAX-WFC; Jager et al., 1997) with the largest spectral resolution (usually about 1 keV at 6 keV).

The baseline for the observatory response time to targets of opportunity within the 50% part of the sky accessible to

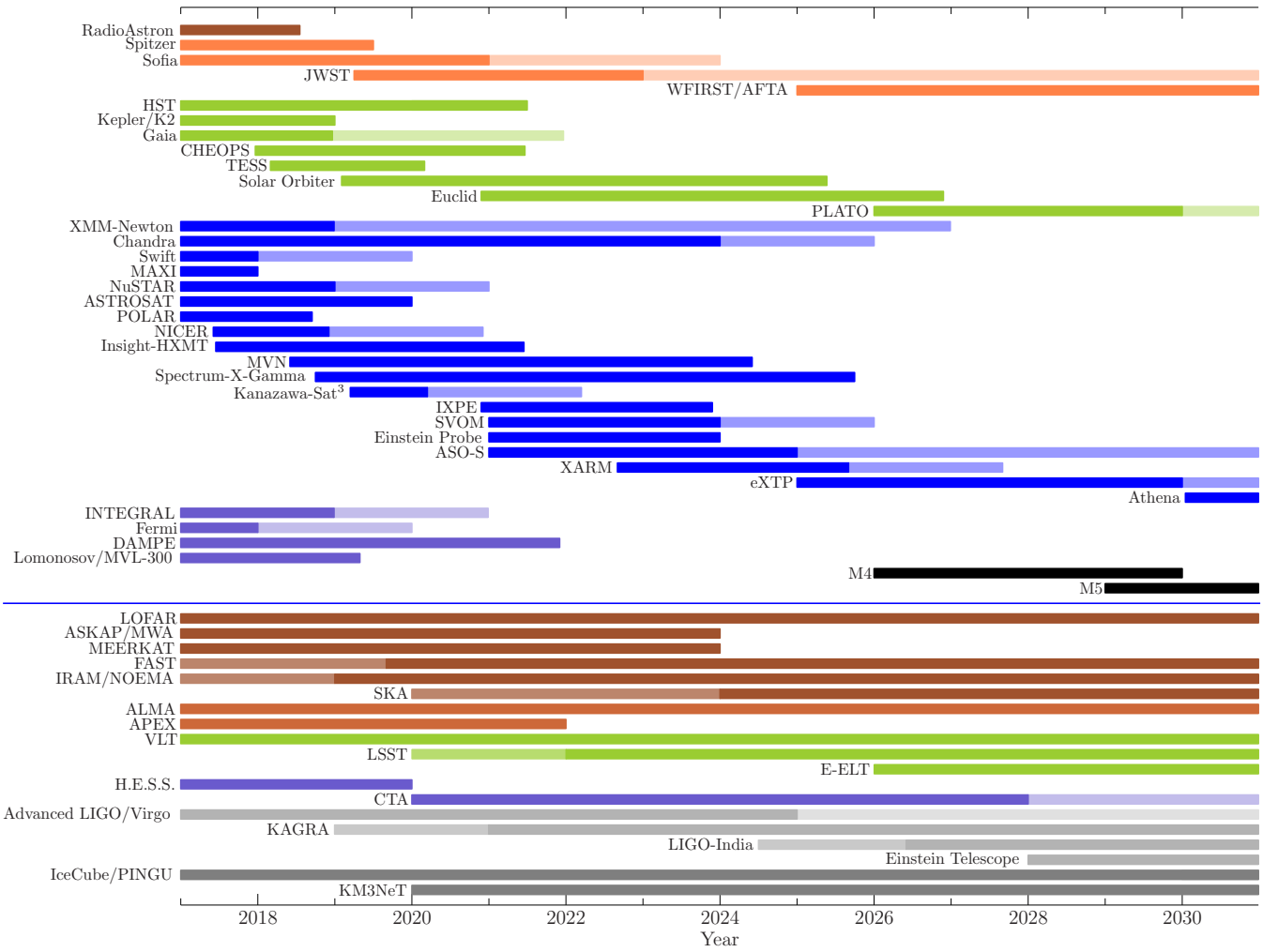

Figure 1 Multi-wavelength and multi-messenger facilities relevant to *eXTP* with timelines as known in January 2018. The thin line separates space-based (top) from ground-based (bottom) facilities. Colors indicate similar wavebands from the radio (brown) via IR (red) and optical (green) to X-rays (blue) and gamma rays (purple). Grey bands: gravitational wave and neutrino detectors. Dark colors: funded lifetime, light colors: expected lifetime, where known, independent of funding decisions. Missions might last longer.

eXTP is 4–8 hours. Depending on the the outcome of mission studies, this may improve to 1–3 hours. The launch is currently foreseen in the mid 2020s.

With a uniquely high throughput, good spectral resolution, polarimetric capability and wide sky coverage, *eXTP* is an observatory very well suited for a variety of studies complementing the core science of strong gravity (De Rosa et al., 2018), dense matter (Watts et al., 2018) and strong magnetism (Feng et al., 2018). The SFA will provide high sensitivity in a soft but wide bandpass, the PFA will provide X-ray polarimetry capability, the LAD will provide the best timing and spectroscopic studies ever for a wide range of high energy sources brighter than ~1 mCrab in the 2 to 30 keV band, and the WFM, with its unprecedented combination of field of view and imaging down to 2 keV, makes *eXTP* a discovery machine of the variable and transient X-ray sky. The WFM will reveal many new sources that need to be followed up with the SFA, PFA, LAD and other facilities. Experience from the past decades shows that newly discovered, unforeseen types of sources will provide unexpected insights into fundamental questions. The WFM will also be monitoring daily hundreds of sources, to catch unexpected events and provide long-term records of their variability and spectroscopic evolution. Several targets of the *eXTP* core program (e.g., low-mass X-ray binaries) allow one to address scientific questions beyond those related to the key mission science goals. Thus, they can be used to fulfill the observatory science goals without requiring additional exposure time. Other targets are instead uniquely observed as part of the observatory science program (e.g., accreting white dwarfs, blazars, high mass X-ray binaries), in turn providing useful comparative insights for the core science objectives.

eXTP will be a unique, powerful X-ray partner of other new large-scale multi-messenger facilities across the spec-

trum likely available in the 2020s, such as advanced gravitational wave (GW) and neutrino experiments (Advanced LIGO and Virgo, KAGRA, LIGO-India, Einstein Telescope in GWs and KM3NeT and Icecube in neutrinos), SKA and pathfinders in the radio, LSST and E-ELT in the optical, and CTA at TeV energies (Fig. 1). First *eXTP* and 4 years later Athena will be the major facilities in the X-ray regime and as such cover the hot and energetic non-thermal phenomena of any cosmic object, Athena focusing on diffuse constituents in the early Universe and *eXTP* focusing on bright, variable and transient phenomena. *eXTP* will be particularly suitable for electromagnetic (EM) studies of GW sources, an exciting field of research whose birth we witnessed through GW170817/GRB170817A (Goldstein et al., 2017; Abbott et al., 2017e). The combined EM/GW signal is expected to provide us new insights of neutron stars through their merger events, see Sect. 11 and Watts et al. (2018). Steady GW sources related to spinning neutron stars and ultracompact X-ray binaries may also be detected and identified in the coming decades, providing new diagnostics for these multi-wavelength sources that are particularly bright in the radio and X-ray bands, see Sect. 5 and Watts et al. (2018).

To explain the science case for *eXTP* as an observatory in a kaleidoscopic manner in this White Paper, material is drawn from eleven White Papers that were written for the *LOFT* study by scientists from the community at large (Amati et al., 2015; de Martino et al., 2015; Donnarumma et al., 2015; Drake et al., 2015; in 't Zand et al., 2015; Maccarone et al., 2015; Marisaldi et al., 2015; Mignani et al., 2015; Orlandini et al., 2015; Rossi et al., 2015; De Rosa et al., 2015). *LOFT* was an ESA mission concept with two of the three primary science goals of *eXTP* and larger versions of the LAD and WFM. The outstanding capabilities of all four *eXTP* instruments will enable to answer key questions that could not be addressed for many years, due to a lack of facilities with sufficient sensitivity. These questions, across a broad swath of topics, will not be answered by any other planned future X-ray facility. The *eXTP* science involves a wide range of objects, from normal stars to supermassive black holes in other galaxies. These objects have a wide range of fluxes. The wide range in capabilities of the instrument package allows one to deal with this range in fluxes: bright sources with the LAD, WFM, and PFA; faint sources mainly with the SFA. In this White Paper, the main questions are briefly discussed per category of objects, in order of approximate distance, that can be addressed with *eXTP* and that are not dealt with in the other *eXTP* White Papers on strong gravity, dense matter and strong magnetism. Due to the breadth of the science, this paper can only summarize those questions.

2 Flare stars

On the Sun, flares occur in close proximity to active regions that are characterized by boosted localized kG-strength magnetic fields (Carrington, 1859; Guo & Zhang, 2006; Güdel & Nazé, 2009; Benz & Güdel, 2010). Loops from these regions extend into the solar corona and, as the footpoints of these loops are jostled by solar convective motions, they are twisted and distorted until magnetic reconnection occurs. There is then a sudden release of energy, resulting in the acceleration of electrons and ions in these loops up to MeV energies, emitting non-thermal radio (gyrosynchrotron) and non-thermal hard X-ray emission (bremsstrahlung and Compton back scattering). These energetic particles both stream away from the Sun and down the loops where they deposit substantial amounts of energy to the lower solar atmosphere (the chromosphere), producing the observed intense hard X-ray emission at the loop footpoints (Benz & Güdel, 2010; Huang & Li, 2011). Flares are also observed on other late-type stars, with luminosities up to 10^{33} erg s^{-1} and durations from less than an hour to several days or longer (Nordon & Behar, 2008; He et al., 2015). The high temperatures result in spectral peaks in the soft to hard X-ray regime, which make them particularly visible with wide-field high duty cycle monitoring devices such as the WFM.

eXTP can contribute greatly to our understanding of stellar flares. Expanding our knowledge of stellar flaring is crucial to examining the influence of transient sources of ionizing radiation from a host star on exoplanet systems, important for habitability concerns and space weather which other worlds might experience (e.g. Segura et al., 2010). Such studies extend the solar-stellar connection in determining the extent to which solar models for conversion of magnetic energy into plasma heating, particle acceleration and mass motions apply to the more energetic stellar flares. Extrapolating from lower efficiency high-energy monitoring observatories, we estimate that *eXTP* will detect at least 35 superflares per year from stars exhibiting the extremes of magnetic activity. The anticipated source types include young stars, fully convective M dwarfs, and tidally locked active binary systems. The wide-field monitoring capability of *eXTP* will also likely enable the detection of flares from classes of stars hitherto not systematically studied for their flaring, and will be important for expanding our understanding of plasma physics processes in non-degenerate stellar environments. Four important questions that *eXTP* can address are:

- *What are the properties of the non-thermal particles responsible for the initial flare energy input?* The study of the flare distribution with energy and of their temporal behavior, e.g., spikes, oscillations, etc., will be enabled by

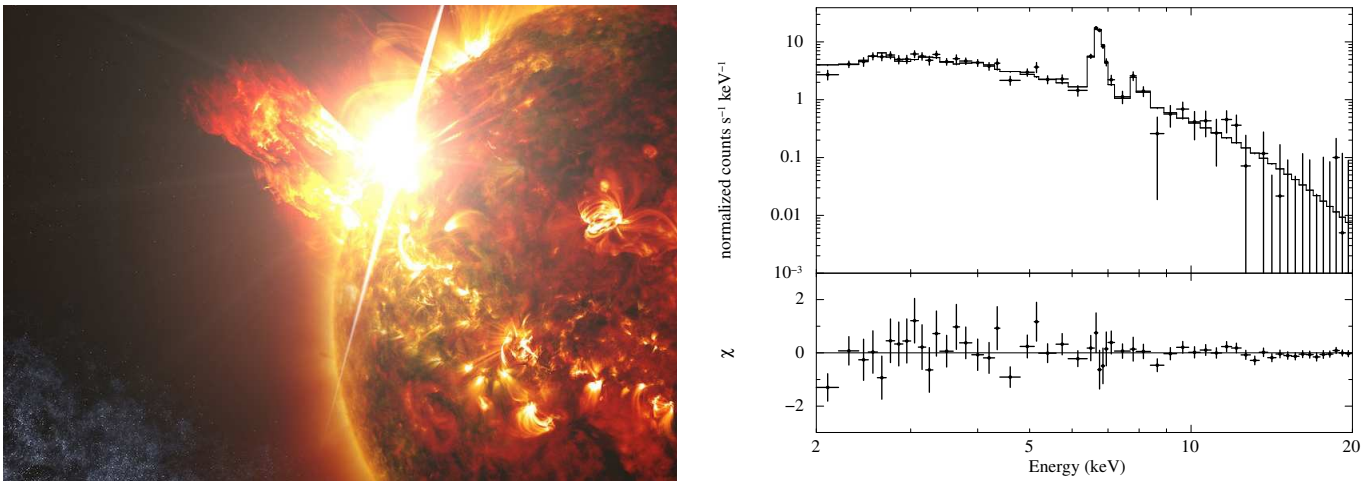

Figure 2 *Left:* artist's impression of the 2014 April 23 "superflare" of one of the stars in the wide M dwarf binary DG CVn (credit Scott Wiessinger of the NASA/GSFC Scientific Visualization Studio). *Right:* Simulated LAD spectrum of a 1000 s time segment of a flare with similar flux and spectrum to the second, slightly less powerful flare of DG CVn 3 hours after the first outburst. Notice the well-exposed He-like Fe lines at 6.7 keV and 7.9 keV which would enable an accurate coronal Fe abundance to be derived (e.g., Phillips et al., 2006, and references therein) .

eXTP's sensitive hard X-ray capability provided by the LAD, far in excess of previous missions.

- *What are the physical conditions of the thermal plasma whose emission dominates the later stages of stellar flares?* Through its soft X-ray capabilities, *eXTP* will enable us to study the variation of properties such as the temperature and elemental abundances as a function of time during flares.
- *What is the maximum energy that stellar flares can reach?* The wide-field, broad X-ray band and high-sensitivity capabilities of *eXTP* will enable us to detect the rare "superflares" that have been only sporadically detected by previous and current missions: better understanding of the prevalence of such powerful events is important both for the physics of stellar flares and for the implications of their effect on potential planets orbiting these stars (see Fig. 2).
- *What is the origin of flares from stars in nearby young associations?* *eXTP* sensitivity will allow one to detect flares from stars in nearby young associations, such as the TW Hya group, at distances up to 60 pc. As discussed by Benz & Güdel (2010), young stars with accretion disks like TW Hya are expected to have a second type of flares due to interactions between the magnetic fields of the active regions and the disk. It is an open question as to whether these flares have different properties than the better known in situ stellar flares (especially due to the very limited detections of these events in the X-rays).

3 Supernova remnants

Supernova remnants (SNRs), including pulsar wind nebulae (PWNe), are important Galactic producers of relativistic particles and emitters of diffuse X-ray synchrotron radiation (Reynolds et al., 2007; Reynolds, 2008). *eXTP* is expected to provide breakthroughs in some longstanding problems in the studies of shell SNRs and PWNe via fine measurement of the distribution of magnetic fields and polarized emission.

The strong shocks driven by supernova explosions are commonly regarded as the main factory of the cosmic rays (CRs) with energy up to 3×10^{15} eV (the so called "knee"), and accumulating evidence has also pointed to this notion (Blasi et al., 2015; Caprioli, 2015). Despite the well established theory of diffusive shock acceleration for CRs, many crucial problems in the acceleration process remain unsolved, such as the injection mechanism of particles and energy, the efficiency of acceleration, the size of the acceleration region, and the upper limit of particle energy (Hillas, 2005; Blasi et al., 2013). Clues to solve the problems can be provided by the non-thermal X-ray emission of the relativistic electrons arising from the strong shocks of SNRs.

In particular, *eXTP* will be powerful in addressing the following questions about SNRs and PWNe:

- *What effect does the orientation of injection with respect to the direction of the magnetic field have on the shock acceleration efficiency in SNRs?* In the acceleration mechanisms, it remains unclear how the orientation of injection with respect to the magnetic lines affects the acceleration efficiency ("quasi-parallel scenario" or "quasi-perpendicular scenario"; Fulbright & Reynolds, 1990). SN1006, a SNR with a bilateral-like non-thermal X-ray morphology, is an ideal example to study this problem. The most recent radio polarization observation favors the case of quasi-parallel injection (Reynoso et al., 2013). *eXTP* can resolve the X-ray structures in the SNR (30'

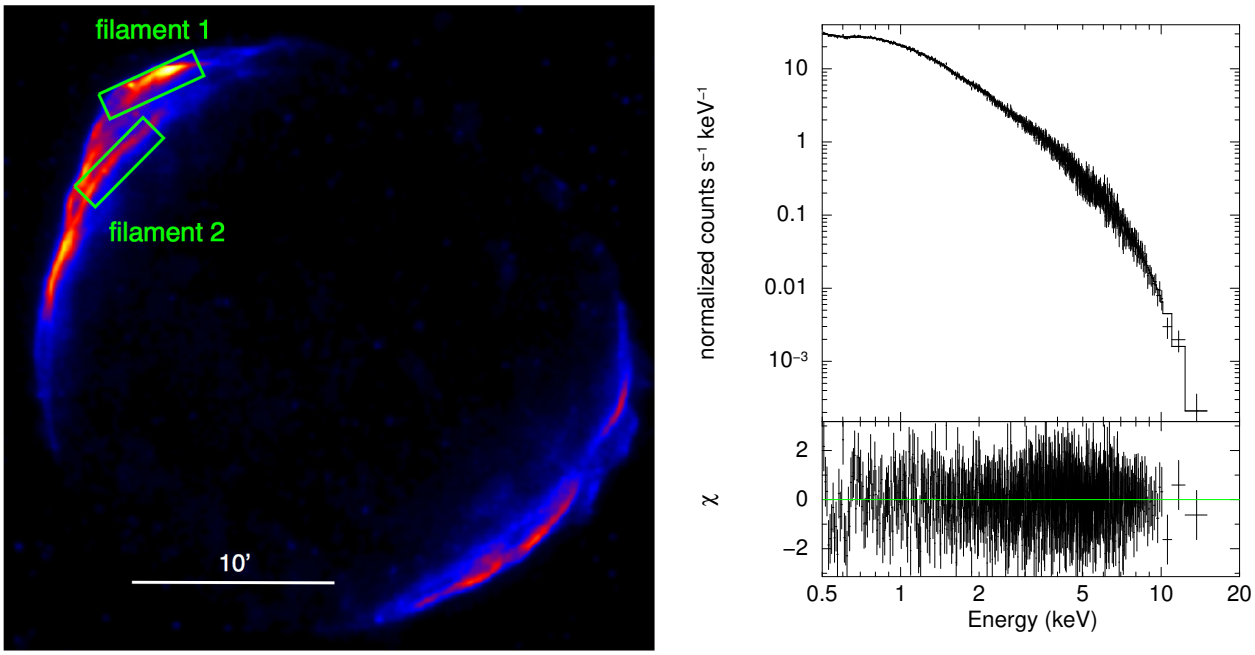

Figure 3 (Left) The 2–8 keV image of SN1006 convolved with the PFA angular resolution (15″). For the boxes around filaments 1 and 2, the polarization can be measured with accuracies of $\sigma_{\rm dop}$ = 1.8% and 2.1% and $\sigma_{\rm PA}$ = 2.9 and 3.2 deg for an exposure time of 0.5 Ms, respectively. (Right) Simulated SFA spectrum of region 'filament 1' in the northeast of SN1006 with a 10 ks observation. A model is employed of synchrotron radiation from an exponentially cutoff power-law distribution of electrons with the parameters hydrogen absorption column density $N_{\rm H}$ = 6.8×10^{20} cm^{-2}, power-law photon index of -0.57 and cut-off energy of 0.5 keV.

in diameter) and provide spatially resolved physical information for them. The PFA polarimeter can measure the polarization degree and angle in the post-shock region of SN1006 with 15" angular resolution (see Fig. 3-left). The measurement accuracy will be about 2% for the polarization degree ($\sigma_{\rm dop}$; assuming a polarization degree of 17%) and 3° for the position angle ($\sigma_{\rm PA}$) after a 0.5 Ms observation of filaments 1 and 2. With a 10 ks observation, the SFA can obtain spatially resolved spectra of the non-thermal emission of the shell (see Fig. 3-right for the simulated spectra of 'filament 1' in the northeast of the SNR). The *eXTP* polarization measurement and spectral analysis are thus expected to give a precise answer to a specific physical problem.

- *What is the intensity of the synchrotron radiation and the orientation of the magnetic field in the forward shock and, especially, the reverse shock in SNRs?* While CR acceleration has been extensively studied at the forward shocks of SNRs, how the reverse shocks accelerate CRs became an intriguing question in recent years. Using a 1 Ms *Chandra* observation towards Cas A, most of the non-thermal emission from the SNR was found in the reverse shock (Helder & Vink, 2008; Uchiyama & Aharonian, 2008). *eXTP* will be able to test this result and compare the polarization parameters between the forward and reverse shocks. With an exposure time of 2 Ms, the PFA polarimeter can measure the polarization degree and angle of 0.5′×1′ sub-structures in Cas A (4.2-6 keV) with accuracies of $\sigma_{\rm dop}$~3% and $\sigma_{\rm PA}$~10° for the forward shock (assuming a polarization degree of 10%), and $\sigma_{\rm dop}$~1.5% and $\sigma_{\rm PA}$~8° for the reverse shock (assuming a polarization degree of 5%). The spatially resolved polarization measurements with *eXTP* will provide crucial information on the magnetic field at the reverse shock where CRs are effectively accelerated.
- *What is the spatial distribution of the non-thermal X-ray emitting components with respect to that of the thermally emitting regions in SNRs?* Since the first detection in SN1006 (Koyama et al., 1995), non-thermal X-ray emission has been detected at the rims of several SNRs. This is believed to be due to synchrotron radiation of the CR electrons accelerated by the SNR shocks (e.g. Ballet, 2006).

In addition to the non-thermal X-ray dominant SNRs (such as SN1006 and RX J1713-3946) and a few young SNRs (such as Cas A and Tycho) in which non-thermal and thermal X-ray emission can be spatially/spectroscopically resolved, there are several SNRs in which potential non-thermal X-ray emission can hardly be distinguished from the thermal emission. These SNRs include N132D, G32.4+0.1, G28.6-0.1, CTB 37B, W28, G156.2+5.7, etc. (e.g. Nakamura et al., 2012). Thanks to the large collecting area of *eXTP* in the hard X-ray band, short exposures of SFA towards these SNRs can collect enough photons for

spectral analysis to clarify whether the hard X-ray emission is non-thermal. The enlarged sample of non-thermal X-ray emitting SNRs in various environments and at different ages will allow one to study the mechanism of CR electron acceleration and to constrain the leptonic emission, acceleration efficiency, magnetic field and other interstellar conditions.

- *Which are the mechanisms of amplification of the magnetic field at the SNR shocks?* Several high-energy observations of SNRs are consistent with a magnetic field at the shock far exceeding the theoretically predicted shock-compressed strength. The joint capability of *eXTP* to measure X-ray emission and polarization will allow one to test current models of amplification of magnetic fields by SNR shocks. It is believed that such shocks propagate into a generally turbulent interstellar medium (Armstrong et al., 1995). The turbulence can be pre-existing or caused by the shock itself via, e.g., a non-resonant streaming instability of cosmic-rays as first found by Bell (2004). In the former case, the density inhomogeneities traversed by the shock front are expected to produce corrugation of the shock surface; such a surface, as it propagates further, triggers differential rotation of over-densities during their shock-crossing generating vorticity, therefore amplifying the magnetic field via a small-scale dynamo process in the downstream fluid (Giacalone & Jokipii, 2007; Inoue et al., 2012; Fraschetti, 2013). The field growth is exponentially fast, as short as years or months (see, e.g., the rapid changes in hot spots brightness observed in the SNR *RXJ*1713.7 − 3496 and in Cas A; Uchiyama et al., 2007; Patnaude & Fesen, 2009), likely due to synchrotron electron cooling in a strong magnetic field.

  eXTP's polarimetric capability will be a valuable asset here in the sense that it will provide, for the first time, the polarization in those hot spots, leading to estimates of the coherence scale of the magnetic turbulence. This will be of the order of the Field length (i.e., about 0.01 pc; Field, 1965) if the vortical mechanism dominates. Indeed, the growth time scale of the magnetic turbulence is approximately equal to the ratio of the Field length to the local shock speed. As described above, a 1 Ms exposure on Cas A would allow one to measure the polarization degree (angle) with an accuracy better than 1% (3°) for the forward shock. The proposed analysis requires relatively high SNR shock speeds (not too high to have a growth time at least of a few months) colliding with dense clouds or propagating into a region with significant clumpiness. By observing the X-ray emission during the early phases of the shock/cloud collision, *eXTP* will allow one to constrain the growth time scale of the magnetic field.

- *What is the configuration of the magnetic field in PWNe and what physical insight can we infer from that?* PWNe, such as the Crab nebula, are high-energy nebulae composed of relativistic particles and magnetic fields created by the central pulsars. The energy input of pulsars, the particle acceleration at the terminal shocks, the PWN structures (including the equatorial ring and bipolar jets) and other physical properties (such as particle transport and magnetization factor) are not fully understood yet (e.g., Reynolds, 2017; Kargaltsev et al., 2015). *eXTP* can perform X-ray polarization measurements towards the Crab nebula with high spatial resolution, and obtain the detailed distribution of magnetic field and polarization degree. The PFA polarimeter can measure the polarization degree and angle of the sub-structures (15″) in the Crab nebula with a mean accuracy of about 1.7% ($\sigma_{\rm dop}$, assuming an polarization degree of 19%) and 2.6° ($\sigma_{\rm PA}$), respectively (we considered an exposure time of 10 ks). The unprecedented X-ray polarization imaging of the Crab nebula will play an important role in the study of PWNe. Another PWN worth following up with *eXTP* is MSH 15–52 which has a size of 10′ and a total flux of $\sim 5.5\times10^{-11}$ erg s^{-1}cm^{-2}. *eXTP* mapping will provide polarization accuracies of $\sigma_{\rm dop}$=2% and $\sigma_{\rm PA}$=3.7° for 10 pointings with a 300 ks exposure (assuming a photon index of -2 and polarization degree of 15%).

4 Accreting White Dwarf Binaries

White dwarfs (WDs) accreting from a companion star in a binary exhibit themselves as cataclysmic variables (CVs; e.g., review by Knigge et al., 2011). CVs represent the most common end products of close binary evolution. These binaries display a wide range of time scales in variability (from seconds-minutes up to months-years) that make them ideal laboratories for the study of accretion/ejection processes in the non-relativistic regime. Disk instabilities, the disk-jet connection and magnetic accretion are common processes occurring in a wide variety of astrophysical objects. Accreting WDs provide an excellent perspective of these phenomena. Furthermore, thermonuclear runaways giving rise to novae (e.g., review by José, 2016) have the potential to probe the accretion/ignition mechanisms, outflows and subsequent chemical enrichment of the interstellar medium, as well as to address the question of whether accretion dominates over outflow, possibly bringing the WD mass over the Chandrasekhar limit yielding type Ia supernovae. This is a key aspect for understanding Type Ia supernova progenitors. In addition, population studies of galactic X-ray sources have recently recognized a crucial role of accreting WD binaries

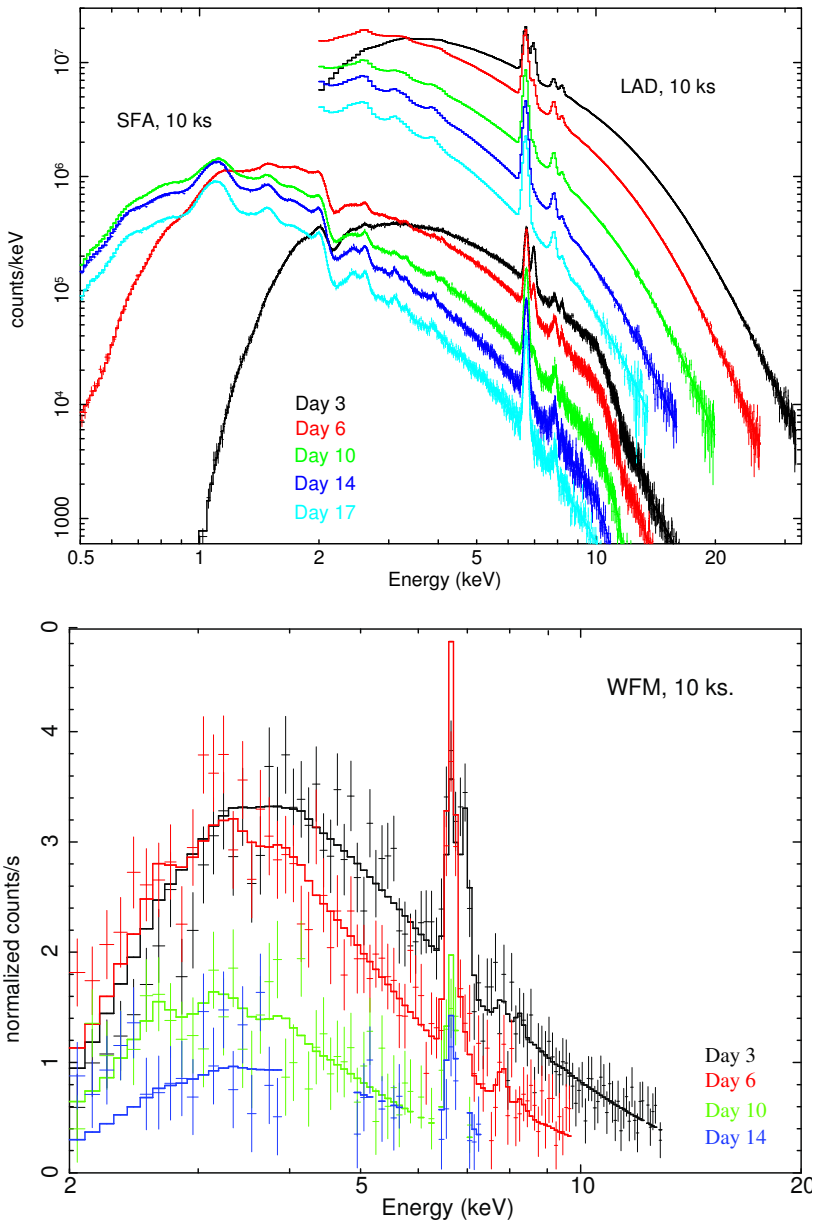

Figure 4 Simulations of the spectral evolution of the symbiotic recurrent nova RS Oph over its outburst, as seen by the LAD and SFA (upper panel) and by the WFM (lower panel). The spectra include a thermal plasma model (*mekal*) with solar abundances, evolving from kT= 8.2 keV and a flux of 3.2×10^{-9} erg s^{-1} cm^{-2} (0.5-20 keV) on day 3, down to kT= 2.5 keV and a flux of 4.3×10^{-10} erg s^{-1} cm^{-2} (0.5–20 keV) on day 17 (after Sokoloski et al., 2006). The high X-ray flux during the first 17 days would trigger the WFM in full resolution mode and a detailed study of the spectral evolution will be possible with the LAD and SFA.

in the origin of the Galactic Ridge X-ray Emission (GRXE), one of the great mysteries in X-rays (Warwick, 2014; Perez et al., 2015; Hailey et al., 2016; Hong et. al., 2016; Koyama, 2017).

The X-ray domain is crucial to understand the physical conditions close to the compact star (e.g., review by Kuulkers, 2006). Progress in many open questions is hampered by the low quiescent luminosities ($L_X \sim 10^{29-33}$ erg s^{-1}) and the unpredictability of large-scale variations that can reach luminosities as low as $\sim 10^{32} - 10^{34}$ erg s^{-1} in dwarf novae (DNe) outbursts and as high as $\sim 10^{38}$ erg s^{-1} in nova explosions. The majority of persistent, steadily nuclear-burning accreting white dwarfs thought to exist in the Milky Way, its satellites, and M 31 have yet to be detected (Di Stefano & Rappaport, 1994; Woods & Gilfanov, 2016). These "supersoft X-ray sources" are candidate Type Ia supernova progenitors, and can exhibit oscillations on very short timescales ($\lesssim 100$ s) for as yet unknown reasons (Ness et al., 2015).

The unique combination in *eXTP* of large effective area, fair spectral resolution and excellent sensitivity of the LAD

and SFA instruments, as well as the wide field of the WFM instrument, can uncover the wide range of variabilities to understand better the underlying physical processes. The three main questions that can be addressed are:

- *How does matter accrete onto white dwarfs and mix with the CO/CNe substrate?* Fast (seconds to minutes) X-ray variability, both periodic and aperiodic, allow one to trace the accretion flow close to the WD surface. In magnetic CVs, periodic coherent pulsations are a signature of magnetically funneled accretion and their spectral study allows one to infer the physical conditions of the post-shock region, the hot spot over the WD surface as well as complex absorption from pre-shock material. Furthermore, quasi-periodic oscillations (QPOs) at a mean period of a few seconds are expected to arise from shock oscillations (Wu, 2000), but so far these were only detected in a handful of systems at optical wavelengths. The high shock temperatures (~20-30 keV) imply that QPO searches need to be extended into the hard X-rays.

  In non-magnetic CVs, when accreting at high rates, a variety of low amplitude variability has been detected. DN oscillations with a period of a few seconds were found in the optical and soft X-rays, changing frequency during outburst. Slower (with a time scale of minutes) low-coherence QPOs were detected in a few systems in the hard X-rays during the decline (Warner, 2004). Their appearance is related to the transition of the boundary layer from optically thick to optically thin and thus have a great potential to infer details of boundary layer regimes. Their frequencies stay in ratio, like the low and high frequency QPOs seen in low-mass X-ray binaries. Furthermore, the presence of a break in the power spectra during quiescence can allow one to infer disk truncation (Balman & Revnivtsev, 2012). The striking similarities with X-ray binaries make CVs interesting for a unified accretion scenario.

  Peak temperatures reached during a nova explosion are constrained by the chemical abundance pattern inferred from the ejecta and do not seem to exceed 4×10^8 K, so it is unlikely that the large metallicities reported from the ejecta can be due to thermonuclear processes. Instead, mixing at the core-envelope interface is a more likely explanation. The true mixing mechanism has remained elusive for decades. Multidimensional models of the explosion suggest that mixing may result from Kelvin-Helmholtz instabilities at the core-envelope interface (e.g., Casanova et al., 2011).

  eXTP can address all this by studying selected samples of magnetic and non-magnetic systems, to detect for the first time low-amplitude fast aperiodic and periodic variabilities over the broad energy range offered by the LAD and SFA and to perform time-resolved spectroscopy.
- *How does mass ejection work in nova explosions?* Novae are, after thermonuclear supernovae, the second most luminous X-ray sources among accreting WDs with emission ranging from the very soft to the hard X-rays. The soft X-rays probe the continuous nuclear burning on the WD surface, while the hard X-rays are believed to trace the early shocks inside the ejecta and between the ejecta and the circumstellar material, as well as the onset of resumed accretion. The details of the mass outflow and the shaping and evolution of the ejected matter are still poorly known. A recent challenge is the unprecedented detection by *Fermi* LAT of high-energy gamma rays ($E > 100$ MeV) in an increasing number of novae (Ackermann et al., 2014; Cheung et al., 2016) indicating that these systems are the site of particle acceleration. This was predicted for RS Oph (Tatischeff & Hernanz, 2007), a symbiotic recurrent nova where the early strong shock between the nova ejecta and the red giant wind was traced in hard X-rays by RXTE (Sokoloski et al., 2006). In classical novae there is not a red giant wind to interact with the nova mass outflow, because the companion is a main sequence star; therefore, particle acceleration is more challenging to explain (Metzger et al., 2015). *eXTP* prompt observations of nova explosions would be crucial to better understand such processes in both nova types (see Fig. 4).

  It is very important to observe over the broadest X-ray range the spectral evolution of these explosions from the early hard X-ray onset to the later super-soft X-ray phase (Schwarz et al., 2011; Sokoloski et al., 2006). Furthermore X-ray variability and periodicities on many different time scales, from days to less than a minute are still to be understood. Short oscillations in the soft X-rays can originate from H-burning instabilities (Osborne et al., 2011) while those in the hard X-rays still remain to be explored.

  Thanks to the WFM, *eXTP* will be able to catch the early X-ray emission from bright novae to be followed-up by the SFA and LAD instruments to monitor over an unprecedented energy range the X-ray spectral evolution including the onset of hard X-ray emission and of the super-soft X-ray phase as well as to characterize for the first time fast variability over *eXTP*'s unique broad range. An example of the *eXTP* potential is shown in Fig. 4.
- *What causes DN outburst diversity and what are the conditions for disk-jet launching?* DN outbursts are believed to be due to disk instabilities but there is still lack of knowledge of what changes occur at the inner boundary layer. The boundary layer is optically thin during quiescence and becomes optically thick during outburst (Wheatley et al., 2003). Hard X-ray suppression during optical outbursts

was believed to be a general behavior. Instead, the few DNe observed so far showed great diversity and not all of them show X-ray/optical anticorrelation (Fertig et al., 2011). The understanding of what fundamental parameters divide the different regimes of the boundary layer is crucial. A further challenge is the detection of radio emission from a DN and from high mass accretion rate CVs (Körding et al., 2008, 2011; Coppejans et al., 2016) interpreted as the presence of a radio jet. CVs were believed to be unable to launch jets. It was recently shown that nova-like CVs can have optically thin inefficient accretion disk boundary layers (Balman et al., 2014), allowing the possibility of retaining sufficient energy to power jets. If this were the case, a radio/X-ray correlation, similar to that observed in neutron star and black hole binaries (Coriat et al., 2011), should be present in these systems.

eXTP can address these challenging issues by following a few DNe with adequate multi-outburst coverage through time-resolved spectroscopy and fast timing in unprecedented detail.

Thus *eXTP* will be crucial to measure the spectral and temporal properties of the poorly known hard X-ray tails in these systems and to correlate them with the soft X-ray emission. When *eXTP* is expected to be operational, wide field area surveys will have provided statistically significant samples to allow detailed investigation in coordination with ground-based optical and radio facilities foreseen in the post-2020 time frame (see Fig. 1).

5 Binary evolution

The evolution of binary stars is one of the most important and challenging problems in modern stellar astronomy. Binary evolution – even when restricted merely to the evolution of binaries with compact objects – touches on a range of key questions (Bhattacharyya & van den Heuvel, 1991; Han & Podsiadlowski, 2008; Tauris & van den Heuvel, 2006; Tauris et al., 2017): the formation of Type Ia supernovae, the formation of merging neutron stars and black holes, the rate of production of millisecond pulsars, and the production rate of a variety of classes of stars with abundance anomalies. The challenges in understanding the populations of binary stars stem from the wide range of physics that goes into them. In addition to normal stellar evolutionary processes, the following must be understood: the stability and efficiency of mass transfer, the common envelope stage, the tides and angular momentum loss mechanisms that keep systems tight (i.e., magnetic braking and circumbinary disks), the spin-up of the accreting star, irradiation effects on the donor star, the details of the supernova explosions of (ultra)stripped stars, the kicks applied to neutron stars and black holes at birth, the spin-down due to the propeller effect, possible gravitational wave emission mechanisms, and the initial parameter distributions of binary and multiple star systems.

Proper testing of theories of binary evolution must come from exploration of substantial samples of close binaries, and good estimates of their system parameters. Because most X-ray binaries, especially with black hole primaries, are transients, the ideal way to detect such objects is with all-sky monitoring. The WFM represents a major step forward in the capabilities of all-sky monitors relative to present monitors.

eXTP will make essential contributions to several major aspects of compact binary populations: the very faint X-ray transient problem (Cornelisse et al., 2002; Degenaar & Wijnands, 2010; King & Wijnands, 2006); the evolutionary link between low-mass X-ray binaries and radio millisecond pulsars; the orbital period distribution of X-ray binaries, by finding the short period systems selected against by shallower all sky monitors (Wu et al., 2010; Knevitt et al., 2014); the "mass gap" between black holes and neutron stars that has been tentatively observed in existing data (Özel et al., 2010; Kreidberg et al., 2012; Wang et al., 2016) and not observed in microlensing data (Wyrykowski et al., 2016); understanding the formation of millisecond pulsars in compact binaries (Roberts, 2013) as well as the details of their spin evolution (Haskell & Patruno, 2017).

eXTP will present a range of new opportunities to study binary stellar evolution processes. These are:

- *What are the characteristics of the population of Very Faint X-ray Binaries?* The WFM will have the necessary sensitivity and large field of view to detect flares and outbursts from the Very Faint X-ray Binaries with luminosities below 10^{36} erg s^{-1}, allowing a census of these sources across a large fraction of the Galaxy. Furthermore, the WFM's large field of view will easily pick up the rare X-ray bursts (see Sect. 6) that very faint X-ray transients exhibit if the accretor is a neutron star Cornelisse et al. (2002). By establishing a substantial sample of such objects through the wide field coverage and good sensitivity of the WFM (Maccarone et al., 2015), it should be possible to engage optical follow-up on enough of them to uncover their nature, which is still poorly understood.
- *What is the evolutionary link between low-mass X-ray binaries and radio millisecond pulsars? eXTP* will provide detailed timing studies of known low-mass and ultracompact X-ray binaries (with an orbital period of less than ~1 hr, e.g. Heinke et al., 2013; van Haaften et al., 2012) which will help us to better understand their evolutionary link to radio millisecond pulsars, such as the so-called redbacks

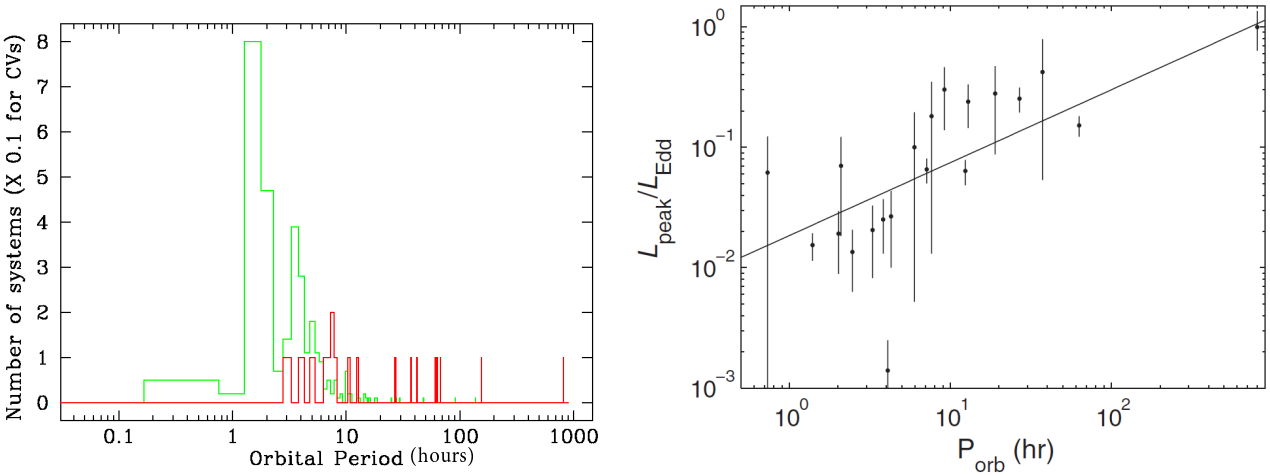

Figure 5 *(Left)* The orbital period distributions of dynamically confirmed black hole X-ray binaries (red curve), and cataclysmic variables (green curve, with the numbers multiplied by 0.1 to fit the two distributions well on the same scale), taken from the Ritter catalog (Ritter & Kolb, 2003). It is apparent that the distributions are very different from one another. Knevitt et al. (2014) find a probability of 0.0012 that these two distributions are drawn from the same parent distribution. *(Right)* Peak luminosity plotted versus orbital period for the black hole X-ray transients seen with RXTE, with a linear fit. Reproduced by permission of the AAS from Wu et al. (2010). Similar relations are also seen for cataclysmic variables (Warner, 1987; Maccarone et al., 2015) and accreting neutron stars (Wu et al., 2010).

and black widow systems (Chen et al., 2013).

A particular class of objects of interest for *eXTP* studies is that of the transitional millisecond pulsars. These represent the most direct evidence for an evolutionary link between radio millisecond pulsars and low-mass X-ray binaries, since they are observed to transit between both states. Three, possibly four, are currently known (Archibald et al., 2010; Papitto et al., 2013; Bassa et al., 2014; Bogdanov & Halpern, 2015). Two of these have relatively low luminosities in their X-ray states of 10^{33-34} erg s^{-1} while the third had an ordinary X-ray outburst as an accretion-powered millisecond pulsar peaking at 10^{36} erg s^{-1}. There may be many more of these systems. Detecting them in larger numbers, and mapping out the statistical properties (e.g., pulse and orbital periods) of the resulting sample will enable a better understanding of the binary evolution. Good candidates may be found among the so-called redbacks, which are radio millisecond pulsars in binaries with an ablated companion star of mass around 0.1 $M_{\odot}$. Observations more sensitive than with XMM-Newton and Chandra are needed to study the common flaring behavior of these systems, for instance how the pulsar behaves on short time scales, to understand better the process behind switching between X-ray and radio states. *eXTP* would make this observational progress possible.

It is worth mentioning the puzzling fact that fully recycled radio millisecond pulsars are seen in systems with orbital periods up to 200 days, but only 3 pulsar-containing low-mass X-ray binaries are known with orbital periods longer than 1 day and the neutron stars hosted are relatively slow pulsars (0.5-4.0 sec). *eXTP* will be able to probe pulsations down to the ms range with an unprecedented sensitivity, hopefully allowing one to reveal the currently missing fast rotators.

- *What is the heaviest neutron star and the lightest black hole?* *eXTP* will allow one to determine whether the orbital period distribution of black hole X-ray binaries follows the predictions of binary evolution. At the present time, the severe selection biases against black hole X-ray binaries with orbital periods less than about 4 hours (Fig. 5-left) lead to a deficit of what is likely to be the largest group of systems. Such systems are likely fainter, see Fig. 5-right. Possibly, these contain the lighter black holes, especially if one includes high-mass X-ray binaries (e.g., Lee et al., 2002). By enhancing the sample of objects for which masses can be estimated, combined with much more sensitive upcoming optical telescopes E-ELT and TMT to obtain dynamical mass estimates, *eXTP* will also help verify or refute the "mass gap" between neutron stars and black holes (Fig. 6) which has profound implications for understanding how supernovae actually explode.
- *How efficient is the process of neutron star spin up?* The process of spin-up of neutron stars in binaries (Fig. 7) can be probed in two ways: by using LAD measurements to expand the sample of neutron stars with good spin period measurements and by using the combination of WFM and LAD to discover and study the population of objects that are in the act of transitioning from low mass X-ray binaries into millisecond radio pulsars.The study of accreting neutron stars and the torques acting on them is important for

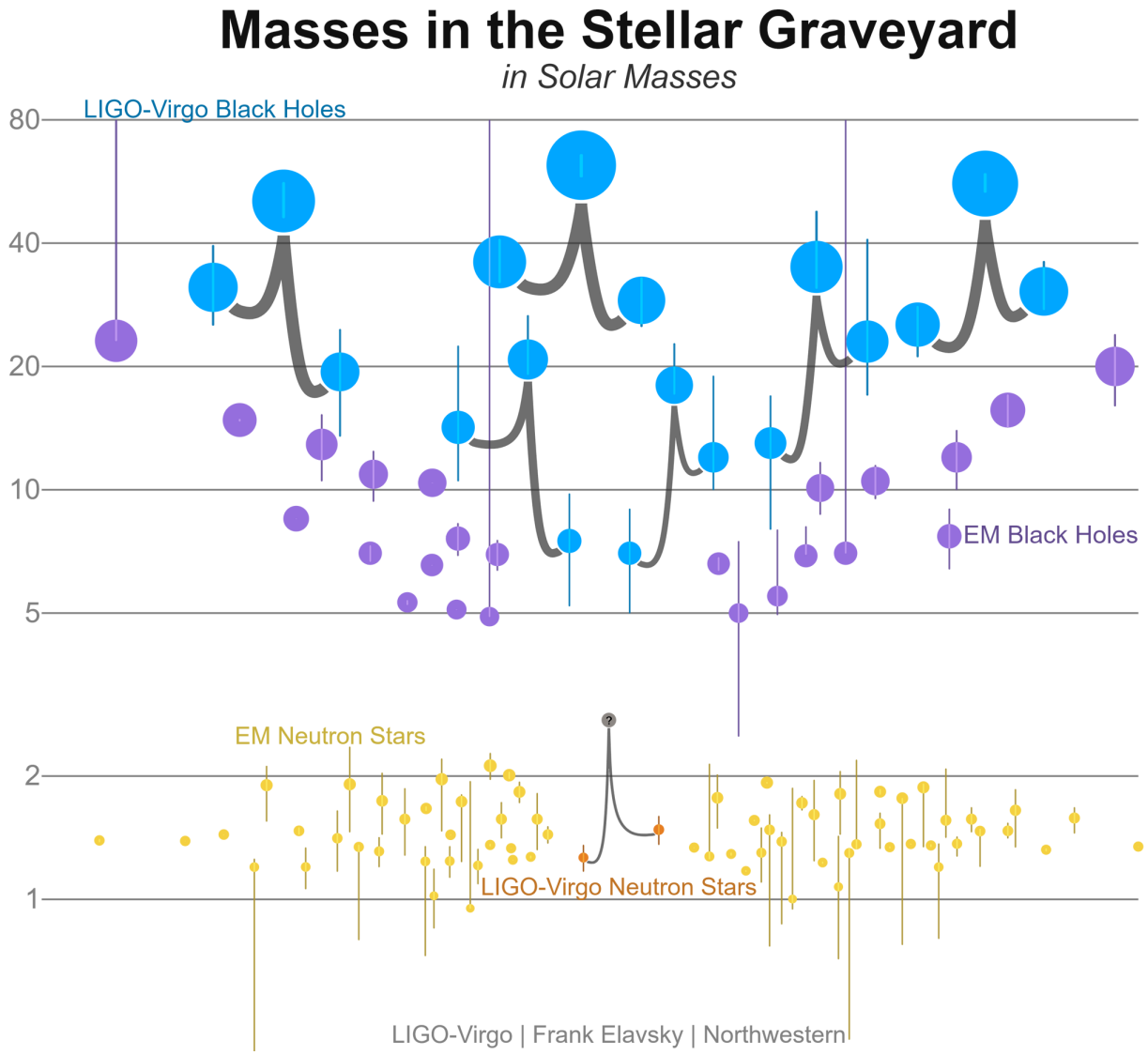

Figure 6 Graphic showing neutron star and black hole mass measurements along the vertical axes (in units of solar mass) (from Wiktorowicz et al., 2014; Özel & Freire, 2015; Casares et al., 2016), including the 16 black holes and 2 probable neutron stars in GW150914, LVT151012, GW151226, GW170104, GW170608, GW170814, GW170817 (Abbott et al., 2016a,b,c, 2017a,b,e,g). The GW measurements are indicated with curved line pointing to the merger event. There is a clear gap between 2 and 5 solar masses. Credit: Frank Elavsky, LIGO-Virgo, Northwestern University.

probing disk-magnetosphere interactions (Rappaport et al., 2004; Bozzo et al., 2009; Tauris, 2012; D'Angelo, 2017) as well as investigating continuous GW emission from the spin of asymmetric neutron stars and the prospects of detecting these sources using second (Advanced LIGO and Virgo, KAGRA, LIGO-India) or third-generation (Einstein Telescope in Europe, Cosmic Explorer in USA Abbott et al., 2015) GW detectors (Haskell et al., 2015; Haskell & Patruno, 2017). Among the promising sources for dual observations in both X-rays and gravitational waves is, for example, Sco X-1, provided its neutron star spin rate is detected (Watts et al., 2008; Abbott et al., 2017c,d) which is where *eXTP* can help through the detection of a weak pulsation. Recent calculations (Bhattacharyya & Chakrabarty, 2017) suggest that transiently accreting millisecond pulsars are promising as well.

- *How can eXTP help find sources for LISA?* The very tight X-ray binaries with orbital periods of less than one hour, the ultracompact X-ray binaries, are ideal sources to be detected in GWs induced by the orbital motion by the upcoming space-borne GW detector LISA (Nelemans et al., 2001) and LISA-like missions like TianQin (Luo et al., 2016) and TAIJI (Gong et al., 2011), missions with envisaged launch dates in the first half of the 2030s. It is expected that *eXTP* will discover a number of new X-ray binaries and may thus find additional ultracompact X-ray binaries (neutron star / white dwarf or double white dwarf binaries) that will provide important and guaranteed sources

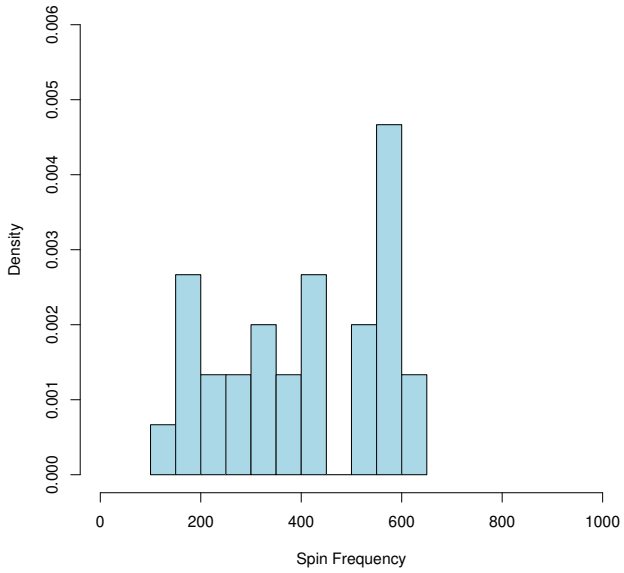

Figure 7 The spin distribution for the fastest known ($\nu > 100$ Hz) accreting neutron stars (adapted from Patruno et al., 2017).

of GWs for detection within the frequency band (~mHz) of LISA and LISA-like missions.

6 Thermonuclear X-ray bursts

While thermonuclear ('type-I') X-ray bursts are well understood as a thermonuclear runaway in the upper freshly accreted layers of a neutron star in a low-mass X-ray binary, many important questions are unanswered (e.g., Lewin et al., 1993; Strohmayer & Bildsten, 2006; in 't Zand et al., 2015; José, 2016; Galloway & Keek, 2017, see reviews by). Some of those are fundamental, pertaining to the structure of the neutron star and exotic nuclear processes, while others are related to interesting physical phenomena such as neutron star spins, convection and radiation transport under strong-gravity circumstances, the geometry of accretion and magnetic field, and unusual stellar abundances. Since *eXTP* is particularly well suited to observe short bright phenomena, it will be able to answer many of these questions.

About 20% of all bursts exhibit oscillations with a frequency very near that of the neutron stars spin (11-620 Hz). The oscillations during the burst rise can be explained by a hot spot expanding from the point of ignition (Strohmayer et al., 1997; Spitkovsky et al., 2002; Bhattacharyya & Strohmayer, 2006; Cavecchi et al., 2013; Chakraborty & Bhattacharyya, 2014; Cavecchi et al., 2015), although this still requires further study. The oscillations during the tail have not yet been explained. They could be caused by non-uniform emission during the cooling phase (e.g., because of different depths of fuel over the surface or cooling wakes; Zhang et al., 2013), but an interesting alternative involves global surface modes that may be excited by the motion of the deflagration front across the surface. This was first suggested by Heyl (2004), and further theoretical work was performed by (among others) Heyl (2005), Cumming (2005), Lee & Strohmayer (2005), Piro & Bildsten (2005) and Berkhout & Levin (2008).

The primary nuclear processes in thermonuclear bursts are the CNO cycle to burn hydrogen (β-limited 'hot' CNO cycle above $\sim 8\times10^7$ K), the triple-α process to burn helium (above several 10^8 K), the αp-process above 5×10^8 K to produce elements like Ne, Na and Mg, and the rapid proton capture process ('rp-process', above 10^9 K) to burn hydrogen into even heavier elements (e.g., Fujimoto et al., 1981; Wallace & Woosley, 1981; Woosley et al., 2005; Fisker et al., 2008; José et al., 2010). In cases of hydrogen-free helium accretion or where the β-limited CNO cycle burns all hydrogen to helium before ignition, bursts are due to ignition in the helium layer. If the CNO burning is not β-limited, it can be unstable leading to a temperature increase that subsequently ignites helium. The ignition of helium may be delayed in that regime (Peng et al., 2007; Cooper & Narayan, 2007), resulting in pure hydrogen flashes. If the CNO burning is β-limited and this burning has no time to burn away the hydrogen, helium ignition occurs in the presence of hydrogen, a situation that leads to the rp-process. Hundreds of proton-rich isotopes are produced during thermonuclear burning, particularly by the rp-process, yielding rare isotopes, whose reaction rates

have not yet been quantified in laboratories (Cyburt et al., 2016).

In the past one and a half decades, two new kinds of X-ray bursts have been discovered that are long and rare: 'superbursts' (Cornelisse et al., 2000; Kuulkers et al., 2002; Strohmayer & Brown, 2002) and 'intermediate duration bursts' (in 't Zand et al., 2005; Cumming et al., 2006) that ignite at 10^2 to 10^4 larger column depths than ordinary bursts. It has been proposed that superbursts are fueled by carbon (Cumming & Bildsten, 2001; Strohmayer & Brown, 2002), but it is unclear how the carbon can survive the rp-process or ignite (Schatz et al., 2003; in 't Zand et al., 2003; Keek et al., 2008; Schatz et al., 2014; Deibel et al., 2016) and whether superbursts are sometimes not fueled by carbon (Kuulkers et al., 2010). In contrast, it seems clear that intermediate duration bursts are fueled by helium on relatively cold neutron stars. The helium may accumulate by slow and stable burning of hydrogen into helium as described above, or by direct helium accretion at low accretion rate (e.g., in 't Zand et al., 2005; Cumming et al., 2006; Chenevez et al., 2007; Falanga et al., 2008). Due to their larger ignition depth, these long bursts can serve as probes of the thermal properties of the crust, one of the outstanding questions of neutron star research. Superbursts have a property which is intriguing in light of this dependence: they ignite sooner than expected on the basis of the measured mass accretion rate and presumed crust properties (Keek et al., 2008). It looks as though the thermal balance in the crust (determined by nuclear reactions in the crust and neutrino cooling in the core) is different from expectations (see also Schatz et al., 2014). Better measurements are needed to constrain more accurately the recurrence time and the time history of the accretion between superbursts. Currently, 26 superbursts have been detected in the last 20 years (in 't Zand et al., 2017). *eXTP* can double that in a few years.

eXTP will provide the opportunity to address the outstanding questions on X-ray bursts. A typical peak photon count rate with the LAD will be 10^5 s^{-1}. Cases with ten times as high rates will also occur. These observations will provide unprecedented detailed insight at processes with sub-ms time scales. With the anticipated observation program, it is expected that the LAD will detect at least several hundreds of X-ray bursts, with about 5 times as much effective area (i.e., 3.5 m^2) and 5 times finer spectral resolution (i.e., 260 eV) than the previous burst workhorse RXTE-PCA (Jahoda et al., 2006) and the currently operational Astrosat-LAXPC (Paul & LAXPC Team, 2009) and about 50 times as much effective area at 6 keV than the currently operational NICER (Gendreau et al., 2016). The coded-mask imaging WFM, thanks to its 4 sr field of view (one third of the sky) will detect as many as ten thousand X-ray bursts in 3 years, which is of the same order of magnitude as all bursts that were detected throughout the history of X-ray astronomy. It is clear that *eXTP* will provide a rich and novel data set on X-ray bursts. While the primary science motives for X-ray burst observations with *eXTP* are dense matter physics and gravity in the strong field regime, the secondary motives relevant to observatory science concern their fundamental understanding, in connection with nucleosynthesis, hydrodynamics, flame spreading and accretion flows (see in 't Zand et al., 2015, and reference therein). As a benefit, the outcome of these studies will help reduce the risk of any systematic errors in studies in the primary science goals.

eXTP will enable substantial advances in the understanding of thermonuclear X-ray bursts, on particularly the following questions:

- *What is the nature of burst oscillations?* Oscillations in burst tails can be studied at much better sensitivity than with previous missions and at photon energies below 2 keV it will improve on *NICER* (Gendreau et al., 2016) by having a four times larger effective area. This will increase the percentage of bursts with detected oscillations, enable the detection of shorter oscillation trains and faster frequency drifts, probe fainter amplitudes and make possible spectro-timing analyses. Thus, *eXTP* will enlarge our knowledge about burst oscillations including the possible persistence of hot spots during the burst decay and the potential roles of surface *r* and *g* modes (see Watts, 2012). Simulations of measurements of burst oscillations are provided in Fig. 8, under different model assumptions (for details, see Mahmoodifar & Strohmayer, 2016). These simulations show that *eXTP* has a diagnostic capability for the cause of burst oscillations in burst tails of a common type of X-ray bursts.
- *Is there a preferred ignition latitude on the neutron star (as expected for fast spinning neutron stars with anisotropic accretion); how do Coriolis, thermal and hydrodynamic effects combine to control flame spread?* A thermonuclear burst is expected to be ignited at one point on the neutron star. The latitude of that point may not be random, but influenced by Coriolis forces. A thermonuclear flame should subsequently spread over the stellar surface in a fashion that is determined again by rotation and by the thermal properties of the ocean in which this happens and the power of the thermonuclear flash (Spitkovsky et al., 2002; Cavecchi et al., 2013, 2015). Observational studies of the rising phases of X-ray bursts show diverse and interesting details (e.g., Maurer & Watts, 2008; Bhattacharyya & Strohmayer, 2007; Chakraborty & Bhattacharyya, 2014; in 't Zand et al., 2014). With the much larger area of the LAD, thermonuclear flame spreading can be studied at an unprecedented level of detail and in many more bursts. For

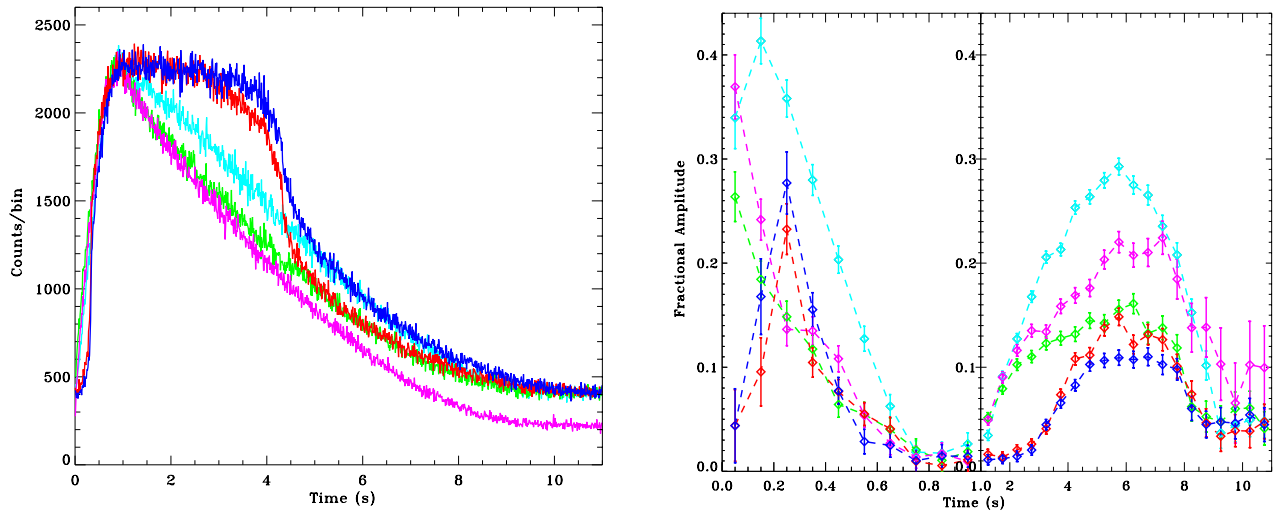

Figure 8 LAD simulations of X-ray burst oscillations for a bright burster similar to 4U 1636-536 that is bursting faithfully for at least 40 years already. For details on the model, see Mahmoodifar & Strohmayer (2016). The simulations were carried out for a neutron star of $M = 1.4 M_{\odot}$, R=10 km and ν=400 Hz, for an observer's inclination angle of $i = 70^{\circ}$ (measured from the spin vector) and with a time resolution of 0.125 ms. The left panel shows the smoothed light curves for the rise and decay of the bursts (with 11 ms time bins). The red, green and blue curves show simulated light curves for ignition co-latitudes (i.e., also measured from the spin vector) $\theta_s = 30^{\circ}, 85^{\circ}$ and 150°, respectively. The hot spot temperature is assumed to be $T_h = 3$ keV and the temperature outside the hot spot $\Delta T = 1.5$ keV lower. The flame spreading velocity goes as $v_{\rm flame} \propto 1/\cos\theta_s$, consistent with strong frictional coupling between different fuel layers (Spitkovsky et al., 2002). The magenta and cyan curves are similar to the green curve ($\theta_s = 85^{\circ}$) but with ΔT=2 keV and $v_{flame} \propto 1/\sqrt{\cos\theta_s}$, respectively, the latter referring to weak frictional coupling. The right panel shows the simulated *eXTP* measurements of the fractional oscillation amplitudes for the same models as on the left panel. Note that the fractional amplitudes are shown on an expanded scale up to $t = 1$ s (burst rise). These simulations show that *eXTP* is capable of diagnosing ignition co-latitude and frictional coupling. They also indicate (see Mahmoodifar & Strohmayer, 2016) that they can constrain the cause of the burst oscillations in burst tails.

example, simulations show (see Fig. 8) that *eXTP* measurements would enable constraining the latitude of the burst ignition.

- *What is the composition of the ashes of nuclear burning; how large is the gravitational redshift on the neutron star surface?* The SFA and LAD combined will be uniquely sensitive to details of the continuum spectrum that are induced by Compton scattering in the atmosphere and to absorption features from dredged-up nuclear ashes such as iron and nickel which may enable direct compositional studies (e.g., Bildsten et al., 2003). Low-resolution evidence for such features has been found in RXTE data of bursts that generated strongly super-Eddington nuclear powers yielding strong photospheric expansion due to radiation pressure (in 't Zand & Weinberg, 2010; Kajava et al., 2017), as predicted by Weinberg et al. (2006). Surface absorption features will be gravitationally redshifted, which can provide additional constraints on the compactness of neutron stars if rest wavelengths are identified. In this respect, the SFA would provide unique data. Most burst data currently have no coverage of sub- 2 keV photon energies. Those that do and are not susceptible to detector saturation, taken for instance with the grating spectrometers on *Chandra* and *XMM-Newton*, are of low statistical quality due to effective areas less than 150 cm^2. The SFA is anticipated to have pile-up fractions of a few percent for typical burst peak fluxes of a few Crab units and has an effective area one order of magnitude larger, at a fair spectral resolution to detect absorption edges. This provides excellent opportunity for the study of narrow spectral features, particularly absorption edges for systems at known distance with Eddington-limited bursts from a slowly rotating neutron star, like IGR J17480-2446 in the globular cluster Terzan 5 (e.g., Strohmayer & Markwardt, 2010; Linares et al., 2012).
- *What characterizes the transition from stable to unstable nuclear burning?* A long standing issue in X-ray burst research is the threshold between stable and unstable helium burning (van Paradijs et al., 1988; Cornelisse et al., 2003; Zamfir et al., 2014; Stevens et al., 2014; Keek et al., 2016; Cavecchi et al., 2017). Thermonuclear burning becomes stable once the temperature becomes so high that the temperature dependence of the energy generation rate levels off to that of the radiative cooling rate (which is proportional to T^4). More than 99% of all X-ray bursts are due to ignition of helium through 3α burning and α-captures. It is predicted that the ambient temperatures in the burning layer only become high enough ($\gtrsim 5 \times 10^8$ K) for sta-

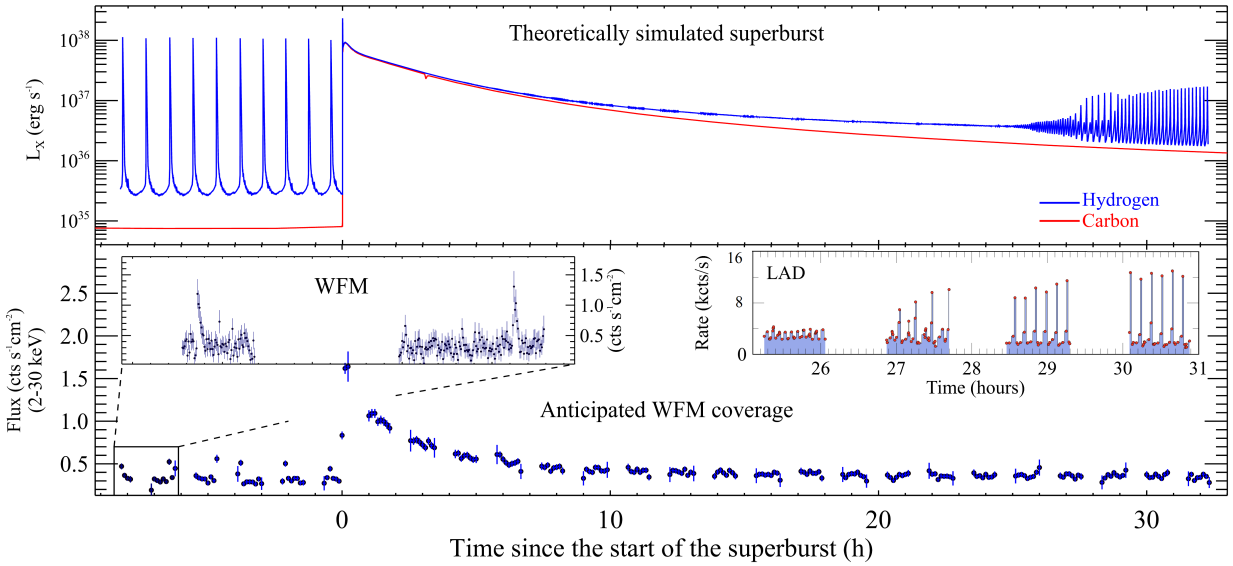

Figure 9 Simulation of the ordinary bursting behavior (blue curve) around a superburst (red curve) in a hydrogen-rich low-mass X-ray binary (from Keek et al., 2012). The superburst quenches ordinary bursts for one day after which a regime of marginal burning commences, characterized by mHz QPOs. The lower panel shows possible WFM and LAD measurements of such a superburst, if it is at 8 kpc, on-axis, placed at 45°from the Galactic center and if the accretion rate is 10% of the Eddington limit.

ble burning when the mass accretion rate is above the Eddington limit (e.g., Bildsten, 1998). However, one finds evidence of stable burning (i.e., absence of X-ray bursts and presence of mHz QPOs indicative of marginally stable burning) already at 10–50% of Eddington (e.g., Revnivtsev et al., 2001; Cornelisse et al., 2003; Heger et al., 2007; Altamirano et al., 2008; Linares et al., 2012). A different perspective on this issue may be provided by *eXTP*, by following extensively the aftermath of superbursts for about a week. The superburst is another means to increase the ambient temperatures. While the neutron star ocean cools down in the hours to days following a superburst, models predict (Keek et al., 2012) that it is possible to follow the transition from stable to unstable burning on a convenient time scale, through sensitive measurements of low-amplitude ($\sim 0.1\%$) mHz oscillations and the return of normal, initially faint, bursting activity (see Fig. 9).

- *What burns in superbursts; what determines the thermodynamic equilibrium of the crust and ocean; what determines the stability of nuclear burning; what is the nature of surface nuclear burning at low accretion rates?* WFM observations will measure more precisely the superburst recurrence time and time profile (e.g., in 't Zand et al., 2017). This will constrain the thermodynamic balance in the ocean and crust, and probe in unprecedented detail the boundary between stable and unstable thermonuclear burning (Cumming et al., 2006). WFM will accumulate large exposure times on all bursters (including yet unknown ones) and thus detect rare classes of events, such as the most powerful intermediate-duration bursts at very low accretion rates.
- *How do bursts impact and influence the surrounding accretion flow; can bursts yield insights into the underlying accretion physics?* X-ray bursts can deliver a powerful impulse to the surrounding accretion disk (e.g., review by Degenaar et al., 2018). The response of the disk to the bursts could include (i) an increase in the accretion rate due to Poynting-Robertson drag, (ii) radiative driven outflows, (iii) an increasing scale height due to X-ray heating or (iv) a combination of all these effects (Ballantyne & Everett, 2005). Unique insights into the properties of accretion disks could be obtained if this response can be measured for bursts with a wide range of durations. The response of the disk can be measured by detecting the X-ray reflection features produced by the burst interacting with the accretion flow (e.g., Ballantyne & Strohmayer, 2004; Keek et al., 2014). The SFA and LAD will be able to detect reflection features from bursts with integration times as short as a few seconds (e.g., Keek et al., 2016). As the evolution of the burst is easily measured, changes in the reflection features can directly map the changes in the accretion disk over the course of the burst.

X-ray burst science is also a high priority for the nuclear science community. X-ray bursts are unique nuclear phenomena, and identified as key problems for nuclear science in the US National Academies report NP2010 "An Assessment and Outlook for Nuclear Physics", the 2015 US Nuclear Science Long Range Plan, and the 2017 NuPECC European

Long Range Plan. Major investments in a new generation of radioactive beam accelerator facilities, in part motivated by X-ray burst science, are now being made around the world, including FRIB in the US, FAIR in Germany, and HIAF in China. New instruments such as the recoil separator SECAR at FRIB or storage rings at FAIR or Lanzhou (China) are being developed to enable nuclear reaction rate measurements for astrophysical explosions such as X-ray bursts.

With a simultaneous advance in X-ray observational capabilities through *eXTP* there is a unique opportunity to combine accurate nuclear physics and precision light curve data to determine stellar system parameters, to identify different nuclear burning regimes, to validate astrophysical 1D and 2D models, and to constrain neutron star properties. In addition, the detection of spectral features from heavy elements on the neutron star surface would be of high importance for nuclear science, as it would provide direct insight into the nuclear processes that power X-ray bursts. The Joint Institute for Nuclear Astrophysics (JINA-CEE) is now fostering the close connections between observational and nuclear science communities that are needed for nuclear physics based model predictions to guide the interpretation of observations, and for new observations to motivate nuclear experiments.

7 High-mass X-ray binaries

Massive supergiant, hypergiant, and Wolf-Rayet stars ($M \gtrsim 10\ M_{\odot}$) have the densest, fastest, and most structured winds. The radiatively accelerated outflows trigger star formation and drive the chemical enrichment and evolution of Galaxies (Kudritzki, 2002). The amount of mass lost through these winds has a large impact on the evolution of the star. The winds can give rise to an extremely variable X-ray flux when accreted onto an orbiting compact object in a high-mass X-ray binary (HMXB). The understanding of the relation between the X-ray variability and stellar wind properties has been limited so far by the lack of simultaneous large collecting area and good spectral and timing resolution.

In the past decades, observational evidence has been growing that winds of massive stars are populated by dense 'clumps'. The presence of these structures affect the mass loss rates derived from the optical spectroscopy of stellar wind features, thus leading to uncertainties in our understanding of their evolutionary paths (Puls et al., 2008). HMXBs were long considered an interesting possibility to probe clumpiness (Sako et al., 2003). As X-rays released by accretion trace the mass inflow rate to the compact object, an HMXB provides a natural in-situ probe of the physical properties of the massive star wind including its clumpiness (in 't Zand, 2005; Walter et al., 2015; Martínez et al., 2017). The so-called 'Supergiant Fast X-ray Transients' (SFXTs) form the most convincing evidence for the presence of large clumps. In X-rays, the imprint of clumps is two-fold: 1) clumps passing through the line of sight to the compact object cause (partial) obscuration of the X-ray source and display photo-electric absorption and photo-ionization; 2) clumps lead to temporarily increased accretion and X-ray flares. A number of hours-long flares displayed by the SFXTs could be convincingly associated with the accretion of dense clumps (Bozzo et al., 2011).

The compact objects in HMXBs are usually young neutron stars (typical age 10^{6-7} yr) that are known to possess strong magnetic fields ($\gtrsim 10^{12}$ G). These channel the accreting material from distances as large as $\sim 10^3$-10^4 km down to the surface of the compact object, yielding X-ray pulsations, and change the spin of the compact object. Large positive and negative accretion torques have been measured in both wind and disk-fed HMXBs on time scales between years and decades. These torques result from the yet unknown coupling between the neutron star magnetic field and the accreting material (Perna et al., 2006; Bozzo et al., 2008; Postnov et al., 2015). Extending the time scale of long-term monitoring of the behavior of pulsars in HMXBs is essential to make progress in understanding this phenomenon. Previous large field-of-view instruments provided the opportunity to monitor many X-ray pulsars in HMXBs, symbiotic X-ray binaries (SyXBs) in which the donor star is a red giant, and in intermediate systems between HMXBs and low-mass X-ray binaries. Particularly striking were the findings for GX 1+4 and 4U 1626-67: after about 15 yr (for GX 1+4) and 20 yr (for 4U 1626-67) of spin-up, both systems showed a torque reversal, which made them switch to a spin-down phase (Bildsten et al., 1997; Sahiner et al., 2012). Other systems, such as Cen X-3, Vela X-1, 4U 1907+09 and Her X-1, often showed torque reversals, sometimes superimposed on a longer term trend of either spin-down or spin-up (Bildsten et al., 1997; Sahiner et al., 2012).

At low mass inflow rates, the accretion might be inhibited completely through the onset of so-called centrifugal and/or magnetic barrier, which could drive the rapid variability observed in the SFXTs and other HMXBs (see, e.g., Bozzo et al., 2008, and references therein). The observed variability is thus often used to probe the strength of the dipolar component of the neutron star magnetic field. This also shapes the geometry of the emission region in X-ray pulsars, which, in turn, influences their observed properties. Most notably, for luminosities above the critical value $\sim 10^{37}\,\mathrm{erg\,s^{-1}}$, the local accretion rate at the neutron star polar areas might exceed the Eddington limit, leading to the formation of an extended accretion columns (Basko & Sunyaev, 1976). The

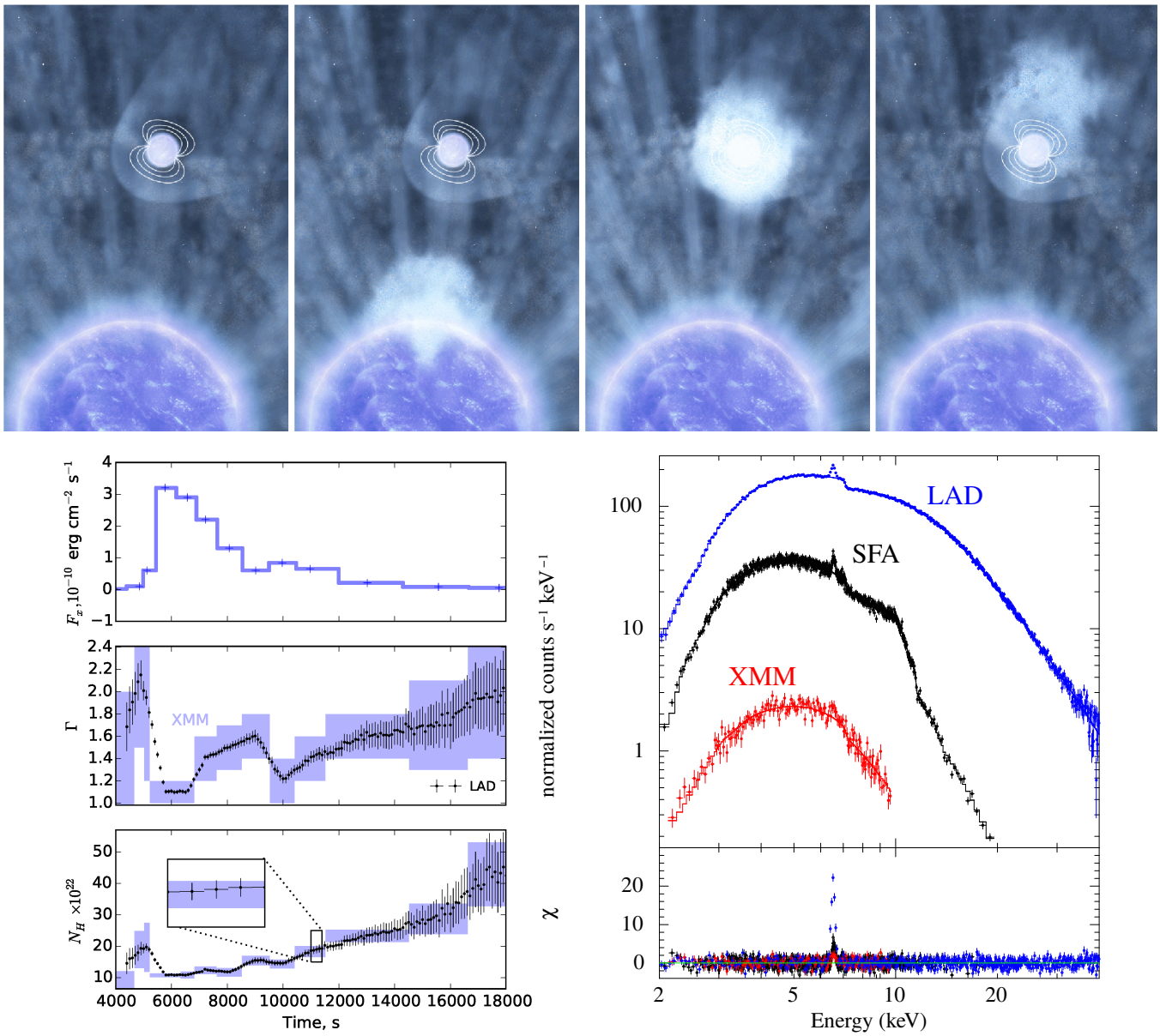

Figure 10 *Top*: Sketch of the accretion by the upper neutron star of a clump ejected by the lower supergiant star (credits: ESA). *Bottom left*: Changes in the flux and spectral parameters during the flare recorded by *XMM-Newton*, from the SFXT IGR J18410-0535 (Bozzo et al., 2011). Violet boxes represent the measurements obtained with *XMM-Newton*, while black points represent values obtained from the simulated LAD +SFA spectra with exposure times as short as 100 s. Compared to *XMM-Newton*, the dynamic process of the clump accretion can be studied in much more details and fast spectral changes can be revealed to an unprecedented accuracy (we remark also that the pile-up and dead-time free data provided by the LAD and SFA greatly reduce the uncertainties affecting the *XMM-Newton*, data obtained so far from HMXBs during bright flares). *Bottom right:* Shown, for comparison, is an example of a *XMM-Newton*, spectrum extracted in a 1 ks-long interval (source flux 3×10^{-10} erg s^{-1} cm^{-2}) during the decay from the flare shown on the left and the corresponding simulated SFA and LAD spectra. The Fe-K line at 6.5 keV, used to probe the clump material ionized by the high X-ray flux, is barely visible in *XMM-Newton*, but very prominently detected in both the SFA and LAD spectra.

transitional luminosity setting the threshold between sub- and super-critical accretion is directly related to the compactness of the neutron star and its magnetic field strength, and can thus be used to constrain these parameters. The presence of an accretion column is expected to alter dramatically the intrinsic beaming of the pulsar X-ray emission, as well as its spectral energy distribution and polarization properties (Basko & Sunyaev, 1976). Observing these changes can thus be used to obtain a direct measurement of the critical luminosity from the observations (Doroshenko et al., 2017).

The propagation of X-ray photons emerging through the strongly magnetized plasma within the neutron star emitting region also affects the observed spectra. The electron scattering cross section in strong magnetic field is largely en-

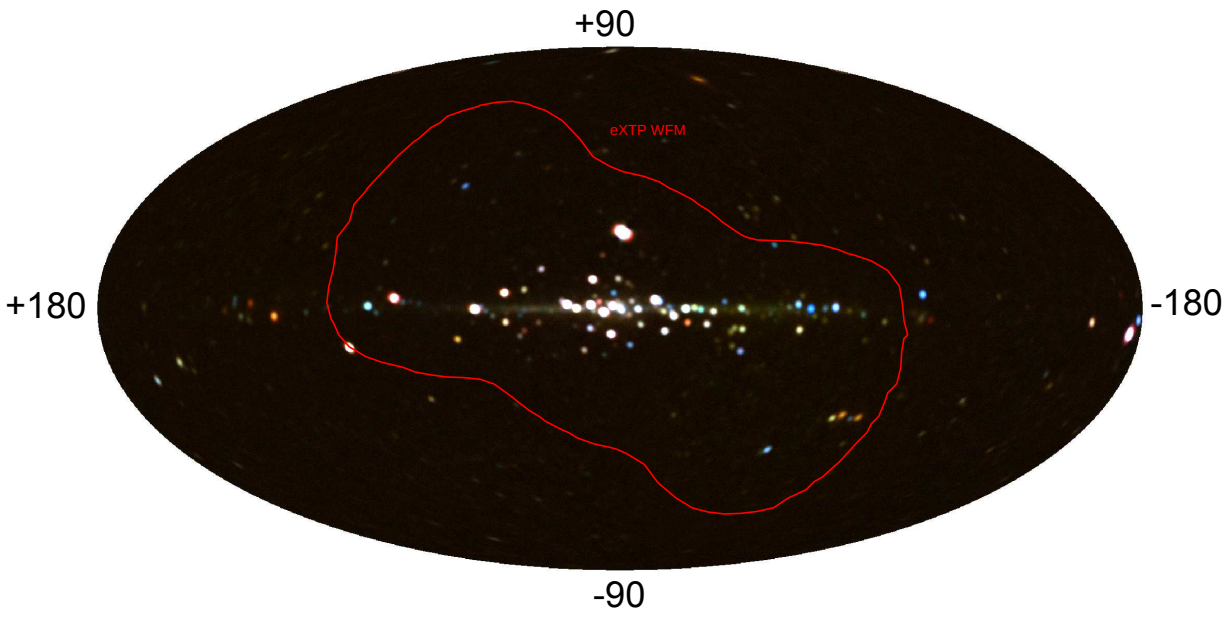

Figure 11 Comparison of WFM's field of view with the 2-20 keV map, in Galactic coordinates, of the X-ray sky as observed with MAXI (courtesy of T. Mihara, RIKEN, JAXA, and the MAXI team). The WFM will have the largest field of view and monitor simultaneously a large fraction of all currently known HMXBs and low-mass X-ray binaries.

hanced around the electrons gyro-frequency, leading to the so-called cyclotron resonance scattering features (CRSFs) often detected in the X-ray spectra of young accreting pulsars (for a recent review see, e.g., Walter et al., 2015). The scattering cross section strongly depends on the angle between the direction of the photon propagation and the magnetic field orientation. This implies that the polarization degree and angle, the X-ray continuum spectrum, and the CRSF parameters depend on pulse phase. Modeling these changes allows us to reconstruct the configuration of the magnetic field and its orientation with respect to the observer and the neutron star.

The mass accretion rate for black holes in HMXBs tends to be less variable compared to the NS case. However, most black holes in HMXB show some hard-to-soft state variability, similarly to what is observed in BH low-mass X-ray binaries. The most studied and observed BH HMXBs are Cyg X-1 (Grinberg et al., 2013, 2014, and references therein) and LMC X-3 (Wilms et al., 2001; Boyd et al., 2001). These sources proved particularly useful to "X-ray" the stellar wind of their donor stars, complementing similar studies carried out on NS HMXBs and discussed above. For example, the Galactic black hole Cyg X-1 shows a periodic modulation of the absorption column, which is due to the absorption of X-rays from the black hole in the massive stellar wind of its donor star, HDE 226868. As shown by Grinberg et al. (2015), the large scatter in individual measurements of the absorption column to the black hole can be used to study the size distribution of clumps in the stellar wind, which is of great interest for understanding the physics of the winds of massive stars (e.g., Sundqvist et al., 2013).

The instruments on-board *eXTP* will dramatically open up perspectives for research in all above mentioned fields. In particular the following questions can be addressed:

- *What are the physical properties of massive star wind structures and how do these affect the mass loss rates from these objects?* With current instruments, integration times of several hundreds to thousands of seconds are needed to get a rough estimate of clump properties and only an average picture of the clump accretion process can be obtained. Similar observations performed with the LAD and SFA onboard *eXTP* will dramatically improve our present understanding of clumpy wind accretion and winds in massive stars in general, by studying (spectral) variability on time scales as short as a few to tens of seconds (see Fig. 10). This will permit a detailed investigation of the dynamics of the clump accretion process and obtain more reliable estimates of the clump mass, radius, density, velocity, and photo-ionization state. In turn, it will improve our understanding on the mass loss rates from massive stars. As structured winds are not spherically symmetric, they are also predicted to emit polarized X-ray radiation. Measurements with the PFA can yield additional information to constrain the stellar mass loss rate (Kallman et al., 2015). The improved capabilities of all *eXTP* instruments compared to the current facilities will permit to conduct also similar studies on the SyXBs (Enoto et al., 2014), thus exploring the structure and composition of the still poorly known winds of red giants stars (which might be accel-

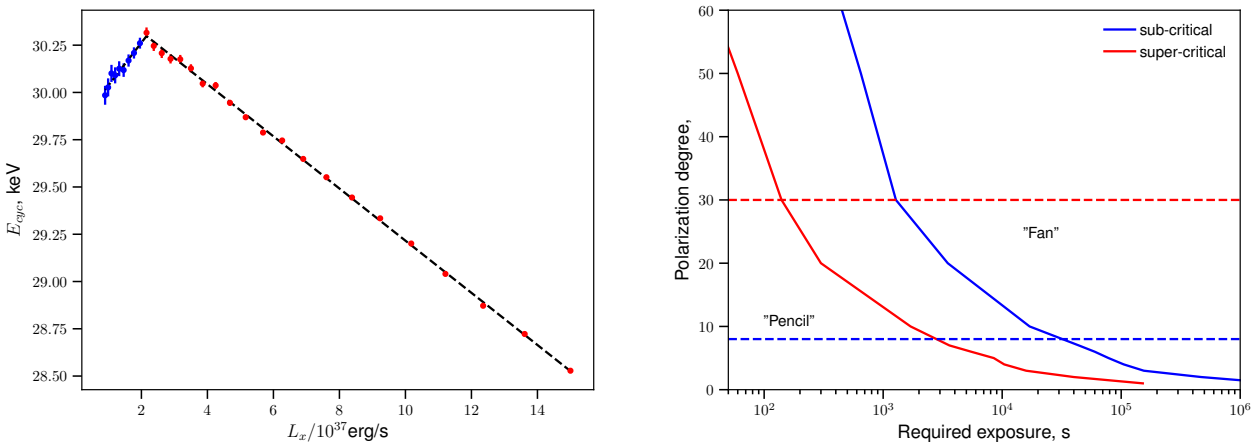

Figure 12 The combination of the LAD large effective area and energy resolution will allow us to monitor the luminosity-related changes of the observed CRSF energy in transient X-ray pulsars with unprecedented accuracy. The left panel of the figure shows a simulation of thirty 10 ks LAD observations of the X-ray pulsar V 0332+53, where a transition from super- to sub-critical accretion has been recently detected through a luminosity-dependent change of the observed CRSF energy (Doroshenko et al., 2017). *eXTP* will allow us to investigate the same effect with a much larger accuracy and to investigate changes in pulse profile shape and polarization signatures associated with similar transitions. The right panel of the figure shows the exposure required to measure the polarization of a given strength at a 3σ significance level for the typical super-critical and sub-critical fluxes observed from V 0332+53. The polarization signal strength predicted by Mészáros et al. (1988) in the two cases are also shown. The *eXTP* PFA will allow us to detect and compare the polarized emission in both the sub- and super-critical regime using relatively short exposure times, performing also studies of the dependence of the polarization properties as a function of the pulse phase .

erated through the absorption of the stellar radiation by dust grains rather than heavy ions). Finally, it is important to understand the consequences of inflated envelopes of massive giant stars (Sanyal et al., 2015) on the observational properties of HMXBs in which the donor stars are filling, or close to filling, their Roche lobes. The ability of the *eXTP* instruments (especially the WFM) to detect and monitor transient sources in a very broad range of mass accretion rates will allow us to study the spectral and temporal behavior of accreting neutron stars with strong magnetic fields. Follow-up observations exploiting the high sensitivity of the SFA will allow us to observe the so-called propeller effect in dozens of X-ray pulsars. For the sources with measured cyclotron energies it will make possible to determine the configuration of the neutron star magnetic field. Monitoring observations of long-period pulsars at low mass accretion rates will constrain the physical mechanisms regulating the interaction of plasma in a low ionization state with the neutron star strong magnetic field (Tsygankov et al., 2017).

- *What are the geometry and physical conditions within the emission region of X-ray pulsars, and their relation to the observed pulse profiles, spectra, and polarization in the X-ray band?* Pulse phase-resolved spectroscopy of accreting pulsars has been one of the main tools to diagnose their emission region properties since decades. *eXTP* will bring such investigations to an entirely new level. The large effective area of the SFA and the LAD will provide spectra and pulse profiles of unprecedented statistical quality even within comparatively short integration times. It will be possible for the first time to study the spectral and pulse profile evolution on very short timescales comparable with the spin period of the neutron star. The energy resolution of the LAD in a broad energy band will allow us to perform detailed studies of the complex CRSF shapes observed in some sources (Fürst et al., 1990), and investigate dependence of the CRSF parameters on the pulse phase, which is essential to constrain the line formation models and the emission region geometry.

  In addition, *eXTP* will provide for the first time highly complementary simultaneous X-ray polarization data. The expected strong polarization and high X-ray fluxes of the accreting pulsars make these sources a prime target for X-ray polarimetry studies. The polarization degree and angle carry information on the geometry of their emission region, magnetic field configuration, and orientation of the pulsar with respect to the observer (Mészáros et al., 1988). A major change of the observed polarization signatures is expected with the transition from the sub- to super-critical accretion, i.e. at the onset of extended accretion columns. *eXTP* observations can be used to detect such transitions and the corresponding changes in the polarization properties of X-ray pulsars, as illustrated in Fig. 12.
- *What are the mechanisms triggering torque reversals in HMXBs and what leads to orbital and super-orbital modulation of the X-ray emission from these systems?* For sys-

tems with well known distances, simultaneous measurements of fluxes and spin-rates can provide constraints on the magnetic field (Klus et al., 2014). If the pulsar magnetic field is also known from cyclotron line measurements, then the relationship between the spin rate and the luminosity can be used to constrain the neutron star parameters, probing not only accretion physics but also fundamental physics in these highly magnetized accreting systems. The WFM is a perfectly suited instrument for these studies in that it is a wide field monitor capable of simultaneously measuring the source flux and accurately determining its spin frequency. Its lower energy threshold will make it the most sensitive monitor for these types of systems that has ever flown. Measurements from the WFM of pulsed flux, unpulsed flux, frequency and frequency derivatives of accreting X-ray pulsars will contribute to the solution of the questions mentioned above, and it will also trigger target of opportunity observations with the LAD/SFA at the onset of torque reversals. Early detections of these state changes are critical to initiate early observations by the LAD/SFA in order to understand the associated spectral/timing variation As a byproduct of the monitoring observations, it will be possible to carry out detailed spectroscopic analyses as a function of orbital, superorbital and spin phase. The orbital dependence, for instance, can be used to map long-lived structures surrounding the neutron stars in these systems, like accretion wakes.

Last but not least, it is worth mentioning that many HMXBs are transient and thus the discovery of new sources or new outbursts from previously known objects in this class will greatly benefit from the capabilities of the WFM. Figure 11 shows that a large fraction of all these sources can be efficiently monitored during each single pointing of the WFM, let alone in sequential different pointings.

8 Radio-quiet active galactic nuclei

The standard model of active galactic nuclei (AGN) predicts a supermassive black hole (SMBH) surrounded by a geometrically thin, optically thick accretion disk. Like the case of X-ray binaries, the seed photons from the disk are Compton scattered into the X-ray band in a hot corona, the main difference being that the accretion disk in AGN emits at optical/UV instead of X-ray temperatures. The UV and optical seed photons from the disk are Compton scattered into the X-ray band in a hot corona above the accretion disk which produces the hard power-law spectrum extending to energies determined by the electron temperature in the hot corona, with a cut-off energy ranging from 100 to 200 keV (Perola et al., 2002; De Rosa et al., 2012; Molina et al., 2013; Marinucci et al., 2014b; Ballantyne, 2014). This primary X-ray radiation in turn illuminates the inner disk and is partly reflected towards the observer's line of sight (Haardt et al., 1994), producing a Fe-K line that will be heavily distorted, with a pronounced red wing - a clear signature of strong field gravity effects on the emitted radiation. The phenomenology of AGN is quite similar to stellar black holes accreting from companion stars in X-ray binaries, except for a difference in time scales and a difference in typical temperatures of spectral thermal components from the accretion disk that scales with the black hole mass because the size of the innermost stable circular orbit scales with mass. The inner structure in AGN is surrounded by rapidly rotating clouds of gas - the Broad Line Region (BLR). A toroidal absorber is located at a distance of a parsec from the black hole and within the Narrow Line Region (NLR) clouds. These regions contribute with additional features to the primary continuum: (1) a narrow Fe-K line at 6.4 keV produced in the BLR, in external regions of the accretion disc or in the molecular torus; (2) a reflection hump above 10 keV, due to the reprocessing of the continuum from the optically-thick medium (such as the torus and/or the accretion disk); and (3) the absorption and variable features produced in the ionized and cold material around the inner region (up to the NLR distance scales). The typical broadband spectrum as may be observed by *eXTP* is shown in Fig. 13.

Thanks to the large effective area and the CCD-class spectral resolution of the LAD and SFA, coupled with the large sky coverage of the WFM, *eXTP* will make a decisive step forward in our understanding of the inner structure of AGN. The unprecedented SFA spectral sensitivity will allow one to observe hundreds of AGN down to a flux of 10^{-13} erg s^{-1} cm^{-2} in the local universe with a very good accuracy (i.e., a signal-to-noise ratio in excess of 100). Thanks to the LAD effective area, the brightest AGN (3×10^{-11} erg s^{-1} cm^{-2}) can be characterized with extreme accuracy. Moreover, the WFM will be capable of continuous X-ray monitoring of large numbers ($\gtrsim$100) of AGN on time scales of a few days to weeks. The WFM will thus provide an essential synergy with those observatories that will, in parallel to *eXTP*, be opening up AGN time domain science on those time scales at other wavebands, for example with CTA (TeV energy domain), Meerkat/ASKAP/SKA (radio wavelengths) and LSST (optical band, see Fig. 1). Here, the focus is on three key aspects of AGN physics (related to the accretion properties and variability), which will be specifically addressed by the unique capabilities of *eXTP*:

- *What are the emitting materials around the central supermassive black hole?* The origin of the narrow Fe emission line observed in AGN is not completely clear, while this is a fundamental piece of information about the SMBH cen-

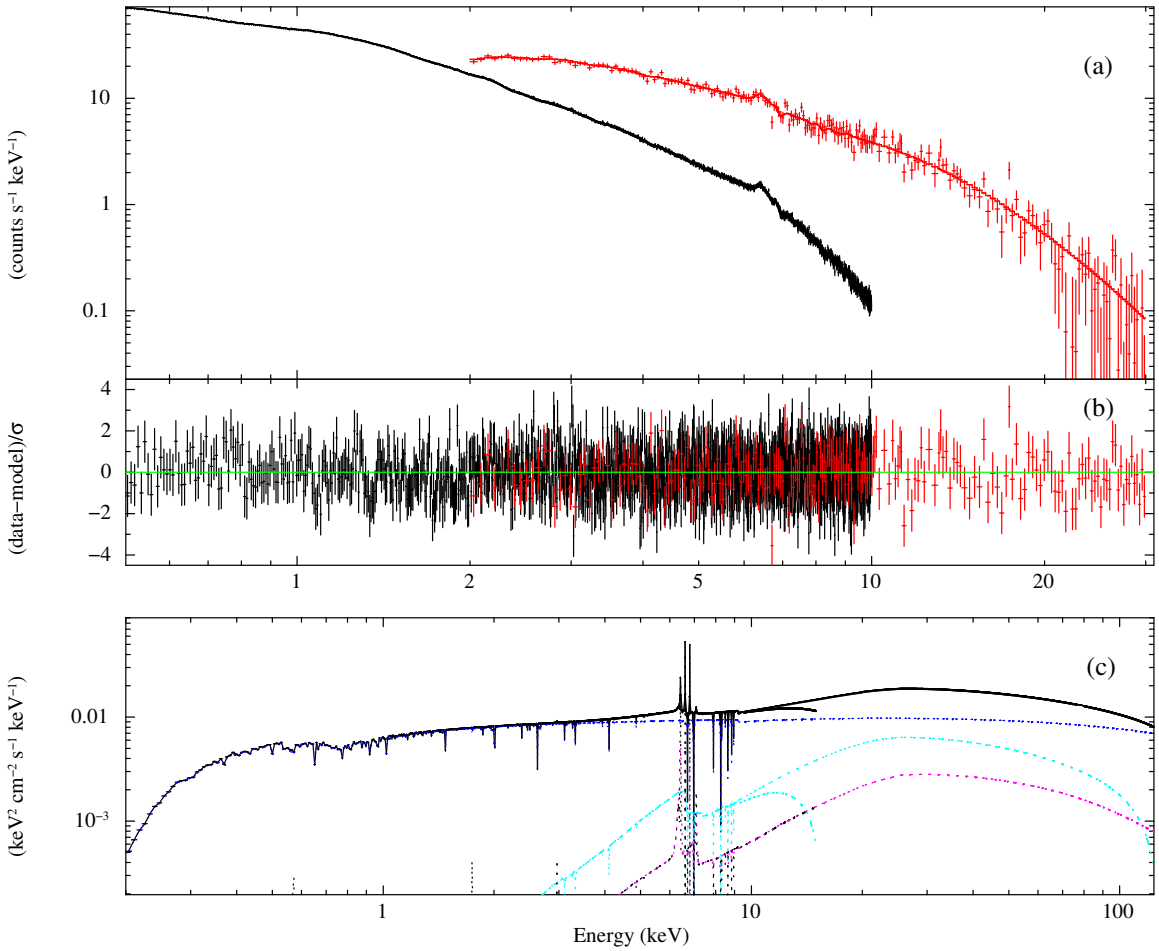

Figure 13 Panel a: *eXTP* (SFA in black, LAD in red) spectrum. Panel b: residuals as obtained by a 100 ks integration of a bright 1 mCrab AGN composed of: the continuum, three components of ionized absorbers, the cold reflection and narrow Fe line Kα, Fe Kβ and Ni Kα, the ionized lines FeXXV and FeXXVI and the blurred ionized reflection component (black hole spin $a = 0.7$). The model complexity we used for the simulation is similar to the case of the AGN SWIFT J2127.4+5654 (Marinucci et al., 2014a; Miniutti et al., 2007) and is shown in panel c where separate spectral components are indicated with different colors (in blue the primary cut-off power–law, in cyan the blurred reflection component originated in the innermost regions nearby the central BH and in magenta the contribution of the a cold reflection component originated in a medium distant from the central BH.

tral engine and its environment. The width of the line is less than few thousand km/s (in terms of full width at half maximum; Yaqoob & Padmanabhan, 2004) and suggests an origin within the BLR or the putative molecular torus (at pc scale) or within the BLR closer to the BH. A powerful method to study the origin of the narrow Fe line is to measure the time lag between the variation of the continuum and the line (Blandford & McKee, 1982). The reverberation mapping methodology is used with the optical and UV broad emission lines with great success (Peterson et al., 2004) and, recently, in X-rays to investigate the origin of the broad Fe line (Fabian et al., 2009; Uttley et al., 2014). However, the uncertainties on the Fe line flux (about 10%) and the low sampling frequency of the X-ray continuum, prevent us applying this method to a large sample of AGN, especially on the daily time scale expected for a BLR origin (Markowitz et al., 2009; Chiang et al., 2000; Liu et al., 2010). *eXTP* will allow one, for the first time, to perform X-ray reverberation of the narrow core and broad component (see the *eXTP* white paper on strong gravity; De Rosa et al., 2018) of the Fe line with a single mission.

The very large field of view of the WFM is a powerful tool to monitor the continuum intensity of virtually all the sources in the sky. To demonstrate the unique capabilities of the WFM we used the 1-year exposure sky map shown in Fig. 14 as a good approximation of the adopted pointing strategy. The WFM can produce continuous light curves with daily 3σ detections for bright sources (i.e., brighter than $\sim 1 \times 10^{-10}$ erg s^{-1} cm^{-2} in the 7–50 keV band, i.e., above the Fe K edge). Weaker objects ($\sim 5 \times 10^{-11}$ erg s^{-1} cm^{-2}) will be detectable in weekly exposures. These time scales are perfectly suited for the narrow Fe line reverberation analysis, since the expected time scales are from days to weeks to years (Markowitz et al.,

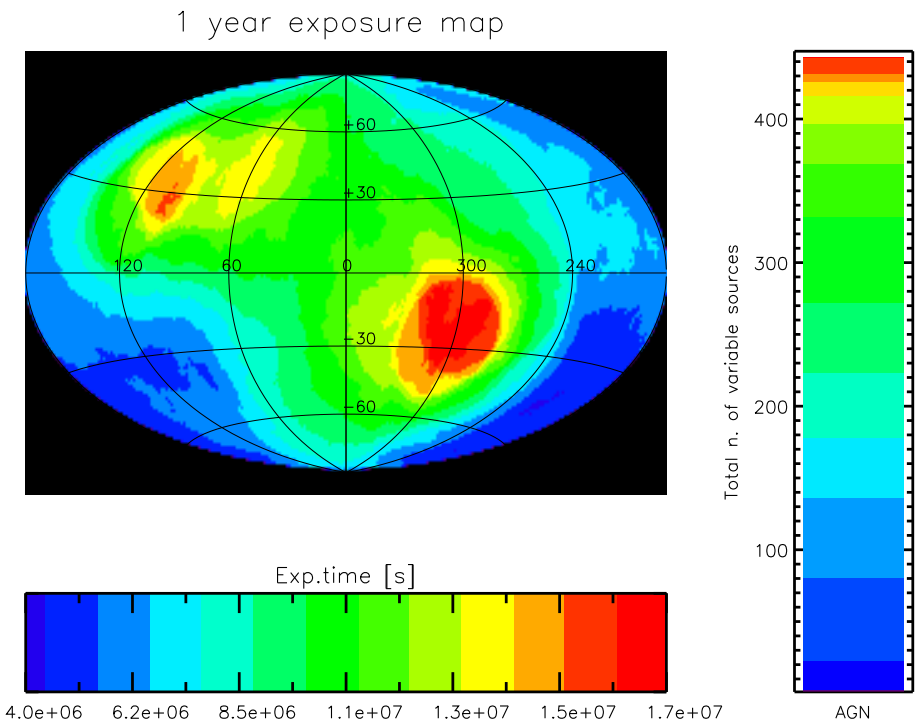

Figure 14 Number of AGN per 4π sr as a function of the position in the sky that are bright enough to be accessible to the WFM for studies of X-ray variability. For these sources, a light curve with at least 10 time bins in a 1-year period can be built, achieving in each bin a signal-to-noise ratio of at least 3. The lateral bar reports the total number of variable AGN observed on the sky, assuming an example of a 1-yr pointing plan. Only regions of the sky covered with more than 10 cm^2 of net detector area have been considered.

2003a), depending on the location and geometry of the material and the intrinsic variability of the sources (therefore, on the black hole mass and the accretion rate). At the same time, the large area available with the SFA and LAD will allow one to perform well-sampled (weekly to monthly) monitoring of the Fe-K line and Compton reflection component with short targeted observations. The CCD-class energy resolution will easily allow one to disentangle the broad Fe line component from the narrow core. In fact, in only 1 ks a narrow Fe line of equivalent width 100 eV can be recovered with an uncertainty of 1-2% for bright sources ($\sim 1\times10^{-10}$ erg s^{-1} cm^{-2} with $\sim 10^3$ SFA plus LAD counts in the line). The same uncertainties can be recovered for weaker sources ($\sim 5\times10^{-11}$ erg s^{-1} cm^{-2}) with 5 ks exposures. Thanks to the broad bandpass of the LAD, *eXTP* will be able to recover the reflection continuum with 10% accuracy in a 1 ks exposure for the brightest sources ($\sim 1\times10^{-10}$ erg s^{-1} cm^{-2}). This measurement, together with the WFM daily monitoring of the continuum above 7 keV (even with a low signal-to-noise ratio), will be a instrumental in identifying the origin of the narrow distant reflection components in AGN.

- *What are the absorbing regions in the environment of supermassive black holes, from kpc to sub-pc scale?* There is strong evidence of at least three absorption components on very different scales: on scales of hundreds of parsecs, on the parsec scale, and within the dust sublimation radius, on sub-parsec scale (e.g., Liu et al., 2010; Bianchi et al., 2012; De Rosa et al., 2012). The most effective way to estimate the distance of the absorber is by means of the analysis of the variability of its column density. In particular, rapid (from a few hours to a few days) $N_{\rm H}$ variability has been observed in most bright AGN in the local Universe (Torricelli-Ciamponi et al., 2014; Maiolino et al., 2010; Risaliti et al., 2013; Sanfrutos et al., 2013; Walton et al., 2014; Markowitz et al., 2003c; Rivers et al., 2015), suggesting that obscuration in X-rays could due, at least in part, to BLR clouds or in the the inner regions of infrared-emitting dusty tori. These observations with *XMM-Newton* and *NuSTAR* have achieved a precision for the covering factor of ~5–10%. Detailed simulations show that such a measurement (assuming the same observed fluxes) will be obtained with *eXTP* with significantly higher precision (1-2%), on even shorter time scales (few ks instead of ~100 ks). This would allow, for the first time, an extensive study of X-ray eclipses, which are frequently seen in local bright AGN (e.g., Markowitz et al., 2014). Following the time evolution of the column den-

sity and of the covering factor over timescales of a few ks will provide unprecedented information on the structure, distance and kinematics of the obscuring clouds. In particular, close to the lower end of the BH mass range in AGN, with a single 100 ks observation it will be possible to fully characterize the circumnuclear absorbing medium by sampling eclipsing events from multiple clouds (e.g., Nardini & Risaliti, 2011). which is now precluded by the short timescales involved. Moreover, the broad-band energy range offered by *eXTP* will allow one to explore in detail also those clouds with larger column densities in Compton thick AGN, whose variability mostly affects the spectrum at high energies.

- *How does the central engine produce the observed variability?* Our knowledge of the X-ray variability in AGN has advanced substantially in the last 15 years, thanks mainly to monitoring campaigns with RXTE and day-long *XMM-Newton* observations of a few X-ray bright AGN (Markowitz et al., 2003b; McHardy et al., 2004; Arévalo et al., 2006; Papadakis et al., 2002; González-Martín & Vaughan, 2012). AGN show red noise in their power spectral density functions (PSD) with a power law that decreases at high frequencies as a power law with index -2. Below some characteristic frequency the PSDs flatten and the break frequencies scale approximately inversely with the BH mass, from BH X-ray binaries to AGN (McHardy et al., 2006). These characteristic frequencies seem linked to both the BH mass and the properties of the accretion flow. Although all the relevant accretion disk time scales depend on the mass of the central object, only a few of them may depend (indirectly) on the accretion rate as well. So far, our knowledge is based on the power-spectral analysis of a few objects. A substantial improvement of the analysis of X-ray variability in AGN would be possible by avoiding the problems introduced by large statistical noise and irregular time sampling. The WFM plays a crucial role in our understanding of the X-ray variability in AGN. The WFM will survey large areas of the sky, allowing one to study long-term X-ray variability of bright/nearby AGN. Using the AGN number counts observed by previous missions, we computed the number density of sources that will be accessible to *eXTP* in each region of the sky (assuming an average AGN spectrum and Galactic absorption). Using the typical AGN flux distribution, we derived the number of sources that are bright enough to build a light curve with a worst resolution of 1 month at signal-to-noise ratio of 3. Fig. 14 shows the number density map of AGN that fulfill these criteria. Allevato et al. (2013) demonstrated that it is possible to retrieve the intrinsic variability (within a factor of 2) even when using sparse light curves with low signal-to-noise ratio, such as the ones expected here for most of the faint AGN population in the WFM sample. Depending on the exact monitoring pattern, much smaller uncertainties are expected for the brightest 20 sources. The WFM, even in its first year of operations, is expected to return light curves with at least 10 data points per year for several *hundreds of variable AGN*, allowing both individual (for the brightest) and ensemble studies of AGN variability on long (monthly) time scales. One will therefore be able to determine accurately the *intrinsic* variability amplitude (on long time scales) for hundreds of AGN and study the variability-luminosity relation with an unprecedented accuracy. This relation will then be compared with similar relations for AGN at higher redshifts (see, e.g., that derived from the *Chandra* Deep Field-South survey; Yang et al., 2016), obtained, however, with much higher statistical uncertainties, due to the limited sample size, that prevent us to probe effectively the luminosity, redshift and timescale dependence of the intrinsic AGN variability) (e.g., Paolillo et al., 2017).

9 Radio-loud active galactic nuclei

eXTP is planned in the same time frame as other observatories that are opening up a window to short time scale variability for AGN, such as the Cherenkov Telescope Array (CTA) at TeV energies and the Square Kilometer Array (SKA) and Atacama Large Millimeter Array (ALMA) in the radio and (sub-)mm bands, respectively (see Fig. 1). This offers a unique opportunity to interpret short time scale variability and connect accretion and jet physics in radio-loud AGN.

eXTP will be able to follow up a large number of AGN. We estimate this to be a few thousand with SFA and a few hundred simultaneously with the LAD. These numbers are derived from the 30–50 keV $\log N - \log S$ reported in Giommi & Padovani (2015), after applying a flux rescaling to match the LAD and SFA energy bands. This extrapolation is well justified by the fact that a hard X-ray survey preferentially selects Flat Spectrum Radio Quasars and low energy peaked BL Lacs due to the hardness of their X-ray spectra, which are generally well described by a single power law in this entire energy range. In addition, the WFM can provide monitoring of bright AGN on time scales of days to weeks thanks to its large sky coverage.

Among the radio-loud AGN, blazars are certainly the most promising in the era of the time domain astronomy. They are among the most powerful persistent (Urry & Padovani, 1995) cosmic sources, able to release (apparent) luminosities in excess of $10^{48}\,\mathrm{erg\,s^{-1}}$ over the entire EM spectrum, from

the radio to the very high energy γ-ray band. This intense non-thermal emission is produced within a relativistic (bulk Lorentz factor Γ = 10–20) jet pointing toward the Earth. Relativistic effects lead to the beaming of the radiation within a narrow cone of semi aperture $\sim 1/\Gamma$ rad with strong apparent amplification of the luminosity and shortening of the variability time scales in the cases in which (as in blazars) the jet is closely aligned to the line of sight.

Blazars come in two flavors: those that show optical broad emission lines (typically observed in quasars that are called Flat Spectrum Radio Quasars or FSRQs) and those that in general display rather weak or even absent emission lines, collectively grouped in the BL Lac object class. The latter generally show the most extreme variability, with variations as fast as a few minutes, and the most energetic photons (above 100 GeV).

The conventional scenario (e.g., Ghisellini & Tavecchio, 2009) foresees a single portion of the jet dominating the overall emission, at least during high activity states. However, this simple idea has recently been challenged by the observation of very fast (minutes) variability, which requires the existence of very compact emission sites. The most extreme example is PKS 2155−304, which experienced two exceptional flares in 2006 - with a recorded luminosity of the order of several times 10^{47} erg s^{-1} - on top of which events with rise times of ∼100 s have been detected. Even assuming that these strong events originated in very compact emission regions, the physical conditions should be rather extreme and Lorentz factors of $\Gamma \sim$ 50–100 seem unavoidable (Begelman et al., 2008). Physical mechanisms possibly triggering the formation of these compact emission regions include magnetic reconnection events (Giannios, 2013) and relativistic turbulence (Narayan & Piran, 2012; Marscher, 2014).

Alternatively, narrow beams of electrons can attain ultra-relativistic energies ($\Gamma \sim 10^6$) in the black hole vicinity through processes involving the black hole magnetosphere (Rieger & Aharonian, 2008; Ghisellini et al., 2009). In this case, it is expected that the emission shows up only in the high energy γ-ray region, giving no signals at lower frequencies (thus resembling the case of the so-called "orphan" flares; different from the simultaneous X-ray and TeV flaring observed from PKS 2155−304 in 2006).

eXTP can address the following questions with regards to radio-loud AGN:

- *What causes the fast γ-ray flares?* Until now, ultra-fast variability has been recorded only in the γ-ray band, especially at TeV energies, at which the Cherenkov arrays are characterized by gigantic collection areas, required to probe such short time scales. Current instruments do not provide an analogous sensitivity in the key X-ray band, at which the low energy component of TeV emitting BL Lacs (the so-called HBLs) peaks and thus it is not possible to study potential ultra-fast variability events at these frequencies. Moreover, such events appear to be quite rare, with a duty cycle of less than 1%. Therefore, monitoring of the sky is required to catch these events.

  The LAD, thanks to its timing capability, will allow one to detect the X-ray counterpart of the very fast variability observed at TeV energies for 2–10 keV fluxes above 2×10^{-11} erg s^{-1} cm^{-2}, shedding light on the nature of the X-TeV connection in HBLs (Kang et al., 2012). Moreover, *eXTP* polarimetric measurements of HBLs will constrain the nature of the electron population(s) responsible for the X-ray emission, providing us with the magnetic field orientation and its change during the flaring activity as compared with the average emission. In these blazars, the polarimeter energy band will cover the region of the synchrotron peak, where flux and polarization degree demand sub-daily integration times. If one assumes a 2–10 keV flux of 2×10^{-10} erg s^{-1} cm^{-2}, one can measure a minimum detectable polarization of ∼ 10% in 5 ks with the PFA. This value is in the range of polarization measurements for synchrotron emission as derived from optical measurements (between 3% and 30%). A highly ordered magnetic field would imply higher polarization degrees. In this respect, *eXTP* will be able to probe the evolution of the magnetic field lines and their role in powering fast variations as detected by the LAD (flare rise over 100 s as detected in the TeV range).
- *What accelerates highly energetic electrons?* A further potential of *eXTP* in the study of HBLs is measuring the change in spectral curvature of their synchrotron spectra which will enable a direct study of the mechanism of acceleration of highly energetic electrons. These studies will benefit from the simultaneous observations of the LAD and SFA that provide the broad band coverage (0.5–30 keV) of the synchrotron emission.
- *Where is the high-energy dissipation region?* The SFA sensitivity is very promising for the study of FSRQs with a 0.5-10 keV flux $\gtrsim 2 \times 10^{-13}$ erg s^{-1} cm^{-2}. For these objects, *eXTP* will probe the rise of the inverse Compton (IC) emission whereas new generation radio and (sub-)mm instruments will provide excellent timing capabilities to study short time-scale correlations with the synchrotron spectral domain. The nature of the photon seeds for the IC emission responsible for the high-energy emission is still strongly debated. Tight constraints are expected to come from the investigation of time scales of variability and polarimetry. In this respect, the SFA will be crucial in a multi-frequency context providing: a) temporal inves-

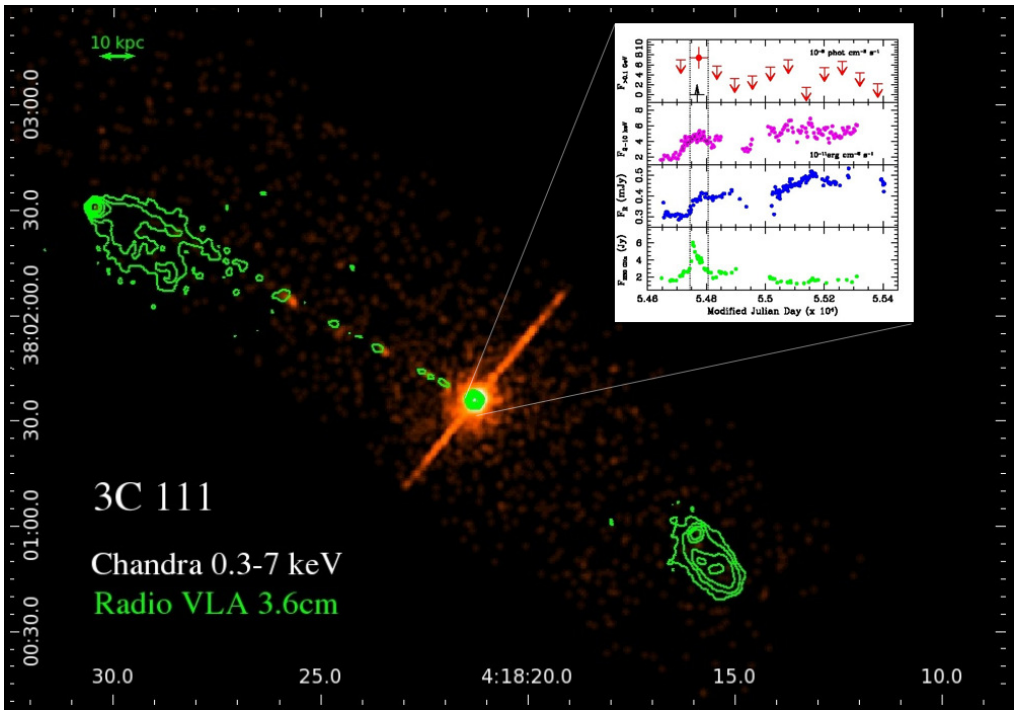

Figure 15 *Chandra* 0.3–7 keV image of the FRII radio galaxy 3C 111 with 3.6 cm radio contours overlayed (Leahy et al., 1997). In the inset the multi-wavelength light curve from mm to γ-rays is shown (from Grandi et al., 2012, reproduced by permission of the AAS). The simultaneity of the flare is impressive: the core luminosity was increasing from millimeter to X-ray frequencies exactly when the greatest flux of γ-ray photons occurred. This is a clear indication of the cospatiality of the event. The outburst of photons is directly connected to the ejection of a new radio knot (the time of the ejection is indicated by the black arrow).

tigation on second time scales; b) spectral trend investigation on minute time scales. With CTA, this may provide a multi-wavelength perspective to understand better the rapid (unexpected) TeV emission recently detected in some FSRQs. The WFM will provide not only an excellent trigger for both CTA and (sub-)mm observatories but also long-term monitoring of a large sample of blazars.

Moreover, polarimetric measurements performed in the 2–10 keV band, in comparison with polarization at lower frequencies, represent a powerful tool to solve the long-standing problem of the origin of the seed photons and therefore constrain the high-energy dissipation region for the brightest objects and flares on daily time scale. The average X-ray fluxes of FSRQs are actually much lower than those of high synchrotron-peak blazars (in the range 10^{-12}-10^{-11} erg cm^{-2} s^{-1}) and small amplitude variations have been detected during the flaring activity. This implies much longer integration times to achieve MDP values of the order of a few %, important to disentangle among different leptonic models (external Compton versus synchrotron self Compton, SSC) by modeling the X-ray emission. In particular, in the case of FSRQs with flux $\sim 2 \times 10^{-11}$ erg s^{-1} cm^{-2}, a minimum detectable polarization of 7% will be obtainable in 100 ks.

- *What is the disk-jet connection in misaligned AGN?* WFM long term monitoring (monthly time scale) of radio galaxies hosting efficient accretion disks (mainly Fanaroff-Riley II sources, hereafter FRIIs; see Figure 15) will provide an optimal tool to investigate the disk-jet connection by triggering both radio and LAD X-ray follow-ups. *eXTP* will investigate the disk-jet connection in a similar manner as in X-ray binaries, that exhibit the same behavior (Wu et al., 2013).

Recent detections of radio galaxies hosting inefficient accretion flows (Fanaroff-Riley I, hereafter FRI) at high and very high energies (e.g., IC 310; Aleksić et al., 2014) are providing a further sample of radio-loud sources well suited for follow-up observations with *eXTP*. Combining SFA and LAD with CTA simultaneous observations will be crucial in constraining the TeV emitting region, likely connected with the magnetosphere surrounding the central engine, as derived by the rapid variability observed by MAGIC (Aleksić et al., 2014). FRI behave like high synchrotron-peak blazars (with lower luminosities) and therefore simultaneous observations in X-rays and at TeV energies are the key to interpret their spectral energy distribution in terms of SSC rather than hadronic models (not ruled out so far). Given the typical fluxes of TeV FRI (a few $\times 10^{-12}$ erg s^{-1} cm^{-2}), SFA (combined with LAD for the brightest flares) observations will allow one to detect

the X-ray counterpart of the fast TeV variations, providing tight constraints on the location of the TeV emitting region and the particle acceleration process (Ahnen et al., 2017).

- *How important is reflection in spectra of radio-loud narrow-line Seyfert 1 galaxies (NLSy1s)?* NLSy1s are often considered as a third class of AGN with relativistic jets (Foschini et al., 2011; D'Ammando et al., 2015). LAD observations will be very promising not only for studying the physical mechanisms responsible for the higher energy emission (in γ-rays or at TeV energies) and then the blazar-like behavior, but also for determining the role of the thermal component. The combination of SFA and LAD follow-up of the high energy flares from NLSy1 detected in γ-rays or at higher energy γ-rays will allow one to follow the X-ray spectral variations of these sources in the broad energy range (0.5–30 keV) down to a 10^{-12} erg s^{-1} cm^{-2}, unveiling the interplay between the Comptonized radiation from the corona and the non-thermal emission from the jet. The LAD observations extending up to 30 keV will play an important role in the detection and characterization of the Fe-K line, and test with high accuracy the reflection model applied to the X-ray spectra of NLSy1. This is to investigate the possible link between accretion and jet properties.

10 Tidal disruption events

Observational evidence is mounting to support a scenario where most galactic nuclei host SMBHs. Gas inflow causes a small (~1%) fraction of SMBHs to accrete continuously for millions of years and shine as AGN. Most are expected to be quiescent, accreting if at all at a very sub-Eddington rate (Shankar et al., 2013). Observationally, it is therefore hard to assess the presence and mass of most SMBHs beyond the local universe. Occasionally, a sudden increase of the accretion rate may occur if a large mass of gas, for instance a star, falls into the tidal sphere of influence of the black hole and finds itself torn apart and accreted. One calls these events 'tidal disruption events' (TDEs, see Rees, 1988). TDEs can result in a sudden increase of EM emission. They can reach the luminosity of a quasar but they are rare ($\sim 10^{-4}$ yr^{-1} per galaxy; in particular types of galaxies, it may be $\sim 10^{-3}$ yr^{-1} per galaxy; French et al., 2016; van Velzen, 2018) and last several months or years. TDEs are a multi wavelength phenomenon, that has so far been detected in radio, optical, UV, soft and hard X-rays. They display both thermal and non-thermal emission from relativistic and non-relativistic matter (for a recent review on observations, see Komossa, 2015).

The detection and study of these flares can deliver other important astrophysical information beyond probing the presence of a SMBH. First, TDEs can allow one to discover intermediate mass black holes, as their peak bolometric luminosity is expected to be inversely proportional to the black hole mass. Second, TDEs are signposts of supermassive *binary* black holes, as their light curves look characteristically different in the presence of a second black hole, which acts as a perturber on the stellar stream (Liu et al., 2009). Recently, a disruption by a SMBH binary candidate was claimed (Liu et al., 2014). Thirdly, as also mentioned below, TDEs give us the opportunity to study accretion and jet formation in transient (~month to year time scale) accretion episodes around SMBHs in contrast to AGN. Fourthly, dormant SMBHs represent the majority of the SMBHs in our universe. X-ray flares from TDEs provide us with the opportunity to probe the mass and spin distribution of previously dormant SMBHs at the centers of normal galaxies as well as the geometry of the debris flow of the accretion flare through X-ray line reverberation (Zhang et al., 2015). Finally, in X-rays TDEs represent a new probe of strong gravity, for instance tracing precession effects in the Kerr metric (see, e.g., Hayasaki et al., 2016; Franchini et al., 2016).

The first TDEs were discovered in *ROSAT* surveys of the X-ray sky (e.g., Komossa & Bade, 1999; Grupe et al., 1999), see Komossa (2002) for a review. Later, *GALEX* allowed for the selection of TDEs at UV frequencies (Gezari et al., 2009, 2012). Many of the most recent TDE candidates are found in optical transient surveys (van Velzen et al., 2011; Cenko et al., 2012; Chornock et al., 2014). An alternative method to select TDE candidates is to look for optical spectra with extreme high-ionization and Balmer lines (Komossa et al., 2008; Wang et al., 2012). This class of TDEs is called 'thermal', and the spectral energy distribution is believed to be associated with phenomena that lead to mass accretion onto the black hole.

Currently, the theoretical picture proposed to interpret the observational properties of TDEs is as follows. After stellar disruption, part of the stellar material is accreted onto the black hole, causing a luminous flare of radiation. If the star is completely disrupted, its debris is accreted at a decreasing rate according to $\dot{M} \propto t^{-5/3}$ (Rees, 1988; Phinney, 1989). Therefore, TDEs allow one to study the formation of a transient accretion disk and its continuous transition through different accretion states. The super-Eddington phase - which occurs only for SMBH masses $M < 10^7$ M$_\odot$ - is theoretically uncertain, but it may be associated with a powerful radiatively driven wind (Rossi & Begelman, 2009) that thermally emits 10^{41} – 10^{43} erg s^{-1} mainly at optical frequencies (Strubbe & Quataert, 2009; Lodato & Rossi, 2011). The disk luminosity (10^{44} – 10^{46} erg s^{-1}) peaks instead in the far-UV/soft X-rays (Lodato & Rossi, 2011). As an alternative scenario to thermal emission from an accretion disk, the optical emission

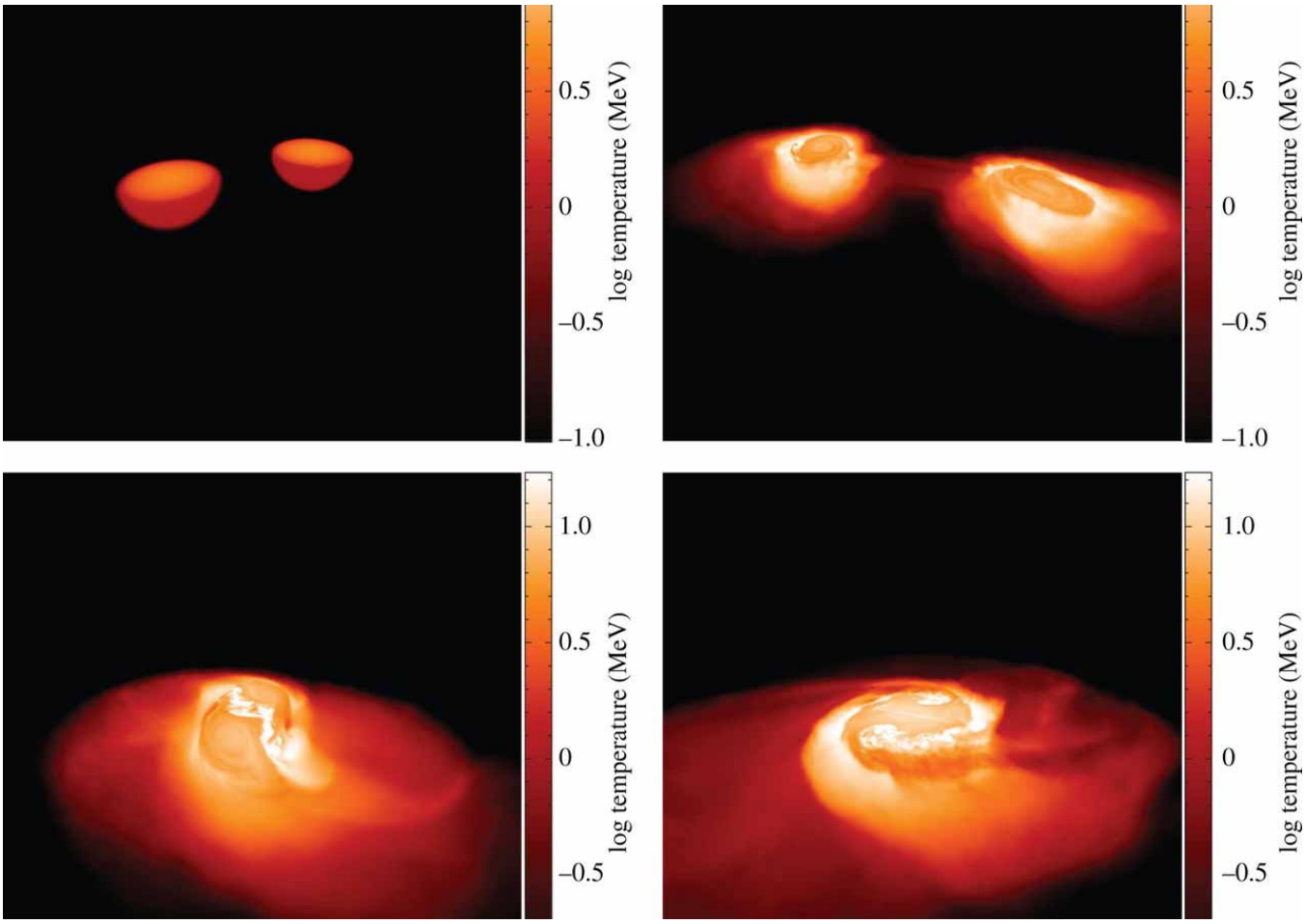

Figure 16 Simulation of a neutron star - neutron star merger. The four frames are timed within 6.8 ms. From Rosswog (2013).

has been suggested to come from shocks as the stellar debris self-crosses or from reprocessed X-ray light (e.g., Piran et al., 2015).

A few years ago, the *Swift* Burst Alert Telescope (BAT) triggered on two TDE candidates in the hard X-ray band (Bloom et al., 2011; Cenko et al., 2012). A multi-frequency follow-up from radio to γ-rays revealed a new class of *non-thermal* TDEs. It is widely believed that emission from a relativistic jet (bulk Lorentz factor $\Gamma \approx 2$, Zauderer et al., 2013; Berger et al., 2012) is responsible for the hard X-ray spectrum (with a negative power-law photon index between -1.6 and -1.8) and the increasing radio activity (Levan et al., 2011a) detected a few days after the trigger. More recently, Brown et al. (2015) reported another candidate relativistic TDE (Swift J1112.2–8238). Hryniewicz & Walter (2011) found nine TDE candidates in BAT data after searching the data from 53,000 galaxies out to 100 Mpc. Finally, Alexander et al. (2016) and van Velzen et al. (2016) discovered the first radio outflow associated with a thermal TDE, suggesting that jets may be a common feature of TDEs.

The best studied of the relativistic events is Swift J1644+57 (Sw J1644 in short; Levan et al., 2011b; Burrows et al., 2011). The two main features that support the claim that Sw J1644 is a TDE are i) the X-ray light curve behavior, that follows $L_{\rm X} \propto \dot{M}(t-\tau)^{-5/3}$ after a few days ($\tau \approx 3$ day) from the trigger (Donnarumma & Rossi, 2015), and ii) the radio localization of the event within 150 pc from the center of a known quiescent galactic nucleus (Zauderer et al., 2011).

If one uses the Sw J1644 radio and X-ray light curves to estimate prospects for any future planned missions, one obtains that non-thermal TDEs can be discovered at a higher rate thanks to triggers provided by radio surveys and to follow-ups at higher energies. The wide field-of-view survey of SKA will effectively detect TDEs in the very early phase, allowing follow-up X-ray observations in the very early phase (Yu et al., 2015; Donnarumma et al., 2015). In synergy with SKA in survey mode, the SFA can in principle successfully repoint to each radio candidate in the sky accessible at any moment to *eXTP* (i.e., 50% of the time), and measure its light curve decay index and spectral properties. The X-ray counterpart of radio-triggered events can be followed up with the LAD too (see Fig. 6 in Donnarumma & Rossi, 2015), thus extending

the energy coverage up to 30 keV with a better characterization of the non-thermal process and of the jet energy budget. The X-ray polarimeter will definitely play the major role. For events followed up within a few weeks from the beginning, a fraction of ~10% of the radio-triggered events will have a 2–10 keV flux greater than 10^{-10} erg s^{-1} cm^{-2}. For these events, it is possible to derive a minimum detectable polarization of ~10% over a 5 ks time scale. This will allow one to test the variation of magnetic field over a time scale of one hour and derive the time needed for the transient jet to build up a large scale coherent magnetic field. Moreover, if *eXTP* were able to follow-up TDEs within 1 day, with the trigger provided by LSST, SKA, the Einstein Probe or WFM and if the source is bright enough in 2–10 keV ($> 10^{-10}$ erg s^{-1} cm^{-2}), it will be possible to investigate also polarization angle variations aimed at assessing the role of jet precession in the early phase of the event. In this case, one foresees a set of daily (50 ks) observations (Saxton et al., 2012; Tchekhovskoy et al., 2014) spread over 10 days in order to appreciate angle variations within a few degrees.

eXTP is therefore very well suited for the X-ray follow-up of jetted TDEs in the SKA era. The expected rate is between a few to several tens per yr (depending on the value of Γ). The attractive prospect is that of building for the first time a sample of well studied TDEs associated with non-thermal emission from jets. This will allow one to study disk-jet formation and their connection, in a way complementary to other more persistent sources such as AGN and X-ray binaries. In addition, jetted TDEs can uniquely probe the presence of SMBHs in *quiescent* galaxies well beyond the local universe (redshift range 1.5-2).

Moreover, the SFA energy band and sensitivity will enable the follow-up of thermal TDEs, that are expected to be triggered in a large number with LSST. These will be studied with eXTP in a tight connection with the X-ray binary transients. The combination of the soft telescopes, the broad energy coverage and the polarimetric capabilities makes eXTP a great X-ray mission to study all the variety of tidal disruption events and to provide the unique opportunity to answer the following questions:

- *What is the rate of non-thermal TDEs?* The SFA sensitivity will allow one to follow up and identify any radio triggered TDEs. The WFM can allow the serendipitous detection of non-thermal TDEs in X-rays at a higher rate (between one and a few tens per year) than any current missions. The combination of the two will provide a unique tool to establish the rate of non-thermal TDEs and study the mechanisms powering the hard X-ray emission.
- *Do TDEs exhibit similar spectral states as X-ray binary transients?* The SFA energy band and sensitivity will enable the follow-up thermal TDEs that are expected to be triggered in large numbers with LSST. Several thousands per year are expected to be triggered up to $z \sim 1$ (Strubbe & Quataert, 2009). The X-ray follow-up with SFA will make it possible to study the evolution of the thermal TDEs and possibly see the transition from soft to hard spectra as expected at later stages due to the coronal Comptonized component (Lin et al., 2017).
- *What are the masses and spins of the previously dormant SMBHs at the centers of normal galaxies?* AGN cover only a small portion of the SMBHs in our universe. The distribution of the masses and the spins of these SMBHs is important to our understanding of the cosmological growth of mass and evolution of the spin of the majority SMBHs. At present and in the near future, we are only able to study the properties of these dormant SMBHs (also some intermediate-mass black holes in dwarf galaxies) through these flaring events. Among them, X-ray flaring TDEs allow us to probe the mass and spin with X-ray line reverberation (e.g., Zhang et al., 2015). For future X-ray bright relativistic TDEs or thermal TDEs, it is possible to detect spectral features with 1 ks SFA and LAD exposures.

11 Gamma-ray bursts and supernovae

Gamma-ray bursts (GRBs; for reviews, see Piran, 2004; Mészáros, 2006; Gehrels et al., 2009) are short (~10 s), bright (up to 10^{-5} erg s^{-1} in 10 keV – 1 MeV), energetic (with fluences up to more than 10^{-4} erg cm^{-2}) and frequent (about one per day). Observational efforts since the 1990s have provided, among others, 1) the accurate localization and characterization of multi-wavelength afterglows (Costa et al., 1997; van Paradijs et al., 1997), 2) the establishment of cosmological distances and supernova-like radiated energies (Metzger et al., 1997), 3) the identification of two classes of GRBs, long and short, with a division at 2 s (Kouveliotou et al., 1993a), and 4) the connection of long GRBs with Type Ib/c supernovae (Galama et al., 1998). The most important open questions in our current understanding of GRBs involve: the physical origin of sub-classes of GRBs (i.e., short, X-ray rich, sub-energetic and ultra-long GRBs), the physics and geometry of the prompt emission, some unexpected early afterglow phenomenology (e.g., plateaus and flares), the connection between GRBs and particular kinds of supernovae, the nature of the 'central engine' and the use of GRBs as cosmological probes.

Short GRBs were long suspected to be connected to binary neutron-star merger events (Eichler et al., 1989; Kouveliotou et al., 1993b). The detection of short GRBs associated with old stellar populations, their offsets from their host galaxies

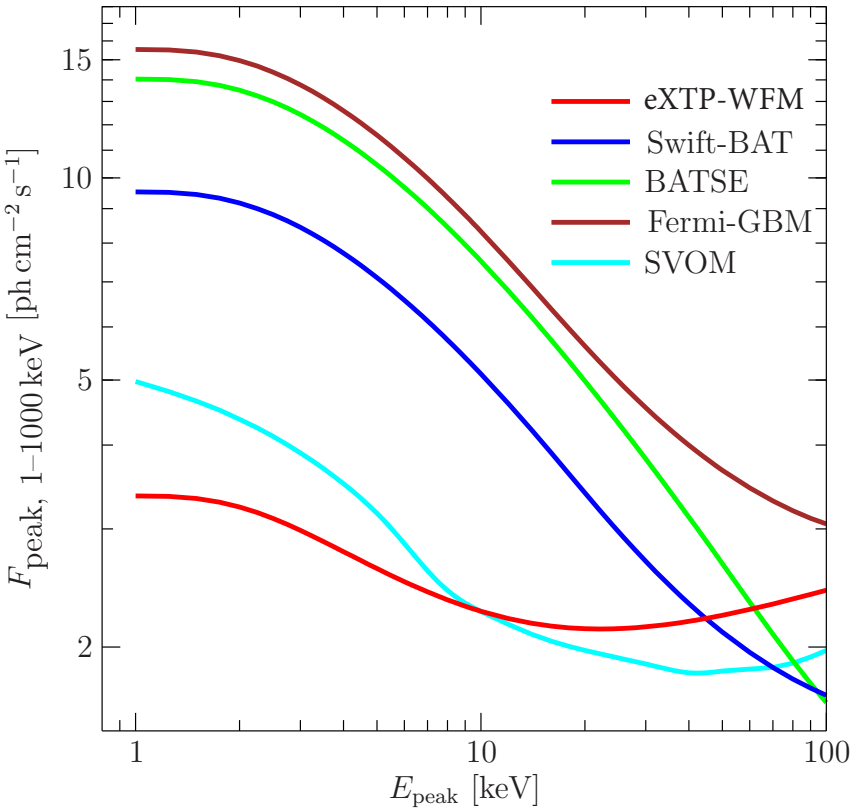

Figure 17 GRB detection sensitivity in terms of peak flux sensitivity as a function of the spectral peak energy E_p (Band, 2003) of the WFM (red) for M4 configuration compared to those of *CGRO* BATSE (green), *Swift* BAT (blue), *Fermi* GBM (brown), and *SVOM* ECLAIRs (cyan).

and the identification of a candidate kilonova explosion supported this association (e.g. Gehrels et al., 2005; Fong et al., 2010; Tanvir et al., 2013). The suspicion received unprecedented support through the coincident detection of the short GRB170817A (Goldstein et al., 2017) and the binary merger gravitational-wave event GW170817 (Abbott et al., 2017e,f). The masses of the two binary components measured through the GWs are more consistent with a set of dynamically measured neutron star masses than with that of black holes. The tidal disruption of neutron stars (see Fig. 16 for stills from a simulation) is expected to yield EM radiation because of the delayed accretion of part of the expelled matter onto the merger product, the strong radio-active decay of r-process elements produced during the merger, the shocks resulting from an expanding cocoon and/or jets.

The prospect of GW detections with Advanced LIGO and Virgo, KAGRA and LIGO-India in the 2020s have been calculated to be rather promising (tens to hundreds per year) for distances of up to ~300-500 Mpc (Abbott et al., 2016; Yang et al., 2017). So far, very few (4-5; see, e.g., Gehrels et al., 2006; Fong et al., 2015) supernova-less GRBs (including the so-called long-short GRBs and short GRBs) have been localized within this distance regime. This may improve with the softer response by the WFM and its larger field of view. It was thought that, due to the beaming effect in special relativity, only relativistic jets from the mergers of two neutron stars or of a black hole and a neutron star beamed toward the Earth can be detected as short GRBs. The detection of the off-axis GRB170817A (Goldstein et al., 2017), without any noticeable signal of a relativistic jet in our line of sight, suggests better prospects for the detection of off-axis X-ray emission, possibly produced as a result of the shock propagation or by the mildly relativistic cocoon (see, e.g., Salafia et al., 2016; Lazzati et al., 2017). This emission has a much larger opening angle, and despite the much lower luminosity, it might still be observable by *eXTP* within the LIGO-Virgo detection horizon. Moreover, independently from short GRBs, some models predict detectable and nearly-isotropic X-ray emission powered by the merger remnant (Zhang & Mészáros, 2001; Metzger et al., 2008; Rowlinson et al., 2013; Zhang, 2013; Gao et al., 2013; Siegel & Ciolfi, 2016a,b). With its unprecedented large field of view, WFM may help to confirm or exclude these models by possibly detecting EM signals from the remnant on the needed time scale (from ~ 1 s to longer). GRB170817A would have been detectable with the WFM with a signal-to-noise ratio during the peak of up to about 10 if its spectrum would be on the 1σ soft side of the error margins of the spectral shape parameters measured with

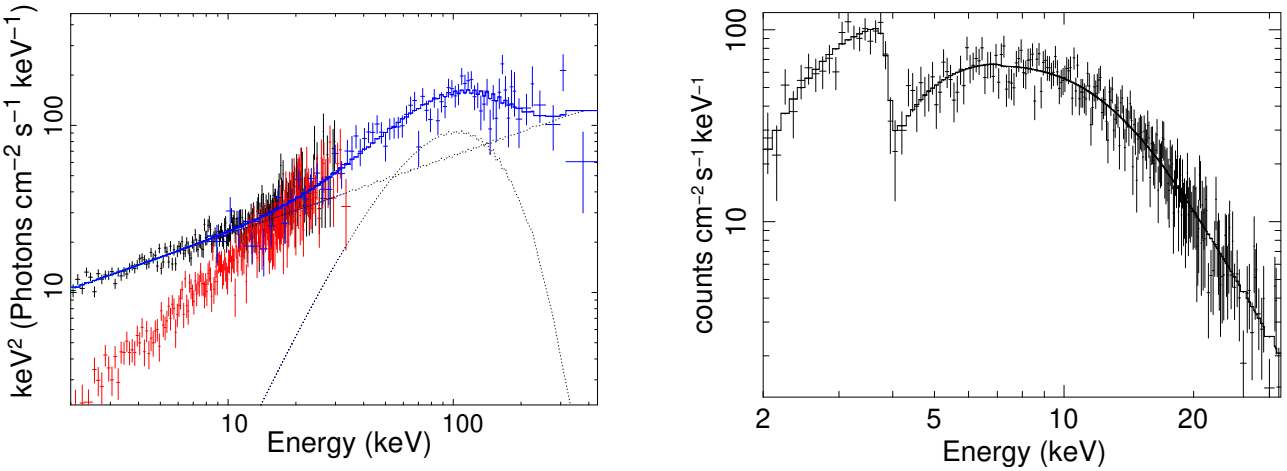

Figure 18 Illustrative plots of WFM capabilities and of their impact on GRB science. *Left:* Simulated WFM spectra of the first ~50 s of GRB 090618 (from Izzo et al. 2012) obtained by assuming either the Band-function extrapolation (black) or the power-law plus black-body model extrapolation (red) to the *Fermi* GBM measured spectrum (blue). The black body and power-law model components best-fitting the *Fermi* GBM spectrum are also shown in black dashed lines. *Right:* Simulation of the transient absorption feature in the X-ray energy band detected by *BeppoSAX* WFC in the first 8 s of GRB 990705 as it would be measured by the WFM (Amati et al., 2000).

Fermi-GBM (Goldstein et al., 2017).

The nature of the second supernova in tight binaries, which are responsible for producing the binary neutron star progenitors of short GRBs and GW sources, is an ultra-stripped supernova (Tauris et al., 2013). These supernovae produce relatively faint and rapidly decaying light curves (Tauris et al., 2015; Moriya et al., 2015). A prime candidate for such a supernova event is SN 2005ek (Drout et al., 2013). Furthermore, as a result of severe mass transfer in the X-ray phase just prior to these supernovae (via so-called Case BB Roche-lobe overflow), such systems are also likely to be observable with eXTP as pulsating ultra-luminous X-ray sources (see Sect. 12.1).

Another interesting class of soft GRBs may arrive from supernova shock breakouts. Wide-field soft X-ray surveys are predicted to detect each year hundreds of supernovae in the act of exploding through the supernova shock breakout phenomenology (Horiuchi et al., 2011; Campana et al., 2006). Supernova shock breakout events occur in X-rays at the very beginning of the supernova explosions, allowing for follow-up at other wavelengths to start extremely early on in the supernova, and possibly shedding light on the nature of the progenitor of some types of supernovae. To date, only one supernova shock breakout has been unambiguously detected, in *Swift* observations of NGC 2770 (Soderberg et al., 2008). It has a fast-rise, exponential decay light curve with a rise time of 72 seconds, and an exponential decay time scale of 129 seconds, and a peak X-ray luminosity of 6.1×10^{43} ergs s^{-1}.

An interesting target for *eXTP* are the recently discovered ultra-long GRBs (Gendre et al., 2013; Levan, 2015). These events are soft gamma-ray bursts lasting hours (instead of seconds). Only a few events are known, and most of their properties remain to be studied. We know however that these events present a possible faint thermal component, and that they may be linked to progenitors very similar to population III stars (i.e. extremely massive, metal poor stars; Ioka et al., 2016). These objects are not brighter than normal long GRBs (albeit the total energy budget is far larger), but last for so long that it is possible to re-point *eXTP* and still to observe the very bright prompt phase. This brightness, combined with the unprecedented large collecting area of the LAD, would allow spectral studies impossible with any other mission to date, studying in detail the evolution of the thermal component and its still debated nature (Piro et al., 2014).

Thanks to its unique combination of field of view, broad bandpass, spectral resolution, large effective area, and polarization capabilities, the instruments on board *eXTP*, particularly the WFM (see Fig. 17), can address questions of fundamental importance to understanding the above phenomena:

- *What are X-ray Flashes?* *eXTP* can enable a substantial increase (with respect to past and current missions) of the detection rate of X-Ray Flashes (XRFs), events commonly interpreted as a softer sub-class of GRBs (but see also Ciolfi, 2016) which likely constitutes the bulk of the GRB population but still lacking a good body of observational data (Heise et al., 2001; Sakamoto et al., 2005, 2008). With respect to *HETE-2* WXM (2–25 keV), the most efficient XRF detector flown so far, WFM will increase the XRF detection rate 7-fold, with an expected rate of 30–40 XRF per year (e.g., Martone et al., 2017). See also Fig. 17.
- *What are the main radiative mechanisms at the basis of*

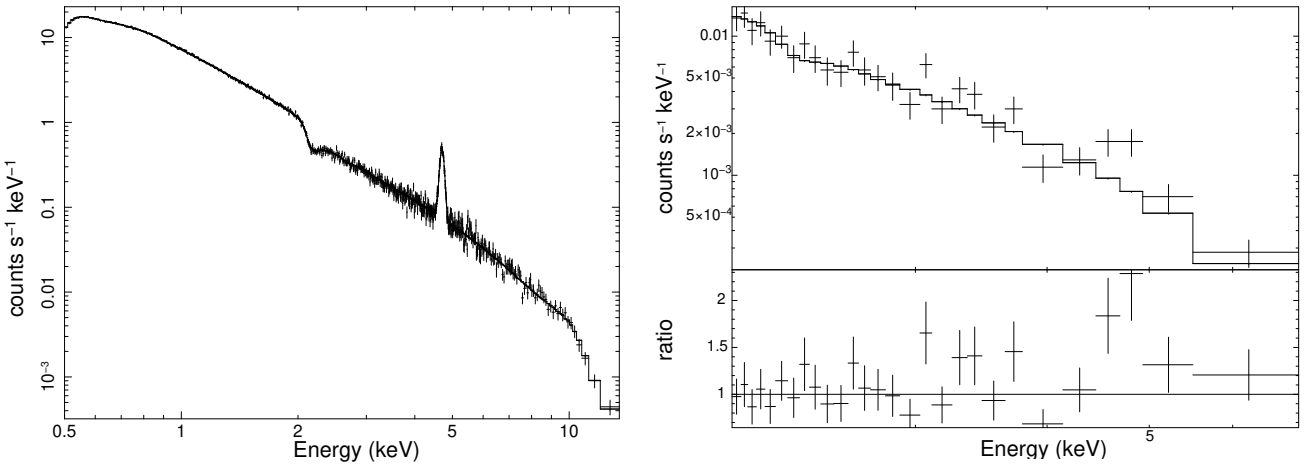

Figure 19 As an example, we considered the redshifted Fe-K line that was measured by *BeppoSAX* in the X-ray afterglow spectrum of GRB000210 (Antonelli et al., 2000). We show in the left panel a simulated SFA spectrum as obtained considering the same afterglow intensity and line equivalent width as detected by *BeppoSAX* 12 hr after the onset of the GRB. An exposure time of 50 ks is assumed (average flux of 8×10^{-13} erg s^{-1} cm^{-2}). The detection of the iron line with the *eXTP* instrument would be outstanding. The right panel shows the same simulation for *Swift*/XRT. No line is detected. This confirms the low sensitivity of XRT to similar features. These unique and unprecedented results would provide an important step forward in the investigation of the circumburst material composition and distribution, with important consequences for shedding light on the nature of GRB progenitors and emission physics.

GRB prompt emission? Measurement of the GRB spectra and their evolution down to 2 keV are an indispensable tool for testing models of GRB prompt emission and will be studied with unprecedented detail thanks to the WFM's unique capabilities (see Fig. 18 left).

- *What is the nature of GRB progenitors?* Transient absorption edges and emission lines in the prompt and afterglow X-ray spectra of long GRBs are expected in several scenarios for their origin. Firm detections or deep limits on such features would be essential for the understanding of the properties of the circumburst matter (CBM) and hence the nature of GRB progenitors. In addition, they could enable us to determine the GRB redshift directly from X-ray observations. Up to now, only a few marginal detections were provided by *BeppoSAX*, *XMM-Newton* and *Chandra*, while no significant evidence for line emission was found in *Swift* afterglow data. As illustrated in Figs. 18 19 (right panels), *eXTP*, thanks to the good energy resolution of both WFM and SFA, combined with a large field of view and a large area, respectively, can greatly contribute to solve this issue and possibly open a new discovery space in the understanding of the GRB phenomenon.
- *Can supernovae be discovered promptly?* Supernova explosions can be detected at their onsets thanks to the shock breakout effect. According to recent supernova rate estimates (Horiuchi et al., 2011), about one to two supernova breakouts per year should be detectable with the WFM out to 20 Mpc. If one takes the case of NGC 2770 as a template, the optimum integration time to detect such events out to 20 Mpc is 240 s (the WFM sensitivity for the detection of impulsive events within this time interval is ~30 mCrab).
- *What is the structure and evolution of GRB jets?* The contribution to GRB science by the LAD and especially the PFA may provide breakthrough information on the jet structure and on the nature of the afterglow flares and plateaus (Burrows et al., 2005; Zhang et al., 2006; O'Brien et al., 2006; Nousek et al., 2006), as different models make different predictions on the evolution of the polarization during these phases (Sari & Mészáros, 2000; Dai, 2004). However, this will strongly depend on spacecraft re-pointing capabilities and is likely limited to the 20% brightest events. For instance, by using the mean parameters of the X-ray afterglow light curves quoted by Margutti et al. (2013) (i.e., a flux normalization at the beginning of the plateau of 6×10^{-10} erg s^{-1} cm^{-2} and 3.96, -0.16 and 1.59 for the decay indices in the three phases - steep, shallow, normal- respectively), we computed the average flux for an exposure of 100 ks starting at different epochs after the trigger. We find that sensitive polarimetric studies with the PFA (i.e., average fluxes above 1 mCrab) can be performed for a typical X-ray afterglow only if it is observed no later than a few minutes after the GRB trigger. However, when considering X-ray afterglows with a bright plateau phase (i.e., 10 times brighter at the start of the plateau), an average flux of few mCrab can be reached for a 100 ks exposure even starting the observations after 6 hours.
- *What is the end product of a neutron star merger?* The end product of a merger of two neutron stars can either be a black hole or a heavy neutron star that may be hypermassive (temporarily supported by for example fast spins)

with magnetic fields of order 10^{15} G (thus a magnetar, e.g., Rowlinson et al., 2013). This probes a very interesting question: what is the threshold mass above which a neutron star cannot exist (see also Sect. 5)? This is intimately related to the neutron star equation of state. A possible observational means to distinguish between both kind of compact objects is, apart from the GW signal (Watts et al., 2018), the detection of a pulsed EM signal after the merger event, for instance in the so-called plateau phase of GRB afterglows that is suggested to be due to rapidly rotating magnetar (e.g. Lasky et al., 2014; Rowlinson et al., 2017). *eXTP* would be well equipped to hunt for such a signal, provided the LAD is pointed quick enough and the prompt signal is very luminous (roughly in the neighborhood of its Eddington limit for a distance of 40 Mpc and a signal duration of 10^4 s, or more).

Finally we note that, as a public community service, *eXTP* will include a capability to localize short transients automatically onboard using data from the WFM. These positions, or a subset of them, will be disseminated via a VHF network and the internet in a similar fashion as for the SVOM mission (Schanne et al., 2015; Zhang et al., 2018).

12 Objects of uncertain nature

12.1 Ultraluminous X-ray sources

Ultraluminous X-ray sources (ULXs) have observed fluxes indicating (assuming isotropic radiation) $L_X > 10^{39}$ erg s^{-1}, and often $> 10^{40}$ erg^{-1}. As these luminosities exceed the Eddington limit (at which released radiation drives away inflowing mass) for typical stellar black hole masses, they indicate the presence of either much larger-mass black holes, of super-Eddington accretion rates, and/or beaming of radiation into limited angles. The recent discovery of X-ray pulsations by XMM-Newton in three ULXs (Bachetti et al., 2014; Fürst et al., 2016; Israel et al., 2017a,b) proves that some ULXs contain neutron stars, and the sinusoidal pulse shape indicates low beaming, so these systems clearly accrete at super-Eddington rates (likely from high-mass donors, e.g., Rappaport et al., 2005; Motch et al., 2011). These systems are now being intensively studied, to try to understand the magnetic fields of their neutron stars, their long-term spin behavior, and the nature of the accretion flows.

eXTP can provide a substantial contribution to ULX science, by finding and timing ULX pulsars. *eXTP* s SFA has an effective area roughly 5.5 times that of XMM-Newtons pn camera at 6 keV (the relevant comparison, since ULX pulsations are stronger at high energies), and an angular resolution of 1′, enabling high count rates for relatively faint objects. As pulsation detection is generally a function of count rate and pulse fraction, the higher SFA effective area means that *eXTP* should be able to detect pulsations over twice as far away (e.g., ∼10 Mpc vs. 5 Mpc for 10^{40} erg/s ULXs with 20% pulsed fractions), and thus within an effective volume 8-10 times larger. A systematic *eXTP* program to survey bright ULXs within 10 Mpc (identified by, for example, eROSITA on Spectrum-X-Gamma, along with Chandra and XMM-Newton surveys), and the brightest ULXs beyond that, may discover ∼30 new ULX pulsars, allowing significant statistical conclusions about the ULX population. Repeated timing of these ULXs will measure their spin-up rates. *eXTP* s high effective area will also allow studies of QPOs (Strohmayer & Mushotzky, 2003), time lags (De Marco et al., 2013), and eclipse searches (e.g., Urquhart & Soria, 2016), opening up substantial discovery space for these extreme objects.

12.2 Fast radio bursts

In recent years, there has been much excitement about the enigmatic Fast Radio Bursts (FRBs; Lorimer et al., 2007). These are bright, millisecond duration, radio bursts with large dispersion measures pointing at extra-galactic distances and large luminosities. A few tens have been detected since 2001 and estimates about their all-sky rate range into the thousands per day (e.g., Keane & Petroff, 2015). Radio telescopes are being adapted to detect many more and aiming to distribute alerts in close to real time (e.g., Petroff, 2017). The origin of these bursts is undetermined and the models range from neutron-star collapse to black holes, neutron star or white dwarf mergers and non-cataclysmic pulsar events (for a review, see Rane & Lorimer, 2017). There is one FRB source which has repeated tens of times (Spitler et al. 2016), while all other observed FRBs have not been observed to repeat (although it is possible that repeats have been missed due to instrument sensitivity limitations and survey strategies; Petroff et al., 2015). The case of the repeater gives rise to a models where the energy is from magnetic reconnection events from a young magnetar (e.g., Katz, 2016) or giant pulses from a rapidly rotating neutron star (e.g., Lyutikov et al., 2016). However, there is no consensus yet (Rane & Lorimer, 2017).

To date FRBs have no counterparts outside the radio band. However, there are models predicting FRBs associated with some GRBs and, hence, a faint, broadband afterglow may be expected (e.g., Zhang, 2014). Coordinated searches of FRBs in the repeating source revealed no detection in X-rays and gamma-rays with 0.5- 10 keV flux limits of order 10^{-7} erg s^{-1} cm^{-2} (e.g., Scholz et al., 2017). This limit can be vastly improved with LAD and SFA to values of 10^{-10} to 10^{-11} erg s^{-1} cm^{-2}. Because of the WFM s large field of view, the possibility of a FRB being detected inside that field of view is

enhanced. Detection of the prompt few millisecond duration emission will be difficult though given the flux limit of approximately $10^{-6.5}$ erg s^{-1} cm^{-2}. If there is a longer duration X-ray counterpart, chances will become better.

Conversely, eXTP could instead provide candidates for targeted searches for FRBs. Many of the progenitor theories require a young neutron star that is rapidly rotating and/or has a high magnetic field (e.g., Rane & Lorimer, 2017). Neutron stars of this type are proposed to be the central engines of some GRBs and superluminous supernovae (see Section 11). Additionally, the host galaxy of the repeating FRB is consistent with the host galaxies of long GRBs and superluminous supernovae (Metzger et al., 2017). However, for long GRBs and superluminous supernovae progenitors, it will take a few decades to clear the surrounding medium to allow the radio emission to escape (Metzger et al., 2017). The short GRB progenitors do not have this issue and bursts may escape much sooner. eXTP will be able to identifying the plateau phase (the signature of the formation of a magnetar Zhang & Mészáros, 2001) following GRBs and these sources can be targeted with rapid response and late-time FRB searches (see Chu et al., 2016, and references therein).

Acknowledgements: We thank the external referees for their advise prior to submission and A. Patruno for a revision of Fig. 7. The Chinese team acknowledges the support of the Chinese Academy of Sciences through the Strategic Priority Program of the Chinese Academy of Sciences, Grant No. XDA15020100. D. Altamirano acknowledges support from the Royal Society. A. Bilous, F. Chambers and A. Watts are supported by ERC Starting Grant 639217. Y. Cavecchi is supported by the European Union Horizon 2020 research and innovation programme under the Marie Sklodowska-Curie Global Fellowship (grant no. 703916). Y. Chen acknowledges support through NSFC grant 11233001, 11773014 and 11633007 and the 973 Program grant 2015CB857100. B. Gendre acknowledges support through NASA grant NNX13AD28A. A. Heger was supported by an ARC Future Fellowship (FT120100363) and by NSF grant PHY-1430152 (JINA Center for the Evolution of the Elements). K. Iwasawa acknowledges support by the Spanish MINECO under grant AYA2016-76012-C3-1-P and MDM-2014-0369 of ICCUB (Unidad de Excelencia 'María de Maeztu'). M. Linares is supported by EU's Horizon programme through a Marie Sklodowska-Curie Fellowship (grant nr. 702638). A. Rozanska was supported by Polish National Science Center grants No. 2015/17/B/ST9/03422and 2015/18/M/ST9/00541. Z. Yan is supported by the National Natural Science Foundation of China under grant numbers 11403074 and 11333005. A. Zdziarski has been supported in part by the Polish National Science Center grants 2013/10/M/ST9/00729 and 2015/18/A/ST9/00746. Zhou acknowledges the support from the NWO Veni Fellowship, grant no. 639.041.647, and NSFC grants 11503008 and 11590781.

Author contributions: This paper is an initiative of *eXTP*'s Science Working Group 4 on Observatory Science, whose members are representatives of the astronomical community at large with a scientific interest in pursuing the successful implementation of *eXTP*. The paper was primarily written by S. Drake (stellar flares), Y. Chen and P. Zhou (supernova remnants), M. Hernanz, D. de Martino (accreting white dwarfs), T. Maccarone (binary evolution), J. in 't Zand (thermonuclear X-ray bursts), E. Bozzo (high-mass X-ray binaries), A. de Rosa (radio-quiet active galactic nuclei), I. Donnarumma (radio-loud active galactic nuclei), E. Rossi (tidal disruption events) and L. Amati (gamma-ray bursts), with major contributions by C. Heinke, G. Sala, A. Rowlinson, H. Schatz, T. Tauris, J. Wilms, W. Yu and X. Wu. The contributions were edited by J. in 't Zand, E. Bozzo, J. Qu and X. Li. Other co authors provided input to refine the paper.

References

Abadie J., et al., 2013, Classical and Quantum Gravity 27, 173001
Abbott B.P., et al., 2016, Living Review in Relativity (arXiv:1304.0670v4)
Abbott B.P., et al., 2015, Class. Quant. Grav. 34, 044001
Abbott B.P., Abbott R., Abbott T.D., et al., 2016a, Physical Review Letters 116, 061102
Abbott B.P., Abbott R., Abbott T.D., et al., 2016b, Physical Review X 6, 041015
Abbott B.P., Abbott R., Abbott T.D., et al., 2016c, Physical Review Letters 116, 241103
Abbott B.P., Abbott R., Abbott T.D., et al., 2017a, Physical Review Letters 118, 221101
Abbott B.P., Abbott R., Abbott T.D., et al., 2017b, Physical Review Letters 119, 141101
Abbott B.P., et al., 2017c, Physical Review D95, 122003
Abbott B.P., et al., 2017d, ApJ 847, 47
Abbott B.P., et al., 2017e, Physical Review Letters 119, 161101
Abbott B.P., et al., 2017f, ApJ 848, L13
Abbott B.P., et al., 2017g, ApJ 851, L35
Ackermann M., Ajello M., Albert A., et al., 2014, Science 345, 554

Ahnen M.L., Ansoldi S., Antonelli L.A., et al., 2017, A&A 603, A25
Aleksić J., Antonelli L.A., Antoranz P., et al., 2014, A&A 563, A91
Alexander K.D., Berger E., Guillochon J., et al., 2016, ApJ 819, L25
Allevato V., Paolillo M., Papadakis I., Pinto C., 2013, ApJ 771, 9
Altamirano D., van der Klis M.B.M., Wijnands, R., Cumming A., 2008, ApJ 673, L35
Amati L., Frontera F., Vietri M., et al., 2000, Science 290, 953
Amati L., Stratta G., Atteia J.L., et al., 2015 (arXiV:1501.02772)
Antonelli L.A., Piro L., Vietri M., et al., 2000, ApJ 545, L39
Archibald A.M., Stairs I.H., Ransom S.M., et al., 2010, Nature 324, 1411
Arévalo P., Papadakis I. E., Uttley, P., et al., 2006, MNRAS 372, 401
Armstrong J.W., Rickett B.J., Spangler S.R., 1995, ApJ 443, 209
Bachetti M., Harrison F. A., Walton D. J., et al. 2014, Nature 514, 202
Ballantyne D.R., 2014, MNRAS 437, 2845
Ballantyne D.R., Everett J.E., 2005, ApJ 626, 364
Ballantyne D.R., Strohmayer T.E., 2004, ApJ 602, L105
Ballet J., 2006, Advances in Space Research 37, 1902
Balman Ş., Godon P., Sion E.M., 2014, ApJ 794, 84
Balman Ş., Revnivtsev M., 2012, A&A 546, A112
Band D.L., 2003, ApJ 588, 945
Basko M.M., Sunyaev R.A., 1976, MNRAS 175, 395¡
Bassa C., Patruno A., Hessels J.W.T., et al., 2014, MNRAS 441, 1825
Begelman M.C., Fabian A.C., Rees M.J., 2008, MNRAS 384, L19
Belczynski K., Wiktorowicz G., Fryer C.L., et al., 2012, ApJ 757, 91
Bell A.R., 2004, MNRAS 353, 550
Benz A.O., Güdel M., 2010, ARAA 48, 241
Berger E., Zauderer A., Pooley G.G., et al., 2012, ApJ 748, 36
Berkhout R.G., Levin Y., 2008, MNRAS 385, 1029
Bhattacharyya D., van den Heuvel E.P.J., 1991, Phys. Rep. 203, 1
Bhattacharyya S., Chakrabarty D., 2017, ApJ 835, 4
Bhattacharyya S., Strohmayer T.E., 2007, ApJ 666, L85
Bhattacharyya S., Strohmayer T.E., 2006, ApJ 641, L53
Bildsten L., Chakrabarty D., Chiu J., et al., 1997, ApJ Supp. 113, 367
Bildsten L., 1998, in 'The many faces of neutron stars', eds. R. Buccheri, J. van Paradijs & A. Alpar, Kluwer Academic Publishers, p. 419
Bianchi S., Maiolino R., Risaliti G., 2012, Advances in Astronomy 2012, 782030
Bildsten L., Chang P., Paerels F., 2003, ApJ 591, L29
Blandford R.D., McKee C.F., 1982, ApJ 255, 419
Blasi M.G., Lico R., Giroletti M., et al., 2013, A&A 559, A75
Blasi P., Amato E., D'Angelo M., 2015, Physical Review Letters 115, 121101
Bloom J.S., Giannios D., Metzger B.D., et al., 2011, Science 333, 203
Bogdanov S., Halpern J., 2015, ApJ 803, L27
Boyd P.T., Smale A.P., Dolan J.F., 2001, ApJ 555, 822
Bozzo, E., Falanga, M., & Stella, L. 2008, ApJ, 683, 1031-1044
Bozzo E., Giunta A., Cusumano G., et al., 2011, A&A 531, A130
Bozzo E., Stella L., Vietri M., Ghosh P., 2009, A&A 493, 809
Brown G.C., Levan A.J., Stanway E.R., et al., 2015, MNRAS 452, 4297
Burrows D.N., Kennea J.A., Ghisellini G., et al., 2011, Nature 476, 421
Burrows D.N., Romano P., Falcone A., et al., 2005, Science 309, 1833
Campana S., Mangano V., Blustin A.J., et al., 2006, Nature 442, 1008
Caprioli D., 2015, In: 34th International Cosmic Ray Conference (ICRC2015), Vol. 34. International Cosmic Ray Conference, p. 8
Carrington R.C., 1859, MNRAS 20, 13
Casanova J., José, J., García-Berro E., et al., 2011, Nature 478, 490
Casares J., Jonker P.G., Israelian G., 2016, in Handbook of Supernovae, eds. A.W. Alsabti & BP. Murdin, Springer (arXiv:1701.07450)
Cavecchi Y., Watts A.L., Braithwaite J., Levin Y., 2013, MNRAS 434, 3526
Cavecchi Y., Watts A.L., Levin Y., Braithwaite J., 2015, MNRAS 448, 445
Cavecchi Y., Watts A.L., Galloway D.K., 2017, ApJ 851, 1
Cenko S.B., Krimm H.A., Horesh A., et al., 2012, ApJ 753, 77
Chakraborty M., Bhattacharyya S., 2014, ApJ 792, 4
Chen H.L., Chen X., Tauris T.M., Han Z., 2013, ApJ 775, 27
Chenevez J., Falanga M., Kuulkers E., et al., 2007, A&A 469, L27
Cheung C.C., Jean P., Shore S.N., et al., 2016, ApJ 826 142
Chiang J., Reynolds C.S., Blaes O.M., et al., 2000, ApJ 528, 292
Chornock R., Berger E., Gezari S., et al., 2014, ApJ 780, 44

Chu Q., Howell E.J., Rowlinson A., et al., 2016, MNRAS 459, 121
Ciolfi R., 2016, ApJ 829, 72
Connaughton V., Burns E., Goldstein A., et al., 2016, ApJ 826, L6
Cooper R.L., Narayan R., 2007, ApJ 661, 468
Coppejans D.L., Körding E.G., Miller-Jones J.C.A., et al., 2016, MNRAS 463, 2229
Coriat M., Corbel S., Prat L., et al., 2011, MNRAS 414, 677
Cornelisse R., Heise J., Kuulkers E., et al., 2000, A&A 357, L21
Cornelisse R., in 't Zand J.J.M., Verbunt F., et al., 2003, A&A 405, 1033
Cornelisse R., Verbunt F., in 't Zand J.J.M., et al., 2002, A&A 392, 885
Costa E., Frontera F., Heise J., et al., 1997, Nature 387 783
Coulter D.A., Foley R.J., Kilpatrick C.D., et al., 2017, Science 358, 1556
Cumming A., 2005, ApJ 630, 441
Cumming A., Bildsten L., 2001, ApJ 559, L127
Cumming A., Macbeth J., in 't Zand J.J.M., Page D., 2006, ApJ 646, 429
Cyburt R., Amthor A.M., Heger A., et al., 2016, ApJ 830 55
Dai Z.G., 2004, ApJ 606, 1000
D'Ammando F., Orienti M., Finke J., et al., 2015, MNRAS 446, 2456
D'Angelo C.R., 2017, MNRAS 470, 3316
Degenaar N., Wijnands R., 2010, A&A 524, A69
Degenaar N., Ballantyne D.R., Belloni T., et al., 2018, Sp. Sc. Rev. 214, 15
Deibel A., Meisel Z., Schatz H., et al., 2016, ApJ 831, 13
De Marco, B., Ponti, G., Miniutti, G., et al. 2013, MNRAS, 436, 3782
de Martino D., Sala G., Balman S., et al., 2015 (arXiv:1501.02767)
De Rosa A., Bianchi S., Giroletti M., et al., 2015 (arXiv:1501.02768)
De Rosa A., Panessa F., Bassani L., et al., 2012, MNRAS 420, 2087
De Rosa A., Uttley, P., Gou, L., et al., 2018, Science China Physics, Mechanics & Astronomy, this issue (*eXTP* White Paper on Strong Gravity)
Di Stefano, R., & Rappaport, S. 1994, ApJ, 437, 733
Donnarumma I., Agudo I., Costamante L., et al., 2015 (arXiv:1501.02770)
Donnarumma I., Rossi E.M., 2015, ApJ 803, 36
Donnarumma I., Rossi E.M., Fender R., et al., 2015, Proc. of Advancing Astrophysics with the Square Kilometre Array (AASKA14), , eds. T. Bourke et al., PoS, vol. 215, article 54
Doroshenko V., Tsygankov S.S., Mushtukov A.A., et al., MNRAS 466, 2143
Drake S.A., Behar E., Doyle J.G., et al., 2015 (arXiv:1501.02771)
Drout M.R., Soderberg A.M., Mazali P.A., et al., 2013, ApJ 774, 58
Eichler D., Livio M., Piran T., Schramm D.N., 1989, Nature 340, 126
Feng H., Santangelo, A., Zane, S., et al., 2018, Science China Physics, Mechanics & Astronomy, this issue (*eXTP* White Paper on Strong Magnetism)
Enoto T., Sasano M., Yamada S., et al., 2014, ApJ 786, 127
Fabian A.C., Zoghbi A., Ross R.R., et al., 2009, Nature 459, 540
Falanga M., Chenevez J., Cumming A., et al., 2008, A&A 484, 43
Fertig D., Mukai K., Nelson T., Cannizzo J.K., 2011, PASP 123, 1054
Field G.B., 1965, ApJ 142, 531
Fisker J.L., Schatz H., Thielemann F.K., 2008, ApJ Supp. 174, 261
Fong W., Berger E., Fox D.B., 2010, ApJ 708, 9
Fong W., Berger E., Margutti R., Zauderer B.A., 2015, ApJ 815, 102
Foschini L., Ghisellini G., Kovalev Y.Y., et al., 2011, MNRAS 413, 1671
Franchini A., Lodato G., Facchini S., 2016, MNRAS 455, 1946
Fraschetti F., 2013, ApJ 770, 84
French K.D, Arcavi I., Zabludoff A., 2016, ApJ 818, L21
Fujimoto M.Y., Hanawa T., Miyaji S., 1981, ApJ 247, 267
Fulbright M.S., Reynolds S.P., 1990, ApJ 357, 591
Fürst F., Pottschmidt, K., Miyasaka H., et al., 2015, ApJ 806, L24
Fürst, F., Walton, D. J., Harrison, F. A., et al. 2016, ApJ, 831, L14
Galama T., Vreeswijk P.M., van Paradijs J., et al., 1998, Nature 395, 670
Galloway D.K., Keek L., 2017, to appear in 'Timing neutron stars: pulsations, oscillations and explosions', eds. T. Belloni & M. Méndez (ASSI, Springer), in press (arXiv:1712.06227)
Gao H., Ding X., Wu X.F., et al., 2013, ApJ 771, 86
Garcia M.R., Miller J.M., McClintock J.E., et al., 2003, ApJ 591, 388
Gehrels N., Sarazin C.L., O'Brien P.T., et al., Nature 437, 851
Gehrels N., Norris J.P., Barthelmy S.D., et al., 2006, Nature 444, 1044
Gehrels N., Ramirez-Ruiz E., Fox D.B., 2009, ARAA 47, 567

Gendre B., Stratta G., Atteia J.-L., et al., 2013, ApJ 776, 30
Gendreau K.C., Arzoumanian Z., Adkins P.W., et al., 2016, In: Space Telescopes and Instrumentation 2016: Ultraviolet to Gamma Ray, Vol. 9905. Proc. SPIE, p. 99051H
Gezari S., Chornock R., Rest A., et al., 2012, Nature 485, 217
Gezari S., Heckman T., Cenko S.B., et al., 2009, ApJ 698, 1367
Ghisellini G., Tavecchio F., 2009, MNRAS 397, 985
Ghisellini G., Tavecchio F., Bodo G., Celotti A., 2009, MNRAS 393, L16
Giacalone J., Jokipii J.R., 2007, ApJ 663, L41
Giannios D., 2013, MNRAS 431, 355
Giommi P., Padovani P., 2015, MNRAS 450, 2404
Gong X.-F., et al., 2011, Class, Quant. Grav. 28, 094012
Goldstein A., Veres P., Burns E., et al., 2017, ApJ 848, L14
González Hernández J.I., Suárez-Andrés L., Rebolo R., Casares J., MNRAS 465, L15
González-Martín O., Vaughan S., 2012, A&A 544, A80
Grandi P., Torresi E., Stanghellini C., 2012, ApJ 751, L3
Grinberg V., Hell N., Potschmidt K., et al., 2013, A&A 554, 88
Grinberg V., Leutenegger M.A., Hell N., 2015, A&A 576, A117
Grinberg V., Potschmidt K., Böck M., et al., 2014, A&A 565, A1
Grupe D., Thomas H.C., Leighly K.M., 1999, A&A 350, L31
Güdel M., Nazé Y., 2009, A&ApR 17, 309
Guo J., Zhang H., 2006, In: 36th COSPAR Scientific Assembly, Vol. 36. COSPAR Meeting
Haardt F., Maraschi L., Ghisellini G., 1994, ApJ 432, L95
Hailey C.J, Mori K., Perez KG., et al., 2016, ApJ 826, 160
Han Z., Podsiadlowski P., 2008, In: Deng L., Chan K.L. (eds.) The Art of Modeling Stars in the 21st Century, Vol. 252. IAU Symposium, p.349
Haskell B., Patruno A., 2017, PRL 119, 161103
Haskell B., Priymak M., Patruno A., et al., 2015, MNRAS 450, 2393
Hayasaki K., Stone N., Loeb A., 2016, MNRAS 461, 3760
He H., Wang H., Yun D., 2015, ApJ Supp. 221, 18
Heger A., Cumming A., Woosley S.E., 2007, ApJ 665, 1311
Heinke C.O., Ivanova N., Engel M.C., et al., 2013, ApJ 768, 184
Heise J., in 't Zand J.J.M., Kippen R.M., Woods P.M., 2001, in 'Gamma-ray bursts in the afterglow era', eds E. Costa, F. Frontera & J. Hjorth, Springer Verlag, p. 16
Helder E.A., Vink J., 2008, ApJ 686, 1094
Heyl J.S., 2004, ApJ 600, 939
Heyl J.S., 2005, MNRAS 361, 504
Hillas A.M., 2005, Journal of Physics G Nuclear Physics 31, R95
Hong J., 2012, MNRAS 427, 1633
Hong J., Mori, K., Hailey, C.J., et al., 2016, ApJ 825, 132
Horiuchi S., Beacom J.F., Kochanek C.S., et al., 2011, ApJ 738, 154
Hryniewicz K., Walter R., 2016, A&A 586, A9
Huang G., Li J., 2011, ApJ 740, 46
in 't Zand J.J.M., 2005, A&A 441, L1
in 't Zand J.J.M., 2017, in '7 years of MAXI: monitoring X-ray Transients', eds. M. Serino, M. Shidatsu, W. Iwakiri & T. Mihara, RIKEN, p. 121
in 't Zand J.J.M., Altamirano D., Ballantyne D.R., et al., 2015 (arXiv:1501.02776)
in 't Zand J.J.M., Bagnoli T., D'Angelo C., et al., 2017, in Proc. 11th INTEGRAL Conference 'Gamma-ray astrophysics in multi-wavelength perspective', ed. E.P.J. van den Heuvel, PoS, vol. 285, paper 94
in 't Zand J.J.M., Cumming A., van der Sluys, M.V., et al., 2005, A&A 441, 675
in 't Zand J.J.M., Keek L., Cavecchi Y., 2014, A&A 568, A69
in 't Zand J.J.M., Kuulkers E., Verbunt F., et al., 2003, A&A 411, L487
in 't Zand J.J.M., Weinberg N.N., 2010, A&A 520, A81
Inoue T., Yamazaki R., Inutsuka S.i., Fukui Y., 2012, ApJ 744, 71
Ioka K., Hotokezaka H., Piran T., 2016, ApJ 833, 110
Israel, G. L., Belfiore, A., Stella, L., et al. 2017a, Science, 355, 817
Israel, G. L., Papitto, A., Esposito, P., et al. 2017b, MNRAS, 466, L48
Ivanova N., Justham S., Chen X., et al., 2013, A&ARv 21, 59
Izzo L., Ruffini R., Penacchioni A.V., et al., 2012, A&A 543, A10
Jager R., Mels W.A.., Brinkman A.C., et al., 1997, A&A Suppl. 125, 557
Jahoda K., Markwardt C.B., Radeva Y., et al., 2006, ApJ Supp. 163, 401
José J., 2016, in 'Stellar Explosions: Hydrodynamics and Nucleosynthesis', ed. J. Jose, CRC Press/Taylor and Francis, p. 259
José J., Moreno M., Parikh A., et al., 2010, ApJ Supp. 189, 204
Kaastra J., Kriss G.A., Mehdipour M., et al., 2014, Science 345, 64
Kajava J., Nättilä J., Poutanen J., et al., 2017, MNRAS 464, L6
Kallman T., Dorodnitsyn A., Blondin J., 2015, ApJ 815, 53
Kang S.J., Huang B.r., Kang T., et al., 2012, ChA&A 36, 115
Kargaltsev O., et al., 2015, Space Sci. Rev. 191, 391
Katz J., 2016, ApJ 826, 226
Keane E.F., Petroff E., MNRAS 447, 2852

Keek L., Ballantyne D.R., Kuulkers E., Strohmayer T.E., 2014, ApJ 797, L23
Keek L., Heger A., in 't Zand J.J.M., 2012, ApJ 752, 150
Keek L., Heger A., 2016, MNRAS 456, L11
Keek L., in 't Zand J.J.M., Kuulkers E., et al., 2008, A&A 479, 177
Keek L., Wolff Z., Ballantyne D.R., et al., 2016, ApJ 826, 79
King A.R., Wijnands R., 2006, MNRAS 366, L31
Klus H., Ho W.C.G., Coe M.J., et al., 2014, MNRAS 437, 3863
Knevitt G., Wynn G.A., Vaughan S., Watson M.G., 2014, MNRAS 437, 3087
Knigge C., Baraffe I., Patterson J., 2011, ApJ Supp. 194, 28
Komossa S., 2002, In: Schielicke R.E. (ed.) Reviews in Modern Astronomy, Vol. 15. Reviews in Modern Astronomy, p. 27
Komossa S., 2015, Journal of High Energy Astrophysics 7, 148
Komossa S., Bade N., 1999, A&A 343, 775
Komossa S., Zhou H., Wang T., et al., 2008, ApJ 678, L13
Körding E., Rupen M., Knigge C., et al., 2008, Science 320, 1318
Körding E.G., Knigge C., Tzioumis T., Fender R., 2011, MNRAS 418, L129
Kouveliotou C., Meegan C.A., Fishman G.J., et al., 1993a, ApJ 413, L101
Kouveliotou C., Meegan C.A., Fishman G.J., et al., 1993b, ApJ 413, L101
Koyama K., 2017, PASJ 70, 1
Koyama K., Petre R., Gotthelf E.V., et al., 1995, Nature 378, 255
Kreidberg L., Bailyn C.D., Farr W.M., Kalogera V., 2012, ApJ 757, 36
Kudritzki R.P., 2002, ApJ 577, 389
Kuulkers E., 2006, in 'Compact stellar X-ray sources', eds. W.H.G. Lewin & M. van der Klis, CUP, Cambridge Astrophysics Series 39, p. 421
Kuulkers E., in 't Zand J.J.M., Atteia J.L., et al., 2010, A&A 514, A65
Kuulkers E., in 't Zand J.J.M., van Kerkwijk M.H., et al., 2002, A&A 382, 503
Lasky P.D., Haskell B., Ravi V., et al., 2014, Phys. Rev. D. 89, 047302
Lazzati D., Lopez-Camara D., Cantiello M., et al., 2017, ApJ 848, L6
Leahy J.P., Black A.R.S., Dennett-Thorpe J., et al., 1997, MNRAS 291, 20
Lee C.-H.., Brown G.E., Wijers R.A.M.J, ApJ 575, 996
Lee U., Strohmayer T.E., 2005, MNRAS 361, 659
Levan A.J., Tanvir N.R., Cenko S.B., et al., 2011a, Science 333, 199
Levan A.J., Tanvir N.R., Cenko S.B., et al., 2011b, Science 333, 199
Levan A.J., 2015, JHEAP 7, 44
Lewin W.H.G., van Paradijs J., Taam R.E., 1993, Space Sci. Rev. 62, 223
Lin D., Guillochon J., Komossa S., et al., 2017, Nature Astronomy 1, 0033
Linares M., Altamirano D., Chakrabarty D., et al., 2012, ApJ 748, 82
Liu F.K., Li S., Chen X., 2009, ApJ 706, L133
Liu F.K., Li S., Komossa S., 2014, ApJ 786, 103
Liu Y., Elvis M., McHardy I.M., et al., 2010, ApJ 710, 1228
Lodato G., Rossi E.M., 2011, MNRAS 410, 359
Lorimer D., Bailes M., McLaughin M.A., et al., 2007, Science 318, 777
Luo J., et al., 2016, Class. Quant. Grav. 33, 035010
Lyutikov M., Burzawa L., Popov S.B., 2016, MNRAS 462, 941
Maccarone T.J., Wijnands R.A.M., Degenaar N., et al., 2015 (arXiv:1501.02769)
Mahmoodifar S., Strohmayer T., 2016, ApJ 818, 93
Maiolino R., Risaliti G., Salvati M., et al., 2010, A&A 517, A47
Margutti R., Zaninoni E., Bernardini M.G., et al., 2013, MNRAS 428, 729
Marinucci A., Matt G., Kara E., et al., 2014a, MNRAS 440, 2347
Marinucci A., Matt G., Kara E., et al., 2014b, MNRAS 440, 2347
Marisaldi M., Smith D.M., Brandt S., et al., 2015 (arXiv/1501.02775)
Markowitz A., Edelson R., Vaughan, S., 2003a, ApJ 598, 935
Markowitz A., Edelson R., Vaughan, S., 2003b, ApJ 593, 96
Markowitz A.G., Krumpe M., Nikutta R., 2003c, MNRAS 439, 1403
Markowitz A.G., Reeves J.N., George I.M., et al., 2009, ApJ 691, 922
Markowitz A.G., Krumpe M., Nikutta R., 2014, MNRAS 439, 1403
Marscher A.P., 2014, ApJ 780, 87
Martone R., Izzo L., Della Valle M., et al., 2017, A&A 608, A52
Martínez-Núñez S., Kretschmar P., Bozzo E., et al., 2017, Sp. Sc. Rev. 212, 59
Maurer I., Watts A.L., 2008, MNRAS 383, 387
McHardy I.M., Koerding E., Knigge C., et al., 2006, Nature 444, 730
McHardy I.M., Papadakis, I.E., Uttley P., et al., 2004, MNRAS 348, 783

Mehdipour M., Kaastra J., Kriss G.A., et al., 2017, A&A 607, A28
Mészáros P., 2006, Reports on Progress in Physics 69, 2259
Mészáros P., Novick R., Chanan G.A., et al., 1988, ApJ 324, 1056
Metzger B.D., Berger E., Margalit B., 2017, ApJ 841, 14 2739
Metzger M.R., Djorgovski S.G., Kulkarni S.R., et al., 1997, Nature 387, 878
Metzger B.D., Finzell T., Vurm I., et al., 2015, MNRAS 450, 2739
Metzger B.D., Thompson T.A., Quataert E., 2008, ApJ 676, 1130
Mignani R.P., Bocchino F., Bucciantini N., et al., 2015 (arXiv:1501.02773)
Miniutti G., Fabian A.C., Anabuki N., et al., 2007, PASJ 59, 315
Molina M., Bassani L., Malizia A., et al., 2013, MNRAS 433, 1687
Moriya T.J., Mazzali P.A., Tominaga N., et al., 2015, MNRAS 466, 2058
Motch, C., Pakull, M. W., Grisé, F., & Soria, R. 2011, Astronomische Nachrichten, 332, 367
Nakamura R., Bamba A., Dotani T., et al., 2012, ApJ 746, 134
Narayan R., Piran T., 2012, MNRAS 420, 604
Nardini E., Risaliti G., 2011, MNRAS 417, 2571
Nelemans G., Yungelson L.R., Portegies Zwart S.F., 2001, A&A 375, 890
Ness, J.-U., Beardmore, A. P., Osborne, J. P., et al. 2015, A&A, 578, A39
Nordon R., Behar E., 2008, A&A 482, 639
Nousek J.A., Kouveliotou C., Grupe D., et al., 2006, ApJ 642, 389
O'Brien P.T., Willingale R., Osborne J.P., Goad M.R., 2006, New J. Phys. 8 121
Orlandini M., Doroshenko V., Zampieri L., et al., 2015 (arXiv:1501.02777)
Osborne J.P., Page K.L., Beardmore A.P., et al., 2011, ApJ 727, 124
Özel F., Freire P., 2016, ARAA 54, 401
Özel F., Psaltis D., Narayan R., McClintock J.E., 2010, ApJ 725, 1918
Paolillo M., Papadakis I., Brandt W.N., 2017, MNRAS 471, 4398
Papadakis I.E., Petrucci P.O., Maraschi L., et al., 2002, ApJ 573, 92
Papitto A., Ferrigno C., Bozzo E., et al., 2013, Nature 501, 517
Patnaude D.J., Fesen R.A., 2009, ApJ 697, 535
Patruno A., Haskell, B., Anderson N., 2017, ApJ 850, 106
Paul B., LAXPC Team 2009, In: Kawai N., Mihara T., Kohama M., Suzuki M. (eds.) Astrophysics with All-Sky X-Ray Observations., p. 362
Peng F., Brown E.F., Truran J.W., 2007, ApJ 654, 1022
Perez K., Hailey C.J., Bauer F.E., et al., 2015, Nature 520, 646
Perna R., Bozzo E., Stella L., 2006, ApJ 639, 363
Perola G.C., Matt G., Cappi M., et al., 2002, A&A 389, 802
Peterson B.M., Ferrarese L., Gilbert K.M., et al., 2004, ApJ 613, 682
Petroff E., Johnston S., Keane E.F., et al., 2015, MNRAS 454, 457
Petroff E., 2017, in Proc. 11th INTEGRAL Conference 'Gamma-ray astrophysics in multi-wavelength perspective', ed. E.P.J. van den Heuvel, PoS, vol. 285, art. 10
Phillips K.J.H., Chifor C., Dennis B.R., 2006, ApJ 647, 1480
Phinney E.S., 1989, Nature 340, 595
Pian E., D'Avanzo P., Benetti S., et al., 2017, Nature 551, 67
Piran T., 2004, Rev. Mod. Phys. 76, 1143
Piran T., Svirski G., Krolik J., et al., 2015, ApJ 806, 164
Piro A.L., Bildsten L., 2005, ApJ 629, 438
Piro L., Troja E., Gendre B., et al., 2014, ApJ 790, L15
Postnov K.A., Mironov A.I., Lutovinov A.A., et al., 2015, MNRAS 446, 1013
Pradhan P., Maitra C., Paul B., et al., 2014, MNRAS 442, 2691
Puls J., Vink J.S., Najarro F., 2008, A&A Review 16, 209
Rappaport S.A., Fregeau J.M., Spruit H., 2004, ApJ 606, 436
Rappaport, S. A., Podsiadlowski, P., & Pfahl, E. 2005, MNRAS, 356, 401
Rane A., Lorimer D., 2017, J. Astrophys. Astr. 38, 55
Rees M.J., 1988, Nature 333, 523
Revnivtsev M., Churazov E., Gilfanov M., Sunyaev R.A., 2001, A&A 372, 138
Reynolds S.P., 2008, ARAA 46, 89
Reynolds S.P., 2017, Space Sci. Rev. 207, 175
Reynolds S.P., Borkowski K.J., Hwang U., et al., 2007, ApJ 668, L135
Reynoso E.M., Hughes J.P., Moffett D.A., 2013, AJ 145, 104
Rieger F.M., Aharonian F.A., 2008, A&A 479, L5
Risaliti G., Harrison F.A., Madsen K.K., et al., 2013, Nature 494, 449
Ritter H., Kolb U., 2003, A&A 404, 301 (update 2016, catalog version RKcat7.24)
Rivers E., Risaliti G., Walton D.J., et al., 2015, ApJ 804, 107
Roberts M.S., 2013, in Proc. of the IAU 291, 127
Rossi E.M., Begelman M.C., 2009, MNRAS 392, 1451
Rossi E.M., Donnarumma I., Fender R., et al., 2015 (arXiv:1501.20774)

Rosswog S., 2013, Philosophical Transactions of the Royal Society of London Series A 371, 20120272
Rowlinson A., O'Brien p.T., Metzger B.D., Tanvir N.R., Levan A.J., 2013, MNRAS 430, 1061
Rowlinson A., Patruno A., O'Brien P.T., 2017, MNRAS 472, 1152
Şahiner Ş, İnam S.Ç, Baykal A., 2012, MNRAS 421, 2079
Sakamoto T., Hullinger D., Sato G., et al., 2008, ApJ 679, 570
Sakamoto T., Lamb D.Q., Kawai N., et al., 2005, ApJ 629, 311
Sako M., Kahn S.M., Paerels F., et al., 2003, in Proc. 'High-resolution X-ray Spectroscopy Workshop with XMM-Newton and Chandra' (arXiv:astro-ph/0309503)
Salafia O.S., Ghisellini G., Pescalli A., Ghirlanda G., Nappo F., 2016, MNRAS 461, 3607
Sanfrutos M., Miniutti G., Agís-González B., et al., 2013, MNRAS 436, 1588
Sanyal D., Grassitelli L., Langer N., Bestenlehner J.M., 2015, A&A 580, A20
Sari R., Mészáros P., 2000, ApJ 535, L33
Savchenko, V., Ferrigno, C., Mereghetti, S., et al. 2016, ApJ, 820, L36
Saxton C.J., Soria R., Wu K., Kuin N.P.M., 2012, MNRAS 422, 1625
Schanne S., Cordier B., Atteia J.-L., et al., 2015, in Proc. 'Swift: 10 years of discovery', PoS, vol. 233, article 107
Schatz H., Bildsten L., Cumming A., 2003, ApJ 583, L87
Schatz H., Gupta S., Möller P., et al., 2014, Nature 505, 62
Schwarz G.J., Ness J.U., Osborne J.P., et al., 2011, ApJS 197, 31
Scholz P., Bogdanov S., Hessels, J.W.T., et al., 2017, ApJ 846, 80
Segura A., Walkowicz L.M., Meadows V., et al., 2010, Astrobiology 10, 751
Shankar F., Weinberg D.H., Miralda-Escudé J., 2013, MNRAS 428, 421
Siegel D. M., Ciolfi R., 2016a, ApJ 819, 14
Siegel D. M., Ciolfi R., 2016b, ApJ 819, 15
Soderberg A.M., Berger E., Page K.L., et al., 2008, Nature 453, 469
Sokoloski J.L., Luna G.J.M., Mukai K., Kenyon S.J., 2006, Nature 442, 276
Spitkovsky A., Levin Y., Ushomirsky G., 2002, ApJ 566, 1018
Spitler L.G., Scholz P., Hessels J.W.T., et al., 2016, Nature 531, 202
Stevens J., Brown E.F., Cumming A., 2014, ApJ 791, 106
Strohmayer T., Bildsten L., 2006, New views of thermonuclear bursts, p.113
Strohmayer T.E., Brown E.F., 2002, ApJ 566, 1045
Strohmayer T.E., Markwardt C.B., 2010, ATel 2929
Strohmayer, T. E., & Mushotzky, R. F. 2003, ApJ, 586, L61
Strohmayer T.E., Zhang W., Swank J.H., 1997, ApJ 487, L77
Strubbe L.E., Quataert E., 2009, MNRAS 400, 2070
Sundqvist J.O., Owocki S.P., 2013, MNRAS 428, 1837
Tanvir N., Levan A.J., Fruchter A.S, et al., 2013, Nature 500, 547
Tatischeff V., Hernanz M., 2007, ApJ 663, L101
Tauris T.M., 2012, Science 335, 561
Tauris T.M., van den Heuvel E.P.J., 2006, in 'Compact Stellar X-ray Sources', eds. W.H.G. Lewin & M. van der Klis, CAP 39, p. 623
Tauris T.M., Kramer M., Freire P.C.C., et al., 2017, ApJ 846, 170
Tauris T.M., Langer N., Moriya T.J., et al., 2013, ApJ 778, L23
Tauris T.M., Langer N., Podsiadlowski P., et al., 2015, MNRAS 451, 2123
Tchekhovskoy A., Metzger B.D., Giannios D., Kelley L.Z., 2014, MNRAS 437, 2744
Torricelli-Ciamponi G., Pietrini P., Risaliti G., Salvati M., 2014, MNRAS 442, 2116
Tsygankov S.S., Mushtukov A.A., Suleimanov V.F., et al., 2017, A&A 608, A17
Uchiyama Y., Aharonian F.A., 2008, ApJ 677, L105
Uchiyama Y., Aharonian F.A., Tanaka T., et al., 2007, Nature 449, 576
Urquhart, R., & Soria, R. 2016, ApJ, 831, 56
Urry C.M., Padovani P., 1995, PASP 107, 803
Uttley P., Cackett E.M., Fabian A.C., et al., 2014, A&ARv 22, 72
van Haaften L.M., Nelemans G., Voss R., et al., 2012, A&A 537, A104
van Paradijs J., Penninx W., Lewin W.H.G., 1988, MNRAS 233, 437
van Paradijs J., Groot P.J., Galama T., et al., 1997, Nature 386, 6626
van Velzen S., Anderson G.E., Stone N.C., et al., 2016, Science 351, 62
van Velzen S., Farrar G.R., Gezari S., et al., 2011, ApJ 741, 73
van Velzen S., 2017, ApJ 852, 72
Wallace R.K., Woosley S.E., 1981, ApJ Supp. 45, 389
Woosley S.E., Heger A., Cumming A., et al., 2004, ApJ Supp. 151, 75
Walter R., Lutovinov A.A., Bozzo E., Tsygankov S.S., 2015,
Walton D.J., Risaliti G., Harrison F.A., et al., 2014, ApJ 788, 76
Wang C., Jia K., Li X.D., 2016, MNRAS 457, 1015

Wang T.G., Zhou H.Y., Komossa S., et al., 2012, ApJ 749, 115
Warner B., 1987, MNRAS 227, 23
Warner B., 2004, PASP 116, 115
Warwick R.S., 2014, MNRAS 445, 66
Watts A.L., 2012, ARAA 50, 609
Watts A.L., Krishnan B., Bildsten L., Schutz B.F., 2008, MNRAS 389, 839
Watts A.L., Yu W. Poutanen, J., , et al., 2018, Science China Physics, Mechanics & Astronomy, this issue (*eXTP* White Paper on Dense Matter)
Weinberg N.N., Bildsten L., Schatz, H., 2006, ApJ 639, 1018
Wheatley P.J., Mauche C.W., Mattei J.A., MNRAS 345m 49
Wilms J., Nowak N.A., Potschmidt K., et al., 2001, MNRAS 320, 327
Woods, T. E., & Gilfanov, M. 2016, MNRAS, 455, 1770
Wu K., 2000, Space Sci. Rev. 93, 611
Wu Y.X., Yu W., Li T.P., et al., 2010, ApJ 718, 620
Wu Z., Jiang D., Gu M., 2013, In: Zhang C.M., Belloni T., Méndez M., Zhang S.N. (eds.) Feeding Compact Objects: Accretion on All Scales, Vol. 290. IAU Symposium, p.345
Wyrykowski Ł. Kostrzewa-Rutkowska Z., Skowron J., et al., 2016, MNRAS 458, 3012
Yang G., Brandt W.N., Luo B., et al., 2016, ApJ 831, 145
Yang S., Valenti S, Cappellaro E., et al., 2017, ApJ 851, L48
Wiktorowicz G., Belczynski K., Maccarone T., in Proc. 'Binary systems, their evolution and environments', conference held 1-5 September 2014 at Ulaanbatar, Mongolia (arXiv:1312.5924)
Yaqoob T., Padmanabhan U., 2004, ApJ 604, 63
Yu W., Zhang H., Yan Z, Zhang W., 2015, in 'Advancing Astrophysics with the Square Kilometre Array (AASKA14)', eds. T. Bourke et al., PoS, vol. 215, article 66
Zamfir M., Cumming A., Niquette C., 2014, MNRAS 445, 3278
Zauderer B.A., Berger E., Margutti R., et al., 2013, ApJ 767, 161
Zauderer B.A., Berger E., Soderberg A.M., et al., 2011, Nature 476, 425
Zhang B., 2013, ApJ 763, L22
Zhang B., 2014, ApJ 780, L21
Zhang B., Fan Y.Z., Dyks J., et al., 2006, ApJ 642, 354
Zhang B., Mészáros P., 2001, ApJ 552, L35
Zhang G., Méndez M., Belloni T.M., Homan J., 2013, MNRAS 436, 2276
Zhang S.-N., et al., 2018, Science China Physics, Mechanics & Astronomy, this issue (*eXTP* White Paper on Instrumentation)
Zhang W., Yu W., Karas V., Dovčiak M., 2015, ApJ 807, 89